



**UNIVERSITY OF NAIROBI**

**SCHOOL OF ENGINEERING**

**DEPARTMENT OF ELECTRICAL AND INFORMATION ENGINEERING**

**MSC (ELECTRICAL AND ELECTRONIC ENGINEERING)**

**MOBILE DEVICE MULTIBAND ANTENNA DESIGN OPTIMIZATION AND  
PERFORMANCE TUNING IN THE PRESENCE OF ACTIVE COMPONENTS**

**BY**

**SEGERA RENE DAVIES**

**F56/69924/2013**

**BSC (ELECTRICAL AND ELECTRONIC ENGINEERING), UNIVERSITY OF NAIROBI, 2013**

A thesis submitted in partial fulfillment of the requirement for the degree of Master of Science in Electrical and Electronic Engineering, University of Nairobi.

*MAY, 2016*

## DECLARATION OF ORIGINALITY

**NAME OF STUDENT:** SEGERA RENE DAVIES

**REGISTRATION NUMBER:** F56/69924/2013

**COLLEGE:** Architecture and Engineering

**FACULTY/ SCHOOL/ INSTITUTE:** Engineering

**DEPARTMENT:** Electrical & Electronic Engineering

**COURSE NAME:** Master of Science in Electrical & Electronic Engineering

**TITLE OF WORK:** MOBILE DEVICE MULTIBAND ANTENNA DESIGN OPTIMIZATION AND PERFORMANCE TUNING IN THE PRESENCE OF ACTIVE COMPONENTS

- 1) I understand what plagiarism is and I am aware of the university policy in this regard.
- 2) I declare that this research proposal is my original work and has not been submitted elsewhere for examination, award of a degree or publication. Where other people's work, or my own work has been used, this has properly been acknowledged and referenced in accordance with the University of Nairobi's requirements.
- 3) I have not sought or used the services of any professional agencies to produce this work
- 4) I have not allowed, and shall not allow anyone to copy my work with the intention of passing it off as his/her own work
- 5) I understand that any false claim in respect of this work shall result in disciplinary action, in accordance with University anti- plagiarism policy

**Signature:** .....

**Date:**.....

**DECLARATION**

**This thesis is my original work and has not been presented for a degree in any other university.**

**DAVIES RENE SEGERA**

**SIGNATURE.....DATE.....**

**This thesis has been submitted for examination with my/our approval as University supervisor(s):**

**SUPERVISOR(S):**

**PROF. MWANGI MBUTHIA**

**SIGNATURE.....DATE.....**

## **DEDICATION**

I would like to dedicate this project to the Almighty God for making it possible in bringing me this far in this project.

I also dedicate this project to my family and loved ones in tolerating my excuses throughout my entire lecture period.

## **ACKNOWLEDGEMENT**

I would like to take this opportunity to express my deepest gratitude to all who have provided me with invaluable help over the course of this project.

First I would like to sincerely thank Prof. Mwangi Mbutia for his continuous guidance throughout the whole allocated period of the project and for securing the research funds that have paid for this research and for my M.Sc. studies.

Finally I convey my gratitude to the postgraduate students for their support throughout the entire project period. I say may God richly bless you all.

# TABLE OF CONTENTS

DECLARATION OF ORIGINALITY.....	ii
DECLARATION.....	iii
DEDICATION .....	iv
ACKNOWLEDGEMENT .....	v
TABLE OF CONTENTS .....	vi
LIST OF TABLES .....	ix
LIST OF FIGURES .....	x
LIST OF ACRONYMS .....	xii
LIST SYMBOLS .....	xiii
ABSTRACT .....	xiv
CHAPTER 1 INTRODUCTION .....	1
1.1 Background to the Research .....	1
1.2 Problem Statement .....	1
1.3 Objectives .....	2
1.4 Scope of the research work.....	3
1.5 Organization of the research work.....	3
CHAPTER 2 LITERATURE REVIEW.....	4
2.1 Antenna Theory.....	4
2.2 Radio Frequency.....	5
2.3 Antenna parameters .....	8
2.3.1 Radiation pattern .....	8
2.3.2 Half Power Beam Width (HPBW).....	10
2.3.3 Directivity (D).....	11
2.3.4 Gain (G).....	12
2.3.5 Efficiency ( $e_o$ ).....	13
2.3.6 Scattering Parameters (S-Parameters).....	14
2.3.7 Voltage Standing Wave Ratio (VSWR).....	16
2.3.8 Polarisation.....	16
2.3.9 Input Impedance .....	17
2.3.10 Bandwidth .....	18
2.3.11 Reciprocity.....	19
2.4 Printed Inverted-F antenna (PIFA).....	19

CHAPTER 3	DESIGN OF A MULTI-BAND PIFA ANTENNA FOR TWO GSM FREQUENCY BANDS (900MHZ AND 1800MHZ)	26
3.1	Introduction	26
3.2	Advanced Design System (ADS)	26
3.3	Multiband PIFA Antenna Design methodology	27
3.3.1	Selection of design parameters	28
3.3.2	Design and modeling a multiband PIFA Antenna structure	29
CHAPTER 4	SIMULATION RESULTS FOR THE DESIGNED MULTIBAND PIFA ANTENNA	38
4.1	Introduction	38
4.2	Simulation results for the GSM-900 PIFA antenna	38
4.2.1	An interpretation of the simulation results for the designed GSM-900 PIFA Antenna	43
4.3	Simulation results for the dual band Printed Inverted-FL for GSM-900 and GSM-1800 bands	47
4.3.1	An interpretation of the simulation results for the designed Dual Band PIFA Antenna for GSM-900 and GSM-1800 Bands	54
4.4	Summary of the simulated results	57
CHAPTER 5	PERFORMANCE OF THE DESIGNED DUAL BAND PIFA ANTENNA ON A POPULATED MULTI-LAYER BOARD	58
5.1	Introduction	58
5.2	Basic concepts of RF PCB Design	58
5.2.1	Proper component placement for electrical considerations	59
5.2.2	Multi-layer PCB stack-up planning	60
5.2.3	Bypass capacitors and fan-out	64
5.2.4	Trace width for current carrying capability	65
5.2.5	Trace width for controlled impedance	66
5.2.6	Trace spacing for voltage withstanding	68
5.2.7	Trace spacing to minimize crosstalk	69
5.2.8	Trace with acute and 90° angles	70
5.2.9	Ground Plane requirement for RF PCB design	70
5.2.10	RF PCB design considerations for embedded PCB antennas	72
5.3	Integrating the dual band PIFA antenna into a multilayer board	72
5.3.1	Defining the layer stack-up for designed multilayer PCB board	72
5.3.2	Suitable location and placement of the dual PIFA on the designed PCB board	75
5.3.3	Designing a 50Ω controlled impedance surface microstrip transmission line for connecting the antenna to the GSM module	75
5.3.4	Simulation results of the multiband PIFA antenna in the presence of components	77

5.4 Simulated results of the antenna on a populated PCB board .....	78
CHAPTER 6 CONCLUSION AND RECOMMENDATIONS .....	84
6.1 Conclusion .....	84
6.2 Recommendations for future work.....	85
REFERENCES .....	86



## **LIST OF TABLES**

Table 3.1	Performance requirements for GSM-900 and GSM-1800 standards
Table 4.0	Dimensions for the optimized GSM-900 PIFA antenna
Table 4.1	Parameters for the optimized GSM-900 PIFA antenna
Table 4.2	Dimensions for the optimized dual band PIFA antenna
Table 4.3	Parameters for the optimized dual band PIFA antenna resonant at 925MHz and 1795MHz
Table 5.1	Stack-up for 8-layer PCB
Table 5.2	Minimum conductor spacing in mils for both internal and external traces of a multilayer PCB

## LIST OF FIGURES

- Figure 2.1 An antenna as a transition structure for both a receiving and transmitting antenna
- Figure 2.2 A circuit representing an antenna as a whole structure
- Figure 2.3 Wavelength measurements
- Figure 2.4 Frequency qualities
- Figure 2.5 The size of the EM spectrum
- Figure 2.6 Spherical coordinate system which describes the radiation pattern
- Figure 2.7 Polar diagram of the azimuth plane radiation pattern
- Figure 2.8 Three dimensional directional radiation pattern
- Figure 2.9 Polar diagram of the elevation plane radiation pattern
- Figure 2.10 Polar diagram of the azimuth plane radiation pattern
- Figure 2.11 Three dimensional Omni-directional radiation pattern
- Figure 2.12 Polar diagram of the elevation plane pattern
- Figure 2.13 Radiation pattern lobes
- Figure 2.14 Polar diagram of HPBW
- Figure 2.15 Rectangular diagram of HPBW
- Figure 2.16 Two port network constituted by S-Parameters
- Figure 2.17 Circuit representing input impedance at the entrance terminals of the transmission line
- Figure 2.18 PIFA antenna layout
- Figure 2.19 PIFA antenna structure
- Figure 3.1 Basic PIFA antenna structure
- Figure 3.2 Substrate geometry
- Figure 3.3 PIFA with dimensions
- Figure 3.4 Printed Inverted-FL Antenna
- Figure 3.5 Printed Inverted-FL antenna with dimensions
- Figure 4.0 Steady state surface current magnitudes at 925MHz for the GSM-900 PIFA
- Figure 4.1 Return Loss for the designed GSM-900 PIFA antenna
- Figure 4.2 The simulated Input Impedance of the designed GSM-900 PIFA antenna
- Figure 4.3 3D radiation pattern for the designed GSM-900 PIFA antenna for  $\varphi=0$
- Figure 4.4 XY-plane radiation patterns for the designed GSM-900 PIFA antenna for  $\varphi=0$
- Figure 4.5 Steady state surface current magnitudes at 925MHz for the dual band PIFA
- Figure 4.6 Steady state surface current magnitudes at 1795MHz for the dual band PIFA
- Figure 4.7 Return Loss for the designed dual band PIFA antenna
- Figure 4.8 The simulated Input Impedance of the designed dual band PIFA antenna
- Figure 4.9 3D radiation pattern for the designed dual band PIFA antenna resonant at 925MHz for  $\varphi=0$
- Figure 4.10 3D radiation pattern for the designed dual band PIFA antenna resonant at 1795MHz for  $\varphi=0$
- Figure 4.11 XY- plane radiation patterns for the designed dual band PIFA antenna resonant at 925MHz for  $\varphi=0$

- Figure 4.12 XY-plane radiation patterns for the designed dual band PIFA antenna resonant at 1795MHz for  $\phi=0$
- Figure 5.1 Proper component layout for an optimised RF PCB design
- Figure 5.2 Effects of the soldermask coating on the PCB impedance
- Figure 5.3 Power pin to bypass capacitor
- Figure 5.4 Power pin to via to bypass Capacitor
- Figure 5.5 Minimum trace widths for 1oz copper for  $\Delta T = 10 \text{ }^{\circ}\text{C}$
- Figure 5.6 Representation of a signal propagation on a PCB trace
- Figure 5.7 Typical trace spacing
- Figure 5.8 3W spacing to minimize crosstalk
- Figure 5.9 Trace geometry of a sharp  $90^{\circ}$  corner
- Figure 5.10 An illustration of good and bad trace geometries
- Figure 5.11 Effect of a slotted ground plane on RF return current path
- Figure 5.12 RF PCB design with grounded via shield.
- Figure 5.13 Multilayer PCB stack-up
- Figure 5.14 Top layer of the designed multilayer stacking
- Figure 5.15 Layer 2(L2\_GND\_1) of the designed multilayer stacking
- Figure 5.16 Surface microstrip design equations
- Figure 5.17 Maximum and minimum trace width setting from the nets spreadsheet
- Figure 5.18 Complete PCB with the dual band PIFA antenna model ready for simulation
- Figure 5.19 Return Loss for the designed dual band PIFA antenna on a populated PCB board
- Figure 5.20 Simulated Input Impedance of the designed dual band PIFA antenna on a populated PCB board
- Figure 5.21 Antenna matching circuit

## LIST OF ACRONYMS

AADS	Agilent Advanced Design System
ADS	Advanced Design System
BGA	Ball Grid Array
dB	decibels
DCS	Digital Cellular Service
PCS	Personal Communications Service
UMTS	Universal Mobile Telecommunications System
EM	Electromagnetic waves
GSM	Global System for Mobile Communication
Hz	Hertz
HPBW	Half Power Beam Width
ITU	International Telecommunication Union
IFA	Inverted-F antenna
KHz	Kilo Hertz
MHz	Mega Hertz
PCB	Printed Circuit Board
PIFA	Printed Inverted F antenna
RF	Radio Frequency
RF MEMS	Radio frequency micro electro mechanical system
WLAN	Wireless Local Area Networks
VSWR	Voltage Standing Wave Ratio
TEM	Transverse Electromagnetic waves
LNA	Low Power Amplifier
PLF	Polarization Loss Factor
EMI	Electromagnetic Interference
EMC	Electromagnetic Compatibility
WiMAX	Worldwide Interoperability for Microwave Access

## LIST SYMBOLS

$\Omega$	Ohm
$\theta$	Elevation Plane angle
$\Pi$	Pi
$\varphi$	Azimuth plane angle
$\lambda$	wavelength
$\alpha$	Proportional sign
$\Gamma$	Reflection Coefficient

## ABSTRACT

The latest trend in handset design is slim smart phones that require small, thin, light weight and wideband multiband internal antennas. This trend poses two major challenges in designing a mobile device antenna: how to use a single antenna to cover all the required frequency bands and then how to make the same antenna small enough so that multiple antennas can be deployed within the same device. Although a printed Inverted-F antenna (PIFA) has been a suitable candidate due to its simple modeling and easier fabrication using a printed circuit board (PCB), it has a limitation of a narrow bandwidth characteristic. To address this issue and yet obtain multiband operations for GSM applications, this research presents the structural optimization of a PIFA antenna which is capacitively loaded with an inverted-L element. The antenna covers GSM-900 and GSM-1800. The results obtained show that the PIFL antenna lower and upper bandwidths determined at -10dB is over 110MHz and 500MHz respectively which covers the above mentioned bands very well with very low return losses of -30dB and -30dB at resonant frequencies 925MHz and 1.795GHz respectively.

In addition to this, a ground plane forms the other half for quarter wave PCB antennas. Integration of these type of antennas with other components within the same PCB of a mobile device compromise the uniformity and continuity of the ground plane due to the requirement for dense routing and component mounting to optimize the use of the limited PCB space available. This will not only detune the matching and introduce losses to the antenna, but also degrade the antenna's performance in terms of gain, bandwidth, efficiency and radiation pattern. Again, this research presents a case study of an optimized components placement and stacking, effective PCB partitioning, routing discipline combined with right selection of antenna location to achieve a successful integration of a PCB-PIFL antenna into a mixed multilayer PCB design, which provides improved continuity and uniformity of the antenna's co-planar ground plane, and the antenna's and improves the overall performance. The results obtained show that the lower and upper bandwidths determined at -10dB is over 60MHz and 130MHz with return losses of -30dB and -14dB at resonant frequencies 915MHz and 1.931GHz.

# CHAPTER 1

## INTRODUCTION

### 1.1 Background to the Research

Mobile communications, wireless interconnects, wireless local area networks (WLANs), and cellular phone technologies compose one of the most rapidly growing industrial markets today. All these applications require antennas.

Moreover, the mobile devices have been demanding antennas that are small, lightweight and compact. All these demands can be met by developing a low profile internal antenna with superior performance. This being the situation, portable antenna technology has all along grown with mobile and cellular technologies. Thus there is a great need for one to have a proper antenna for these devices. A proper antenna will improve transmission and reception, reduce power consumption, and improve marketability of these communication devices. However, designing a proper antenna is technically challenging due to the limited antenna volume and influence of the casing for these mobile devices.

Currently, modern mobile devices operate at a number of frequency bands, the most common being GSM-900 (850-960MHz), GSM-1800 (1710-1880MHz), GSM-2100 (1920-2170MHz) and ISM Band at 2400MHz. As these devices are becoming smaller, it is not feasible to simply equip the devices with an array of antennas, each tuned for a specific frequency band. This has resulted in a demand for antennas that can operate at multiple bands without the need for multiple antennas. Modification of the main radiator for an IFA has demonstrated an achievement in multi-band operation [3, 4].

### 1.2 Problem Statement

In the past, most mobile devices were equipped with the monopole antenna. Monopole antennas are simple in design and construction and are well suited for mobile communication applications. The most common  $\lambda/4$  monopole antenna is the whip antenna, which can operate at a range of frequencies and can deal with most environmental conditions better than other monopole antennas. The whip antenna operating at 800MHz was first utilized in the Motorola DynaTAC which happened to be the first commercially available cellular phone in 1983[8]. Although the monopole antenna provides an Omni-directional radiation pattern which is ideal for mobile devices, it poses a number of draw-backs; it is relatively large in size and protrudes from the handset case. This problem with the monopole's obstructive and space demanding structure also complicates any efforts taken to equip a device with several

antennas to achieve multi-band operation. Again monopole antennas also lack any built-in shielding mechanisms to direct any radiating waves away from the user's body, thus increasing the potential risk of producing cancerous tumors growth in the user's head and reducing its efficiency.

Research that was conducted on the monopole antenna in the 1990s concentrated on the developing methods to control the radiation pattern [9, 10] and also investigating the effects of users on the antenna performance [11].

Around mid-1990s, monopole antennas were replaced by helical antennas which were more compact. The helical antenna was utilized in mobile handsets like the Nokia 5510. However, when new telecommunications bands like GSM-1800 were introduced these helical antennas were modified for multi-band operation. [12, 13].

Mobile phone manufacturers begun to use patch antennas in the late 1990s, which due to their low profiles and small footprints, could be integrated internally within these devices. This move by the manufacturers provided two merits; a smaller handset size and the capability to design the antenna for directing less radiation towards a user's head [14, 15]. Since then patch antennas have become the most popular choice for mobile devices.

Later on, more additional telecommunication bands were introduced like the GSM-1900 and GSM-2100 and forced people to investigate on multi-band patch antennas [16, 17, 18, 19]. To capture this growing, diverse and promising market, the functionality of these devices was increased by incorporating additional systems like gyroscopes, accelerometers and magnetometers. This required the patch antenna to even have the smallest possible footprint and several methods were proposed to attain this goal [20, 21, 22].

There are a wide variety of methods being investigated to deal with the deficiencies of the common  $\lambda/4$  monopole antenna; many of these methods are based on micro strip antenna designs. One such promising design is the Inverted-F antenna, a derivative of the monopole. The inverted-F is a modified monopole and has a thin profile which allows for it to be placed next to components in a mobile device. It is well discussed in chapter 2.

### **1.3 Objectives**

The fundamental objective of this research work is to design a multi-band Inverted-F antenna that is suitable for mobile devices. In antenna designs, multi-band operation can be achieved by modification of the main radiator either by creating several radiators for different resonances from a single feeder or elongating the main radiator's physical length to achieve



multiple resonance modes. In this work creating several radiators is proposed and whereby longer radiators are elongated to meet the space constraints.

This research work has primarily the following objectives:

- i) To select and design an efficient and optimized, low-profile and realizable printed Inverted-F antenna that is capable of operating at a number of frequencies bands GSM-900 (850-960MHz) and GSM-1800 (1710-1880MHz).
- ii) To verify the operation of this antenna at the prescribed frequencies in terms of the input impedance, reflection coefficient, field patterns, return loss using the antenna design software, Agilent Advanced Design System (AADS).
- iii) To evaluate the performance of this antenna in the presence of active components.
- iv) To evaluate tuning methods of this antenna in the presence of active components.

#### **1.4 Scope of the research work**

This research work will contribute in the following areas;

- i) Design and selection of a suitable low profile, multi-band antenna for mobile devices.
- ii) Design and optimization a multi-band Inverted-F antenna for mobile devices.
- iii) Simulation of antenna design using an electromagnetic simulation software
- iv) Testing and tuning of the designed antenna in the presence of active components.

#### **1.5 Organization of the research work**

The research begins with a review of antenna theory in Chapter 2 which is followed by a description of the inverted-F antenna and past research works of this type of antenna. The parameters that control the different radiation characteristics of the PIFA are discussed and a design methodology outlined. Various strategies employed to achieve multi-band operation are also discussed.

Using the design methodology presented in Chapter 2, a design for a multi-band PIFA for the GSM frequency bands (900MHz and 1800MHz) is presented in Chapter 3.

The designed multiband PIFA is simulated using the Agilent Advanced Design System software (AADS) and results presented in Chapter 4.

Chapter 5 presents the results obtained when the antenna is tested and tuned in the presence of components.

The conclusion of the research work and suggestions for further work are made in Chapter 6.

## CHAPTER 2

### LITERATURE REVIEW

#### 2.1 Antenna Theory

An antenna can be defined as a metallic device which radiates and receives electromagnetic waves (EM), more specifically radio waves [23]. It can also be defined as a transition between a guided EM wave and a free-space EM wave, and vice versa [24]. This process can be elaborated by a general communication between a transmitting antenna and a receiving antenna as shown in the figure 2.1.

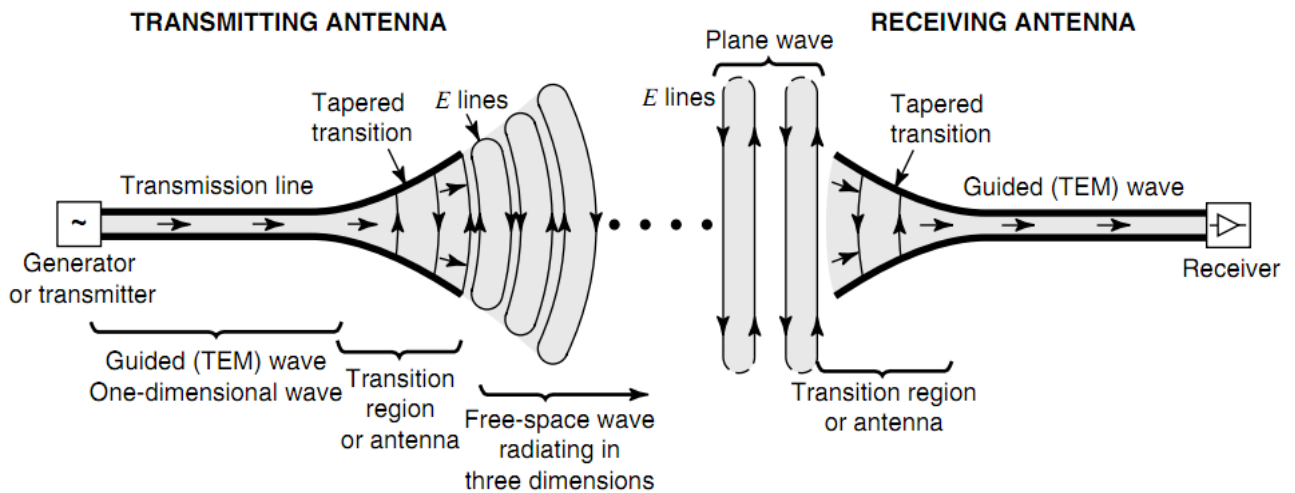


Figure 2.1 –An antenna as a transition structure for both a receiving and transmitting EM waves [25]

As shown above, for both antennas, the transmission line has the form of a coaxial line or a waveguide. The latter, when a transmitting antenna is considered, is connected to a transmitter that generates radio-frequency (RF) energy that is guided through the uniform part of the line as a plane TEM wave with little loss, transformed into a signal that is amplified, modulated and applied to the antenna. Otherwise, when a receiving antenna is considered, the transmission line is connected to the receiver which collects the alternating currents that resulted from the transformation process of the received radio waves by the antenna. Thus we can also state that the antennas convert electrons to photons [25].

The antenna characteristics concerning radiation are basically the same regardless of the antenna type. Thus, if a time-changing current or acceleration (or deceleration) of charge occurs, the radiation will be created in a certain length of a current element. This is described in [23]:

$$\frac{L}{dt} \frac{dI}{dt} = l \cdot q \cdot \frac{dV}{dt} \text{ (A.m/s)}$$

2.1

Where:

$L$  -length of the current element in meters (M)

$\frac{dI}{dt}$  – Time-changing current in ampere per second (A/s)

$q$  -Elementary charge in coulomb C or (A.s)

$$q = It = 1.602 \times 10^{-19}$$

$\frac{dV}{dt}$  -acceleration/deceleration

Moreover, the radiation is always perpendicular to the acceleration and its power is proportional to the square of both parts of equation 2.1. It is also important to mention that the spacing between the two wires of the transition line is just a small part of a wavelength, therefore, the more the transition curve of the antenna opens out the more the order of the wavelength is reached; consequently the more the wave tends to be radiated and launched into free space [25]. Looking at the antenna structure as a whole, the transition region of the antenna is like a radiating resistance ( $R_r$ ) to the transmission line point of view, which represents the radiation that the antenna emits, analyzing it as a circuit of an antenna. Fig.2.2 shows a complete circuit of an antenna; where the source is the ideal generator with tension  $V_g$  and with an impedance  $Z_g$ ; the transmission line has a characteristic impedance  $Z_c$  or  $Z_o$ , and the antenna itself is represented by a load impedance  $Z_A$  that works as an input impedance whose process will be explained later on in this chapter. Therefore, if ideal conditions are applied, the radiation resistance will get all the energy that is generated by the transmitter.

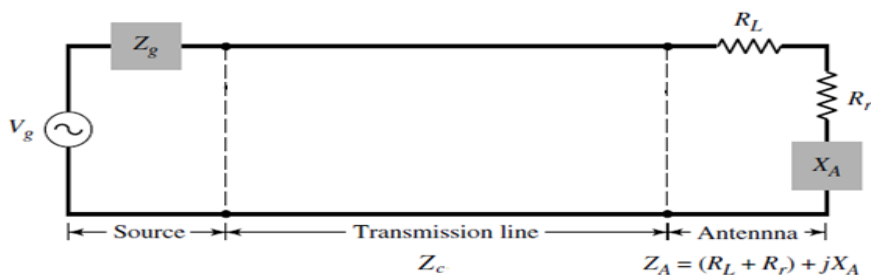


Figure 2.2- A circuit representing an antenna as a whole structure [23]

## 2.2 Radio Frequency

Electromagnetic waves (EM) can be defined as a type of electromagnetic radiation organized according to the frequency (f) of its waves. Frequency (f) counts the number of

incidences that a repetition of an event occurs per unit time. Its SI unit is Hertz (Hz) which means the number of cycles per second. Each cycle is also mentioned as a period (T). Therefore, frequency (f) is the reciprocal of period:

$$f = 1/T \tag{2.2}$$

Wavelength ( $\lambda$ ), is another very important parameter, which is the distance between two consecutive points on the same phase. It is given in meters (M) and is defined as:

$$\lambda = C/f \tag{2.3}$$

Where C is the speed of light in free space ( $3.0 \times 10^8$  m/s)

Figure 2.3 shows the plot of wavelength and whereas Figure 2.4 depicts the difference between highest and lowest frequencies.

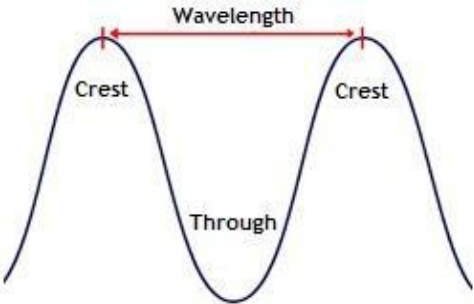


Figure 2.3- wavelength measurements [26]

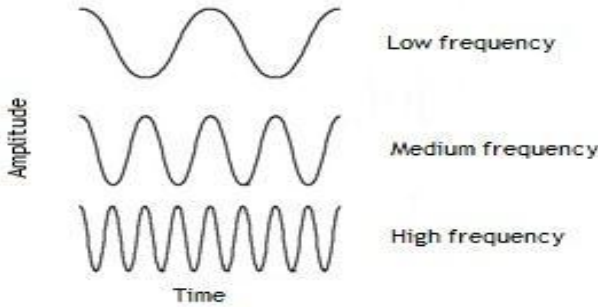


Figure 2.4-Frequency qualities [26]

The electromagnetic spectrum (Figure 2.5) is a diagram that covers a wide range of frequencies of electromagnetic radiation such as: radio, microwave, infrared, visible light, ultraviolet, x-ray, and Gamma rays. Radio waves have the lowest frequency and the highest wavelength, while for the Gamma rays is the opposite. Consequently, the level of energy is higher for the highest frequencies.

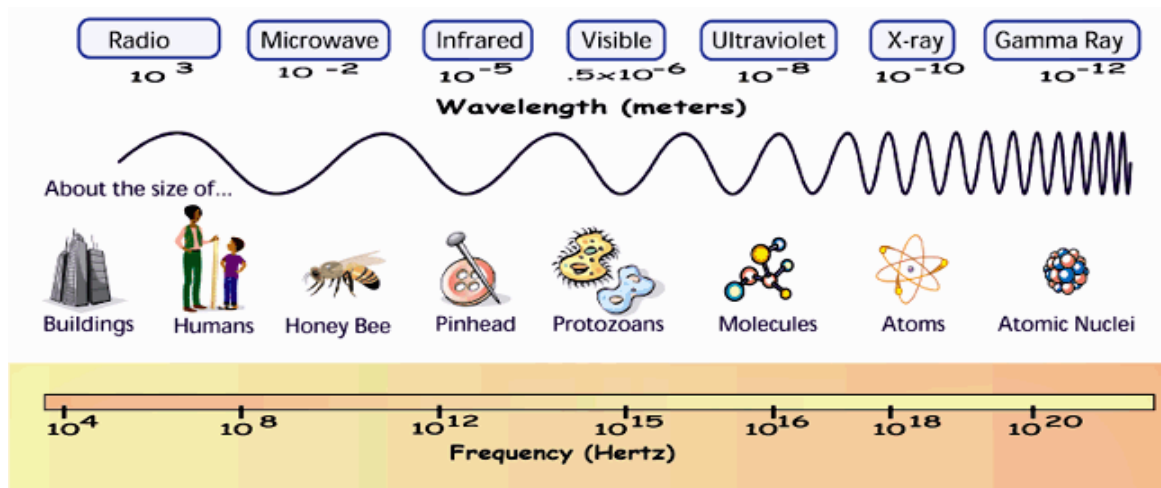


Figure 2.5-The size of the EM spectrum [26]

As shown above, the electromagnetic spectrum is divided into different frequency ranges. For the purpose of this research work, the radio spectrum is the one used. For telecommunications, International Telecommunications Union (ITU), is an entity which regulates the frequency spectrum usage, and determined that the usage spectrum is 3Hz to 300GHz. Meanwhile, radio-frequency (RF) varies in a range of 30 KHz to 300GHz, values for which radio waves start to be emitted in practice.

Radio Spectrum	Frequency	Wavelength
extremely low frequency(ELF)	3Hz to 30Hz	100'000km to 10'000 km
Super low frequency(SLF)	30Hz to 300Hz	10'000km to 1'000km
Ultra low frequency(ULF)	300Hz to 3000Hz	1'000km to 100km
very low frequency(VLF)	3kHz to 30kHz	100km to 10km
low frequency(LF)	30kHz to 300kHz	10km to 1km
medium frequency(MF)	300kHz to 3000kHz	1km to 100m
high frequency(HF)	3MHz to 30MHz	100m to 10m
very high frequency(VHF)	30MHz to 300MHz	10m to 1m
<b>Ultra high frequency(UHF)</b>	<b>300MHz to 3000MHz</b>	<b>1m to 10cm</b>
Super high frequency(SHF)	3GHz to 30GHz	10cm to 1cm
Extremely high frequency(EHF)	30GHz to 300GHz	1cm to 1mm

Table 2.1-Radio spectrum band [27]

Table 2.1 describes the radio spectrum ranges for frequency and wavelength [27] and the highlighted radio spectrum band (UHF) is the one of interest in this research work.

## 2.3 Antenna parameters

There are several parameters that should be considered when choosing an antenna for a wireless device. Some of the most important things to consider are how the radiation varies in the different directions around the antenna, how efficient the antenna is, the bandwidth over which the antenna has the desired performance and the antenna matching for maximum power transfer. And since all the antennas require some space on the PCB, the choice of antenna is often a tradeoff between cost, size and performance [39].

### 2.3.1 Radiation pattern

This is a graphical (three-dimensional or two-dimensional) or a mathematical illustration of the radiation properties of an antenna as function of the space coordinates defined by the spherical coordinates  $\varphi$  and  $\theta$ , as shown in figure 2.6.

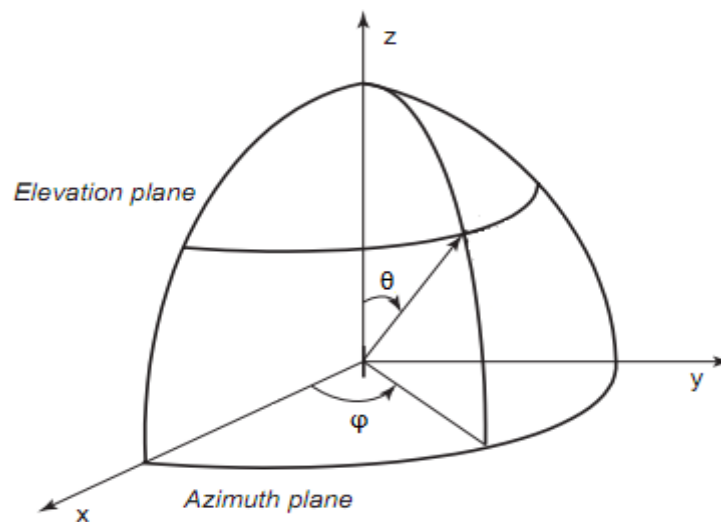


Figure 2.6 - Spherical coordinate system which describes the radiation pattern (adapted from [39])

More specifically, the radiation pattern gives the power that is radiated or received by a transmitting antenna or by a receiving antenna, respectively using the angular distribution already referred. That power can vary depending on the direction of radiation, and is measured far away from the antenna terminals. This radiation pattern can be described in three ways namely:

*Isotropic pattern*-this is evident for an antenna radiating with the same power in all directions. This means too that the antenna is lossless, but in reality they do not exist, though they are only used as a working reference.

*Directional pattern*-occurs when an antenna radiates into one or some directions more power than in other directions. Thus it means that those directions will be preferred for the waves to radiate. Due to the asymmetry of radiation, the pattern will vary only with  $\theta$  (elevation plane), and constant for  $\phi$  (Azimuth plane). An example of the three-dimensional pattern is given in Figure 2.8, and the respective polar diagrams are shown in Figure 2.7 and Figure 2.9.

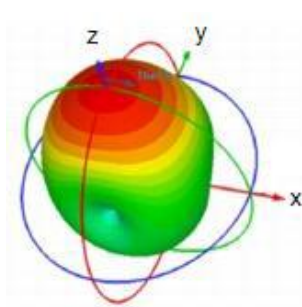


Figure 2.8-three dimensional radiation pattern [27]

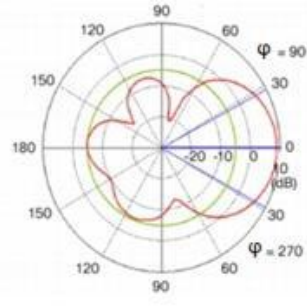


Figure 2.7- Polar diagram of the azimuth plane radiation pattern [27]

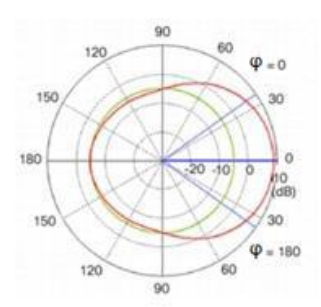


Figure 2.9-Polar diagram of directional elevation plane radiation pattern [27]

*Omni-directional pattern*-this occurs when the radiated power is the same along a given plane, therefore constant, thus concentrating the variation of its pattern along the other plane. An example of the three-dimensional pattern is given in Figure 2.11, and the respective polar diagrams are shown in Figure 2.10 and Figure 2.12.

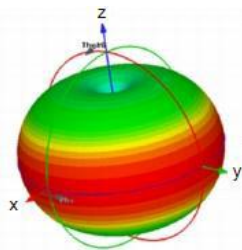


Figure 2.11-Three dimensional directional radiation pattern [27]

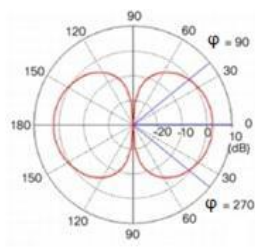


Figure 2.10-Polar-diagram of the azimuth plane radiation pattern [27]

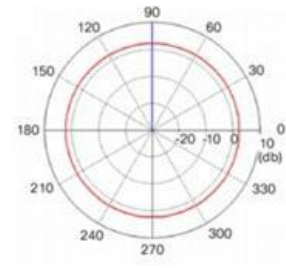


Figure 2.12-Polar-diagram of Omni-elevation plane pattern [27]

From Figure 2.8, it can be deduced that the pattern radiates through the Z-axis; consequently the polar diagrams of Figure 2.7 shows that for the x-y plane (variation of  $\phi$ ) there is no specific direction of radiation, in contrast with the polar diagram of Figure 2.9 which shows that there is a preferred direction of radiation. Also from Figure 2.11, one can ascertain that the radiated power is uniform despite the variation and rotation of angle  $\phi$ ; therefore the variation of angle  $\theta$  forms a directional pattern, in contrast to the Omni-directional pattern of the azimuth plane.

Evaluating the respective polar diagrams, it is easy to see that Figure 2.10 creates a uniform polar radiation and Figure 2.12 doesn't. Finally, both of the three-dimensional

graphics are described by colors around its curves; the red represents the peak powers; the yellow refers to intermediate power; and the green represents the lowest powers.

The radiation pattern of an antenna is also characterized by its lobes (or beams). The part concentrating more radiation is called the *main lobe*. All the other lobes are called minor lobes, but some of them can have a more specific name. When some lobe also radiates in other directions (though in a second plane) than the main lobe is called a *side lobe*. There are also back lobes which make an angle of approximately  $180^\circ$  to main beam. Detailed description of the radiation pattern lobes are shown in a partial polar plot (Figure 2.13) [39].

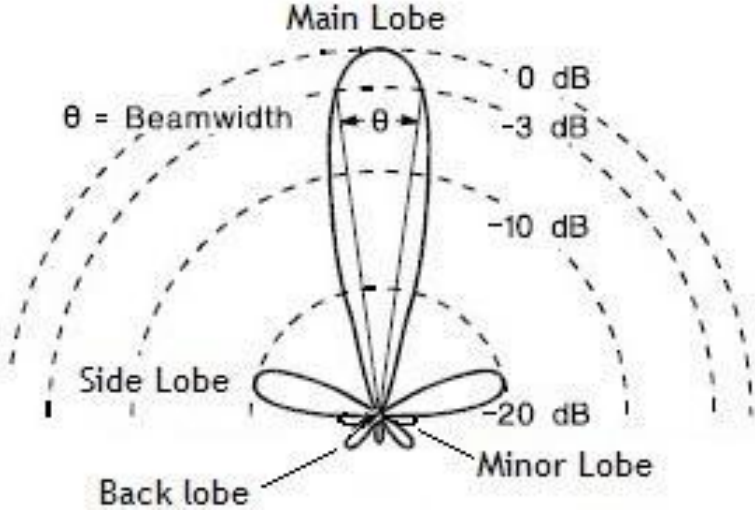


Figure 2.13-Radiation pattern lobes [39]

### 2.3.2 Half Power Beam Width (HPBW)

This is a measure that illustrates the quality of the main beam radiation i.e., if two points of the main beam are defined as the points where the power of the radiation pattern decreases by one half (3dB) from its peak, then the angular distance between these points will give the HPBW. This is depicted in the figures below.



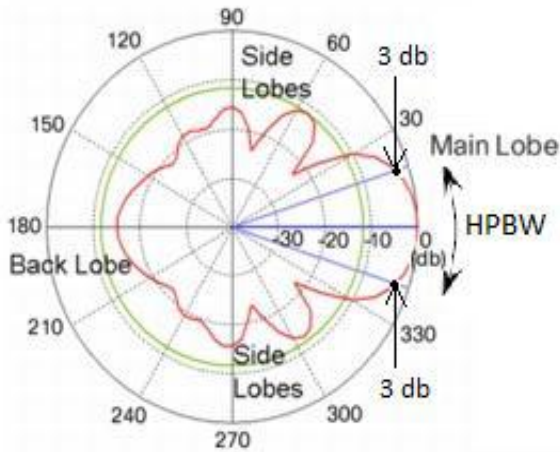


Figure 2.14-Polar diagram of HPBW [27]

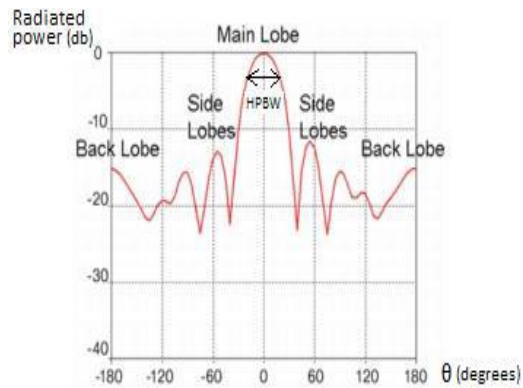


Figure 2.15-Rectangular diagram of HPBW [27]

### 2.3.3 Directivity (D)

This is a quantity indicating how powerful is the radiation of an antenna in a specific direction in relation to the radiated power of an isotropic reference. Thus it is possible to evaluate if the concentration of the emitted power will be higher or smaller than that of the average radiated power in all directions of the antenna. Analytically this can be defined as;

$$D = \frac{U}{U_0} \frac{4\pi U}{P_{rad}} \quad 2.4$$

Where;

$D$ -Directivity

$U$ -Concentration of radiated power in a specific direction

$U_0$ -Concentration of radiated power of an isotropic antenna reference

$P_{rad}$ -Total radiated power

And

$$U_0 = \frac{P_{rad}}{4\pi} \quad 2.5$$

If there is no directivity ( $D=1$ ) in a specific direction, it means that the radiated power will be distributed uniformly in all directions; therefore similarly to the referred isotropic reference. Otherwise there will be directivity in a given specific direction if the concentration of the power radiated in that direction is larger than that of the isotropic reference ( $D>1$ ). This case implies the directivity will increase with the concentration of power in that direction, thus increasing the gain and decreasing the HPBW [31].

### 2.3.4 Gain (G)

This quantity is expressed as a ratio of the power radiated by the antenna in a particular direction, to the power that could be radiated if the antenna was radiating isotropically, emitting the total forward accepted power (at the input terminals) instead of the total radiated power (at the output terminals), as in directivity. This forward power is also divided by a term  $4\pi$ . Therefore, while in directivity a lossless antenna is implicit; in gain the losses are considered. This is called absolute gain, and is given by the formula below [31].

$$G_{abs} = \frac{U}{U_0} = \frac{4\pi U}{P_{in}} \quad 2.6$$

Where:

$G_{abs}$  -Gain of the antenna

$U$  -Power radiated in a given direction

$U_0$ - Power that would radiate isotropically

$P_{in}$  –Forward accepted (input) power

This means, that when the gain is higher than one, the power radiated in the far field will always be higher than the supposed power radiated isotropically. The absolute gain can also be specified in *dBi* units as:

$$G_{dBi} = 10.\log (G_{abs}) \quad 2.7$$

Where;

$G_{dBi}$  -Gain in *dBi*

Sometimes, instead of the absolute gain, it is given in reference to the relative gain; the equation is basically the same, but now  $P_{in}$  is defined as the power radiated by a reference antenna (or by a main lobe) in its specified direction. In this case the gain is given in dB:

$$G_{dB} = 10.\log (G_{rel}) \quad 2.8$$

Where:

$G_{dB}$  -Gain in dB

$G_{rel}$  –relative Gain

The relative Gain can also be referred to that of a half- wavelength dipole antenna that serves as a reference; in that case, it means that  $0 \text{ dBd} = 2.15 \text{ dBi}$ . Usually, that kind of

antenna work in a range less than 1GHz and it is the simplest antennas with the least gain of all antennas.

The relationship between Gain and Directivity is given by:

$$G = \epsilon_r D \quad 2.9$$

Where:

$G$ -Relative Gain or Absolute Gain

$\epsilon_r$  -Antenna radiation efficiency

$D$  -Directivity

The radiation efficiency comes as:

$$\epsilon_r = \frac{P_{rad}}{P_{in}} \quad 2.10$$

Where:

$P_{rad}$ - Total radiated power

Thus, the radiation efficiency parameter ( $\epsilon_r$ ) gives an idea of how much power is radiated by an antenna when compared to the power that was delivered to the input terminals. The bigger the radiation efficiency, the bigger is the Gain and smaller is the Directivity [31].

### 2.3.5 Efficiency ( $e_o$ )

Antenna efficiency is a parameter that measures the losses at input terminals of an antenna. As explained above,  $P_{in}$  is the total power of an antenna at its input terminals and is defined by:

$$P_{in} = P_{rad} + P_{losses} \quad 2.11$$

Where:

$P_{losses}$ -Power that an antenna loses while the EM waves are being transported to its output terminals. Therefore, only the power  $P_{rad}$  will be radiated.

Thus, the antenna total efficiency can be calculated as:

$$e_o = \epsilon_r \epsilon_r \quad 2.12$$

Where:

$e_o$  -Antenna total efficiency

$\epsilon_r$ -Antenna radiation efficiency

$e_r$ -Reflection efficiency, which is given

$$e_r = 1 - |\Gamma|^2 \quad 2.13$$

The efficiency plays an important role in the classification of antenna gain [31].

### 2.3.6 Scattering Parameters (S-Parameters)

This is a very useful system used to characterize the incident and reflected waves in a linear two-port structure. The figure below shows the respective network:

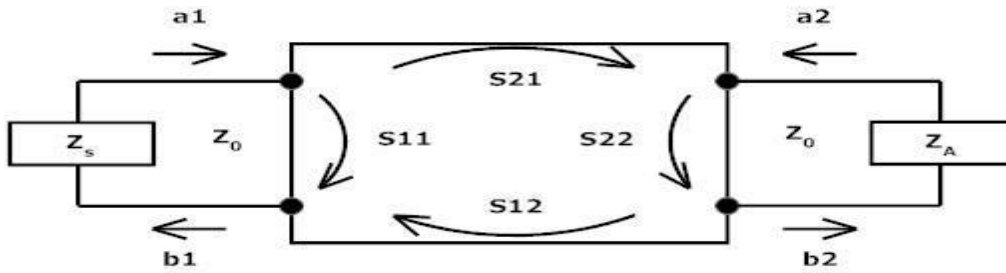


Figure 2.16- Two port network constituted by S-Parameters [31]

The S-parameters are defined as follows:

$$S_{11} = \frac{b_1}{a_1} | a_2 = 0 \quad 2.14$$

$$S_{22} = \frac{b_2}{a_2} | a_1 = 0 \quad 2.15$$

$$S_{21} = \frac{b_2}{a_1} | a_2 = 0 \quad 2.16$$

$$S_{12} = \frac{b_1}{a_2} | a_1 = 0 \quad 2.17$$

Where:

$S_{11}$ -Input reflection coefficient

$S_{22}$ -output reflection coefficient

$S_{21}$ -Forward transmission gain

$S_{12}$ -Reverse transmission gain

$a_1$ -Wave of incident power on the input of the network

$a_2$ -Wave of incident power on the output of the network

$b_1$ -Wave of reflected power from the input of the network

$b_2$ -Wave of reflected power from the output of the network

An antenna can be considered as a one port network and thus only  $S_{11}$  is applicable to it. The reflection coefficient of a network as a whole is defined as the ratio of the amplitude of

the reflected wave to the amplitude of the incident wave. Although, when applied to the transmission line, it comes as:

$$\Gamma = \frac{Z_A - Z_o}{Z_A + Z_o}, \quad -1 \leq \Gamma \leq 1 \quad 2.18$$

Where:

$\Gamma$ -Reflection coefficient

$Z_A$  -Load Impedance

$Z_o$  -Transmission line impedance

For  $\Gamma=1$ ,  $Z_A$  is infinite and there is an open-circuit; otherwise, for  $\Gamma=-1$ ,  $Z_A$  is zero and there is a short circuit. A perfect situation occurs for  $\Gamma=0$  where there are no reflections from the transmission line and subsequently the maximum amount of power is provided to the load. Applying the reflection coefficient formula to  $S_{11}$ , the load will be now given by the input of the network, so the input reflection coefficient comes as:

$$\Gamma_{in} = S_{11} = \frac{Z_1 - Z_o}{Z_1 + Z_o} \quad 2.19$$

Where:

$\Gamma_{in}$ -Input Reflection coefficient

$Z_1$  -Input impedance of port 1

Return Loss ( $R_L$ ) is the parameter used to measure the ratio of both  $S_{11}$  and  $S_{22}$  in dB depending on the port. The Return Loss for  $S_{11}$  is given by:

$$R_{L\text{ dB}} = -20 \cdot \log |S_{11}| \quad 2.20$$

Where:

$|S_{11}|$  -Magnitude of  $S_{11}$

$R_{L\text{ dB}}$  -Return loss in dB

Usually  $R_L$  is a negative number; the more negative  $R_L$  is, the more power is delivered to the load and less is reflected. Thus this indicates that the source and the characteristic impedances are matched to the load. The Smith Charts are a way to represent  $R_{L\text{ dB}}$ . But fortunately, vector network analyzers plot them in a way to find the matching between transmission lines and loads of antennas.

### 2.3.7 Voltage Standing Wave Ratio (VSWR)

VSWR measures the matching between an antenna and a transmission line. It essentially states the power that an antenna will get from a transmission line in order to be able to radiate as much as possible of that received power. VSWR is calculated as the ratio of the maximum amplitude to the minimum amplitude of the voltage of a standing wave:

$$VSWR = \frac{V_{max}}{V_{min}} \quad 2.21$$

Where:

$V_{max}$ -Maximum amplitude of a standing wave in volts (V)

$V_{min}$ -Minimum amplitude of a standing wave in volts (V)

VSWR can also be defined by the following equation

$$VSWR = \frac{1+|\Gamma|}{1-|\Gamma|}, -1 \leq \Gamma \leq 1 \text{ and } VSWR \geq 1 \quad 2.22$$

Where:

$|\Gamma|$ -Magnitude of the reflection coefficient

Since  $S_{11}$  is also a reflection coefficient,  $VSWR$  can also be given by:

$$VSWR = \frac{1+|S_{11}|}{1-|S_{11}|} \quad 2.23$$

A good value for  $VSWR$ (low value) means that the antenna is well matched, and subsequently the amount of power that the antenna receives from the transmission line is very satisfactory; otherwise, a high  $VSWR$  value means that an antenna is mismatched, and then the loss of power delivered to the antenna will be very high. In this case the antenna will not radiate power, once the wave is reflected back and will not approach the antenna terminals [40].

Technically speaking, VSWR is always greater than or equal to one. A great matching can be found in a bandwidth of 2:1, and an ideal matching is given by 1:1 VSWR, where there is no reflected power.

### 2.3.8 Polarisation

When an antenna radiates EM waves in a certain direction at any point in the far field, its characterisation is given by a figure that traces out the magnitude of the electric field vector along the propagation time. This property is called polarisation. Basically, it can be described as a measure of how the EM waves are orientated along its emission. If a polarisation is not settled, one can assume that the direction of the maximum gain will also be

the one for the polarisation [40]. There are three types of polarisation: *linear polarisation*, *circular polarisation* and *elliptical polarisation*.

The linear polarisation is due to the linearity of the electric field vector. When the latter at a certain point in the far field is always described by a line travelling in a single direction as a function of time, it means that its polarisation is linear. On the other hand, the antenna can be horizontally or vertically polarised when linearly polarised, depending on how oriented the field is in order to the ground. Take note that for different types of linear polarisation, different antennas are not able to communicate. Concerning to the circular polarisation, its characteristics are part of an antenna if the electric field vector outlines a circle as a function of time at a certain point in the far field. Lastly, the elliptical polarisation describes an antenna when its electric field vector at a far field point is such that it traces elliptical curves constantly with time [40]. Moreover, both the circular and elliptical polarisations are characterised for being right-hand (RH) or left-hand (LH) polarised, depending on the sense of the field; if the field is flowing in the clockwise direction, the field will be right hand polarised; otherwise it will be left hand polarised.

### 2.3.9 Input Impedance

The input impedance of an antenna is the measure that establishes the ratio of the voltage to the current at its input terminals. Basically, those terminals are a transition between the transformation of the electric current produced by the transmitter and the EM waves that will be radiated, work as a load to the transmission line; therefore, the input impedance is a characteristic that describes and gives an idea of how powerful the radiation will be, once it is possible to calculate the maximum power that is transmitted to the antenna before emitting the EM waves. The general expression of input impedance is given by [40]:

$$Z_{in} = R_A + jX_A \quad 2.24$$

Where:

$Z_{in}$ -Input impedance in Ohms ( $\Omega$ )

$R_A$  -Antenna resistance in Ohms ( $\Omega$ )

$X_A$ -Antenna reactance in Ohms ( $\Omega$ )

All these values are pointed to the input terminals of the antenna.  $R_A$  Is given by:

$$R_A = R_L + R_r \quad 2.25$$

Where:

$R_L$  -Loss resistance in Ohms ( $\Omega$ )

### $R_r$ -Radiation resistance in Ohms ( $\Omega$ )

As shown above, input impedance is the sum of a real number and of an imaginary number. The first specifies the power that antenna radiates or the power that antenna takes in, while the imaginary part specifies the power that is not radiated by the antenna, thus retained not far away from its terminals.

For lower frequencies (higher wavelengths) the length of the transmission line is not significant when compared to wavelength, so the result is a short line. Although for higher frequencies where the transmission line is slightly a big fraction of a wavelength, it can be a problem because the input impedance will be influenced in a large scale by the length of the transmission line. Therefore, the term impedance matching becomes important, because in this case the length of a transmission line is not significant when compared to the wavelength. The input impedance of an antenna will be matched with a transmission line if both impedances are the same ( $Z_A = Z_o$ ). The matching is measured by a parameter called VSWR discussed above. If an antenna is mismatched, the loss of power can be very high, because the power generated by the source will be reflected back. As a measure related with power, input impedance is a crucial quantity for the power that an antenna will receive. Thus, as a definition, a maximum power will be delivered from the source to the antenna, if the input impedance is equal to the conjugate of the impedance generated by the source  $Z_A = Z_s^*$ . Therefore no power will be transmitted when  $Z_A$  or superior than  $Z_s$ . The figure below illustrates this.

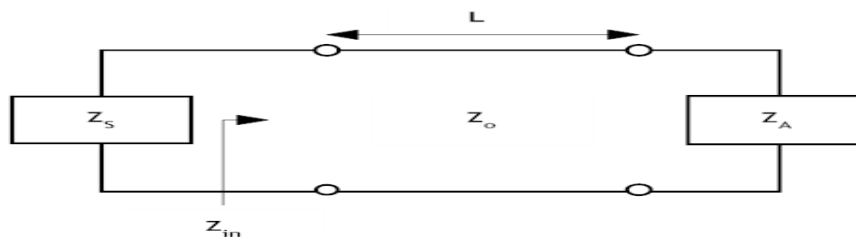


Figure 2.17-Circuit representing input impedance at the entrance terminals of the transmission line [31]

### 2.3.10 Bandwidth

The term bandwidth specifies the range of frequencies which an antenna can achieve, in order to obtain a desirable behaviour of a certain characteristic. It is classified as the first required condition before building an antenna, because it is a measure of how acceptable the performance of an antenna can be. However, as a range, two boundaries define the lower and upper frequency limits, and the ratio of its size to the centre frequency as a percentage define



the percent bandwidth for a narrowband antenna – thus occupying a small space quantity on the RF spectrum, given by the equation 2.26, otherwise, for a broadband (or wideband) antenna the bandwidth is defined as the ratio of the upper to lower frequencies as written in equation (2.27). Both expressions are analytically represented as [24, 25, 31]:

$$B_f = \frac{f_H - f_L}{f_c} \times 100 \quad 2.26$$

$$B_r = \frac{f_H}{f_L} \quad 2.27$$

Where:

$B_f$ -Fractional bandwidth in Hz

$B_r$ -Bandwidth ratio

$f_L$ -Lower frequency in Hz

$f_H$ -Upper frequency in Hz

$f_c$ -Centre frequency in Hz

### 2.3.11 Reciprocity

It is the principle which states that an antenna may send or receive EM waves in an equal manner. That is, the characteristics of an antenna must remain the same while receiving or radiating. Thus, reciprocity can also be measured by analysing the radiation pattern of an antenna, which again, may look the same while transmitting or receiving RF waves. S-parameters are also a notable case of reciprocity [31].

### 2.4 Printed Inverted-F antenna (PIFA)

PIFA is a type of embedded antenna widely used in mobile devices. In the past decade, the PIFA has been used extensively in wireless communication devices operating in the frequency bands for Wireless Local Area Network (WLAN) and Worldwide Interoperability for Microwave Access (WiMAX) and 5GHz. The PIFA is well-suited for these applications because its physical size complies with the dimensions of the intended wireless devices. Besides, the antenna itself provides good gain and radiation efficiency. However, at lower frequencies, such as the telecommunication bands investigated in this research, the physical size of the PIFA is relatively larger and may not always be ideal for fitting on a handset. Fortunately miniaturization techniques such as meandering [30] are used to obtain an acceptably sized antenna.

The F-antenna can be thought of as a tilted whip, where impedance matching is accomplished by tapping the antenna at the appropriate impedance point along its width. The figure below depicts a layout of a PIFA antenna.

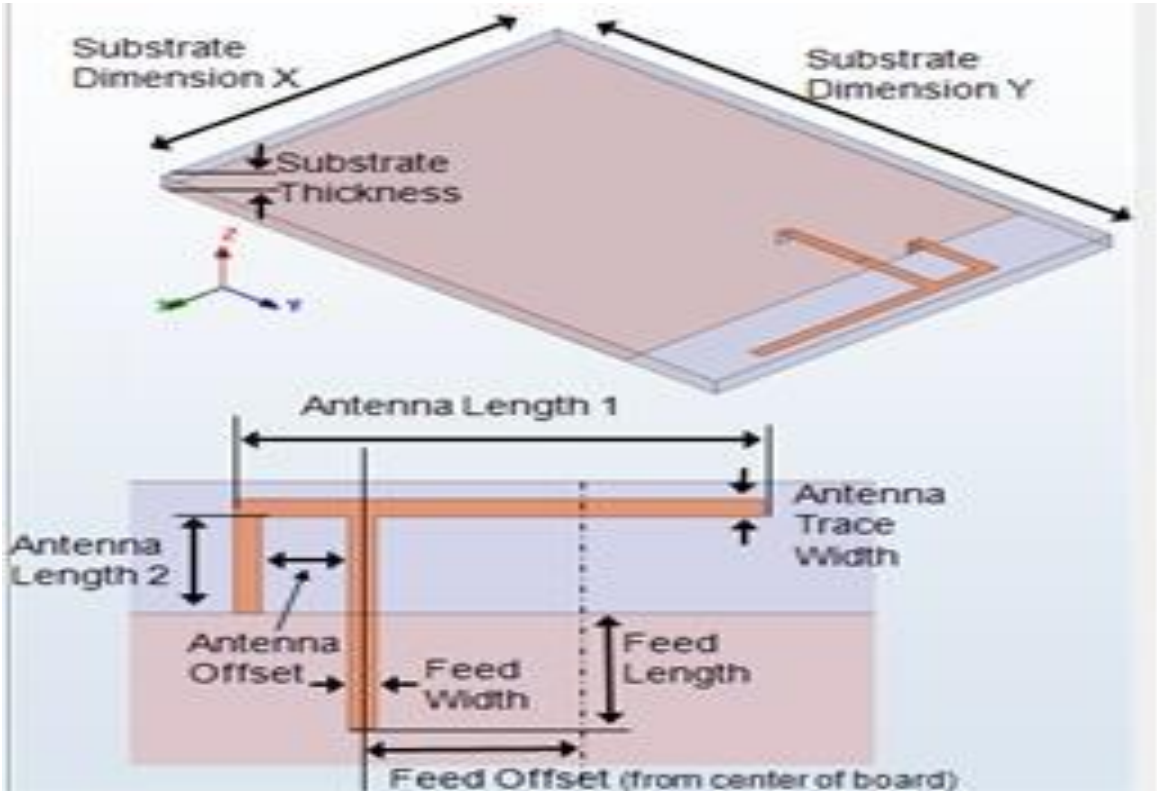


Figure 2.18: PIFA Antenna Layout [31]

The Printed Inverted-F Antenna (PIFA) consists of a main radiating arm that is bent to become parallel with a ground plane. It also has a shorting arm that is added to control its input impedance [31].

**2.5 PIFA Antenna Literature Review**

From the many antenna types that can be incorporated within mobile devices the PIFA antenna has proved to be the best candidate and below is a review of past research works on various techniques employed to achieve optimal performance.

**2.5.1 Bandwidth Enhancement**

One of the major limitations of a PIFA antenna shown in figure 2.19 is its narrow bandwidth but various techniques to improve it are outlined as follows:

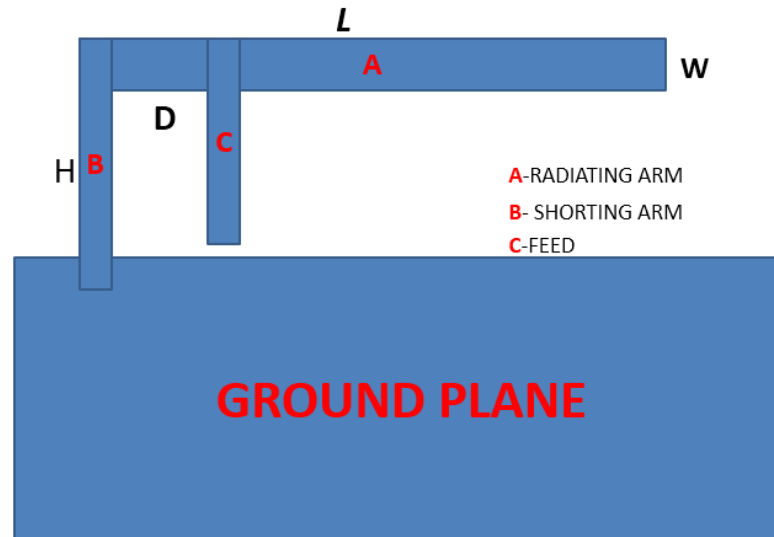


Figure 2.19: PIFA antenna structure

Where:

H-height of the PIFA antenna

D-Gap between the feed of the PIFA antenna and the shorting arm

L-length of the PIFA antenna

W-Width of the radiating arm of the PIFA antenna

**ERIK ÖJEFORS** in [41] suggested that the important design parameters of a PIFA are the height of the PIFA (H), the length of the PIFA (L) and the position of the feed point relative to the ground connection of the radiator (D). Generally, a large distance H from the ground plane is desirable to maximize the radiation resistance and bandwidth of the radiator. A height of 0.8mm was used and the measured results were as follows: a return loss of -16dB at 2.4GHz and the -10dB bandwidth was 2GHz and the measured gain was -0.7dBi that indicated more than 50% efficiency.

**Iulian Rosu** in [42] proposed that the dimensions of a PIFA antenna structure for optimal performance are as follows:  $L=\lambda/4$ ,  $W= \lambda/40$  and  $H= \lambda/14$ . Where H is the height of the PIFA, L is the length of the PIFA and W is the width of the radiating arm. All these combined with a ground of length  $\lambda/4$  even tuning becomes easier.

**C. Soras** in [43] suggested that the bandwidth of a PIFA antenna is directly proportional to the width of the radiating arm of the antenna (W). With a width (W) of 1mm and the antenna tuned at 2.4GHz a bandwidth of 250MHz was obtained.

**Abu Naim Rakib Ahmed** in [44] suggested a triple inverted PIFA operating between the wide frequency ranges 4.75-8.2 GHz, where an I-shaped slot is inserted in between two

IFAs. The width of the I-shaped slot is 4mm and the area covered by this antenna is  $12 \times 20 \text{ mm}^2$ . The proposed antenna provides a small size with a large bandwidth of 3.5GHz (4750-8250MHz) and it also ensures a nearly Omni-directional radiation patterns with peak gain 6.27/5.37/4.47 dBi across the operating bandwidth respectively.

### 2.5.2 Multiband Operation

With the many telecommunication bands introduced, it is of great need for mobile devices to be equipped with antennas that support multiband operation. One of my research objectives considers designing a multiband antenna. Below are various techniques employed to enable a PIFA antenna support multiband operation.

**Ahmad Rashid Razali** in [45] proposed that there are two main considerations that govern planar antenna designs; *antenna miniaturization techniques* and *multiband operation*. Multiband operation can be achieved by using three strategies:

#### A) Modification of the main radiator

- i) *Multi-branching* which involves creating several radiators for different resonances from a single feed. These branches are of monopole strips or arms to create different paths for different resonances. This technique allows the excitation of multiple resonant frequencies at their fundamental mode. *Multi-stacking* or *multi-layering* is another technique that offers similar operation as multi-branching technique. However, creating several radiating branches may occupy more space, hence making the antenna physically larger than the desired volume. For this reason, while designing a multiband antenna, the designers must also apply miniaturization approaches like meandering, wrapping, bending and folding [44].
- ii) Elongating the main radiator's physical length to achieve multiple resonant modes without diminishing the antenna's compact feature through *spiraling*, *looping*, *folding into a 3-D geometry* and *bending* [44].
- iii) *Notch Geometry*-a multi-resonator configuration is also achievable through proper application of some sort of slot or slit. In this approach, the radiator is modified in such a way that its original geometry is introduced with fine-tuned defined configuration of slots or slits. The resulting modification separates the main current stream into several other paths, which in turn creates different resonators. Also designs utilizing slots are not necessarily limited to straight lines or rectangular geometries, other shapes have also been proposed such as a

U-slotted PIFA, a V-slot loaded patch antenna, a Z-shaped slot antenna or an open –ended Rampant-slot antenna [44].

### **B) Modification of the ground plane**

Due to the advancement in RF transceivers, the space allocated for its radiating element has become smaller because of the increase in the number of new circuitry needed to provide data channeling.

Modification of the radiating element in a compact volume has been very challenging. Thus an alternative solution is a better utilization of its ground plane. Even though the geometry of the main radiating element plays a main role in determining the resonant frequency and other performances of the antenna, the importance of the ground plane as a natural complimentary agent to a radiating current must not be neglected. This modification includes *size variation, location of the radiating element within the ground plane area or inserting slots in the ground plane* [44].

Variation in a finite ground plane size and geometry affect the performance of an antenna. The resonant frequency of a conventional PIFA starts to converge to that of the case of an infinite ground plane when the size of the finite ground plane is increased above a unit wavelength.

With respect to the PIFA antenna the bandwidth increases with the length of the ground plane. It was demonstrated in [44] that the increased bandwidth, especially with respect to the lowest resonant frequency of operation is achieved with a longer ground plane.

Secondary radiators are formed by ground slots, which introduce new resonant frequencies or enhance the already existing ones. The feasibility of this approach to enhance an impedance bandwidth has been demonstrated for a PIFA [45, 46].

With proper tuning of slot parameters, new resonant frequencies can be generated to provide multiband operation or increase the bandwidth [47, 46]. This configuration requires ground slots to be in close proximity of the primary radiator to excite efficiently new resonances. A shortfall of such a configuration is a limited means for tuning the slot dimensions. Also the restricted slot locations may limit the antenna integration with the RF circuitry [48]

### **C) Reconfigurable Approach**

With multiband capability, reconfigurable antennas can utilize more efficiently the radio frequency spectrum, facilitating better access to wireless services in modern radio receivers. Reconfigurable antennas are generally divided into two main categories; *frequency tunable and pattern diversity antennas*. Furthermore, selection of electronic switches is of

paramount importance. Depending on the type of antennas, switches such as RF MEMS, varactors and PIN diodes can be used. The choice is governed by electrical specification, fabrication complexity, bias requirement, switching time and price [44].

## 2.6 Inferences drawn

The PIFA antenna has proved to be the best candidate to be incorporated within mobile devices because its physical size complies with the dimensions of the intended wireless devices and has a good gain and radiation efficiency. However, at lower frequencies such as 900MHz, the telecommunication band investigated in this research work, the physical size of the PIFA is relatively larger but fortunately, miniaturization techniques such as meandering, folding and capacitive loading can be employed to obtain an acceptably sized antenna.

The PIFA antenna can be directly printed on the PCB and hence no additional costs are incurred. This makes the manufacturing process easy. Its compact size, acceptable bandwidth, high efficiency and a good Omni-directional radiation pattern meets the many demands of many mobile devices.

The polarization of the PIFA antenna is rather elliptical than linear since the axial ratio rarely reaches 20dB. This makes it able to receive both vertically and horizontally polarized electromagnetic waves, which has proven beneficial in indoor environments where depolarization is a dominant phenomenon and the choice of the best polarization difficult.

Although the PIFA antenna suffers from a narrow bandwidth, techniques like designing a PIFA antenna with a height (H) roughly  $\lambda/14$  can greatly improve the bandwidth. Widening the PIFA width to be roughly  $\lambda/40$  can also improve the bandwidth. The bandwidth of the PIFA antenna increases with the length of the ground plane. A longer ground plane increases the bandwidth, especially with respect to the lowest frequency of operation.

The two main considerations governing the design of planar antennas are antenna miniaturization techniques and multiband operation. Multiband operation can be attained by using three strategies: *Modification of the PIFA's main radiator, modification of the PIFA's ground plane and using a reconfigurable antenna approach.*

For a PIFA antenna its ground plane plays a significant role in its operation. Excitation of currents in the PIFA antenna causes excitation of currents in the ground plane. The resulting electromagnetic field is formed by the interaction of the PIFA and an image of itself below the ground plane. Thus the antenna/ground plane combination will behave as an asymmetric dipole, the differences in current distribution on the two-dipole arms being responsible for some distortion of the radiation pattern.

Generally, the required PCB ground plane length is roughly  $\lambda/4$  in the direction of excitation currents. If the ground plane is much longer than  $\lambda/4$ , the radiation patterns become increasingly multi-lobed. On the other hand, if the ground plane is significantly smaller than  $\lambda/4$  then tuning the PIFA antenna becomes increasingly difficult and the overall antenna performance degrades. The optimal location of the PIFA antenna on the PCB in order to achieve an Omni-directional far-field pattern and a  $50\Omega$  impedance matching was found close to the edge of the PCB.

Introduction of slots to this ground plane creates new resonant frequencies or enhances the already existing ones depending on the slot dimensions and locations. These slots need to be in close proximity of the main/primary radiator to excite efficiently new resonances. Although this approach enhances the PIFA antenna's impedance bandwidth, it suffers from limited means for tuning the slot dimensions. Also restricted slot locations may limit the antenna integration with the RF circuitry.

Lastly, reconfigurable antenna approach for multiband operation can utilize more efficiently the radio frequency spectrum, which in turn facilitates a better access to wireless services in modern radio receivers. Selection of electronic switches to use depends on the antenna type in play. These switches can be RF MEMS, varactors and PIN diodes. The switch choice is also governed by electrical specification, fabrication complexity, bias requirement, switching time and price. This approach though poses great complexity to the antenna design process which happens to be challenging already.

In conclusion, from the research survey carried out, it is evident that few researchers have published details of the designed antennas simulation and performance on real devices populated with active (powered) components which is the appropriate environment where these antennas should be tuned and their performance in terms of gain, return loss, efficiency, VSWR etc. evaluated. This research work will contribute in the area of design and optimization of a multiband PIFA antenna covering two GSM bands 900MHz and 1800MHz, tuning and evaluation of its performance when incorporated on a working device built using a multilayer PCB board populated with active (powered) components.

## **CHAPTER 3**

### **DESIGN OF A MULTI-BAND PIFA ANTENNA FOR TWO GSM FREQUENCY BANDS (900MHz AND 1800MHZ)**

#### **3.1 Introduction**

A single band antenna supports only one frequency of a wireless service. But these days more wireless standards are being supported by mobile devices. This calls for the employment of several antennas for each standard. But utilizing several antennas requires a large space which is not available within a mobile device volume. Thus covering multiple bands with a single antenna structure is the need for the hour.

The printed Inverted-F antenna (PIFA) has been increasingly integrated into the mobile device due to its small size, low profile and Omni-directional pattern. This antenna design consists of a rectangular planar element located above the ground, a shorting plate and a feeding point. The Inverted-F of the antenna is a type of monopole where the top section has been folded down to be parallel with the ground plane. This technique is done to reduce the height of the antenna while maintaining the resonant trace length [38].

#### **3.2 Advanced Design System (ADS)**

Advanced Design System (ADS) is an electronic design automation software system produced by Agilent Technologies. It provides a powerful, easy-to-use interface and integrated design environment for designers of RF electronic products such as mobile phones, pagers, wireless networks, satellite communications, radar systems, microwave, and high speed digital applications.

##### **ADS Momentum**

Momentum is a part of Advance Design System and it provides the simulation tools required to evaluate and design products of modern communication systems. Momentum is an electromagnetic solver in the form of a simulator that computes the S-parameters for general planar circuits which includes microstrip, slotline, stripline, coplanar waveguides and many other topologies. Multilayer communication circuits and printed circuit boards can also be simulated in ADS Momentum with accurate results. Momentum is a complete tool for prediction of the performance of high frequency circuit boards, antennas and integrated circuits [37].

The ADS Momentum optimization tool extends Momentum capability to a real design automation tool. The Momentum Optimization process varies geometry parameters automatically to help in achieving the optimal structure for the circuit or device performance



goals. Momentum optimizations can be done by using layout components (parameterized) from the schematic page.

One of the great advantages that Momentum possesses is the 3-dimensional interface that it provides for the user during simulations and results. Momentum is a 2.5D solver that can do both 2D and 3D computations. For example while computing the antenna parameters, Momentum provides both 2D and 3D graphs of the directivity and the far-field radiation patterns of the antenna [37].

Once the designed antenna is modeled and simulated in ADS momentum, its S-parameters, two- and three- dimensional radiation patterns, excitation models, gain, directivity, and efficiency can be obtained.

### 3.3 Multiband PIFA Antenna Design methodology

Below is a table showing the standard performance requirement for mobile device antennas covering GSM-900 and GSM-1800 standards.

GSM BAND	FREQUENCY	REQUIRED BANDWIDTH	UPLINK BAND	DOWNLINK BAND	REQUIRED REFLECTION COEFFICIENT	REQUIRED ANTENNA EFFICIENCY
GSM-900	(890-960) MHz	70MHz	(890-915) MHz	(925-960) MHz	<-5dB	>45%
GSM-1800	(1710-1880) MHz	170MHz	(1710-1785) MHz	(1805-1880) MHz	<-10dB	>65%

Table 3.1 Performance requirements for GSM-900 and GSM-1800 antennas

The design, simulation and optimization of the PIFA antenna will be carried out using ADS which is a high frequency structure simulator.

From past research works, it was observed that even a slight difference of 0.5mm in the antenna radiation dimensions, feed point location, shorting arm dimensions and in many more parameters can greatly shift the resonant frequency or affect the return loss [13]. This is due to the characteristics of a PIFA antenna structure which is very sensitive to changes in its dimensions and effects of the ground plane. The design criteria of this antenna are as follows:

- i) Selection of design parameters.
- ii) Design and modeling of the multiband PIFA antenna structure.

- iii) Simulating and optimizing the multiband PIFA antenna parameters.
- iv) Comparison and result validation.

### 3.3.1 Selection of design parameters

The objective of this research work is to design a multiband PIFA antenna for mobile devices which is efficient, compact and of low profile. In addition, the antenna must include the operation on GSM-900 (850-960MHz) and GSM-1800 (1710-1880MHz) standards. Thus many multiband transceiver antennas were studied to uncover various designs and their characteristics to support multiband operation. Among these antennas, the PIFA antenna was found to be the most promising candidate for this design. As outlined in chapter two, there are two main considerations that govern any multiband antenna design; *antenna miniaturization techniques* and *multiband operation*. In this antenna design, *multi-branching* technique is employed to achieve multiband operation. Multi-branching involves modifying the main radiating arm by creating several radiators for different resonances from a single feed.

#### Selected geometry

The geometry selected for the designed antenna is that of a basic PIFA containing only the three main parts: *the main radiating arm, the feed* and *the shorting arm*. This PIFA structure with its ground plane is as shown below:

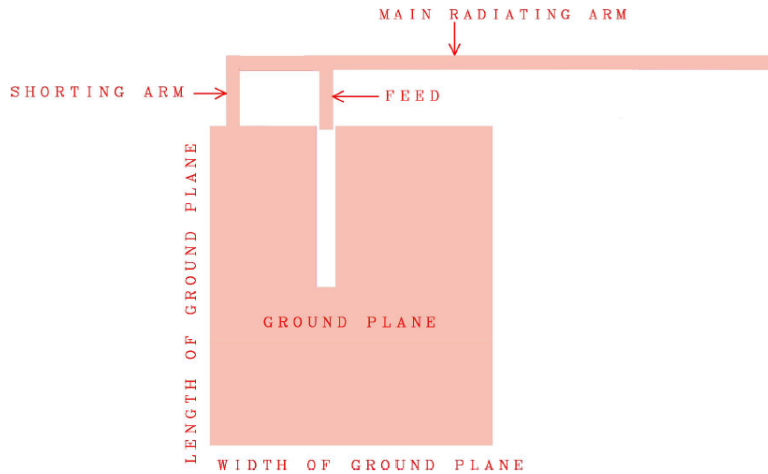


Figure 3.1 Basic PIFA antenna structure

FR4 substrate (see figure 3.2) with a loss tangent ( $\delta=0.02$ ), dielectric constant ( $\epsilon_r = 4.4$ ) and a height, ( $h=1.27\text{mm}$ ) is used as the dielectric material in this research. Copper 7 micron thick with a conductivity of  $5.8e7 \text{ S/m}$  is used as a metal part of the PIFA antenna. Finally, air is used as the dielectric above and below the FR4 substrate.

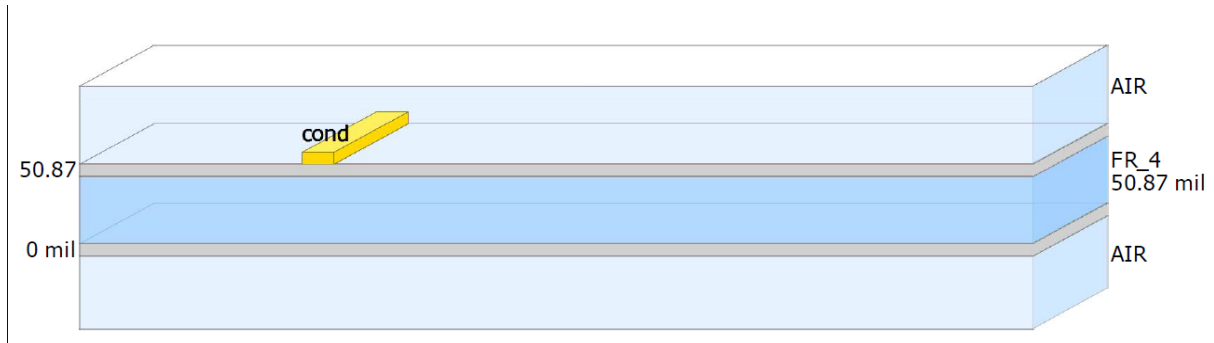


Figure 3.2 Substrate geometry

### 3.3.2 Design and modeling a multiband PIFA Antenna structure

In this section, the stages of designing a multiband PIFA antenna are outlined and discussed. To understand fully the design of this multiband PIFA antenna, a single band PIFA antenna for GSM-900 is designed and analyzed first after which further modifications are made to the structure to obtain the GSM-1800 band as well.

#### Single band PIFA antenna design

The PIFA antenna consists of a main radiating arm that is bent to become parallel with a ground plane. It also has a shorting arm that is added to control its input impedance [46] as shown in figure 3.1 above. A well dimensioned PIFA antenna structure that could help us in understanding the design process is shown in the figure below.

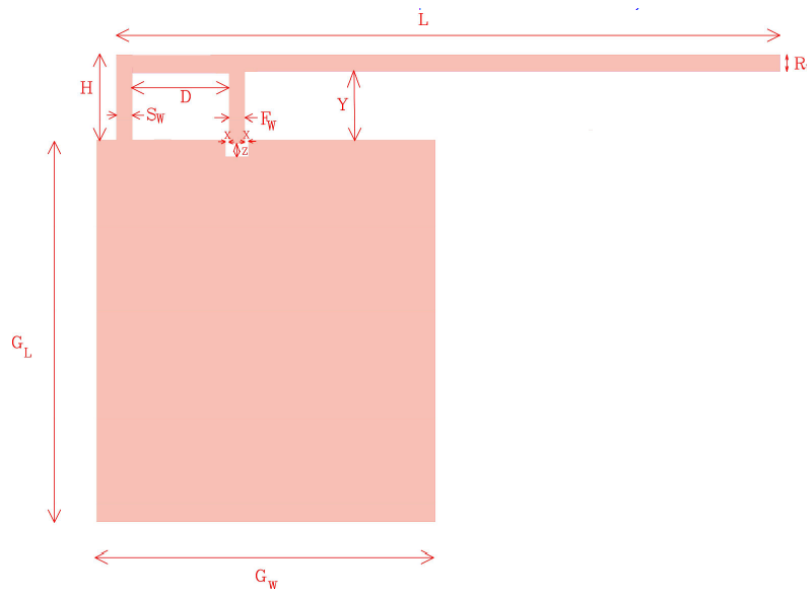


Figure 3.3 PIFA with dimensions

Where:

- $L$ -Length of the radiating arm
- $H$ -Height of the shorting arm
- $R_w$ -Radiating arm width
- $S_w$ -Shorting arm width

$F_w$ -Feed width  
 $D$ -Distance between shorting arm and feed  
 $G_L$ -Length of the ground plane  
 $G_w$ -width of the ground plane  
 $X$ -The side gap between the PIFA feed and the notch on the ground plane  
 $Z$ - Distance between the lower end of the feed and the notch on the ground plane  
 $Y$ -Distance between the main radiating arm and the ground plane

The antenna has complex input impedance which is a function of resonant frequency. To match the antenna with a source with real impedance (often  $50 \Omega$ ), a shorting arm is added to the end of the radiating arm, which introduces additional inductive impedance.

The radiation characteristics of a PIFA can be controlled by varying the parameters that affect its resonance and input impedance. The length of the PIFA ( $L$ ) is inversely proportional to its resonance frequency.

The relationship can be expressed by [40]:

$$f_r \sim \frac{c}{4(L+H)} \quad 3.1$$

Where:

$f_r$ -Resonant frequency  
 $c$ -Speed of light ( $3.0 \times 10^8 \text{ m/s}$ )  
 $L$ -Length of the radiating arm  
 $H$ -Height of the radiating arm

The relationship 3.1 assumes that the PIFA is in a medium with a relative permittivity of approximately 1 (i.e. free space).

The effective length of the current on the above PIFA antenna structure above is  $L + H + R_w$ .

Now the resonant condition can be expressed as:

$$L + H + R_w \sim \lambda/4 \quad 3.2$$

Where;

$$\lambda = c/f_1 \quad 3.3$$

Thus  $L + H + R_w \sim c/4f_1 \quad 3.4$

Making  $f_1$  the subject of the formula;

$$f_1 \sim \frac{c}{4(L+H+R_w)} \quad 3.5$$

The antenna performance is also greatly affected by the relative permittivity of the substrate onto which it is implemented thus the formula above can be written as:

$$f_1 \sim \frac{c}{4\sqrt{\varepsilon_{eff}}(L+H+R_w)} \quad 3.6$$

Where;

$f_1$ -The resonant frequency related to  $R_w$

The other resonant frequency that is part of linear combination with the case  $0 < R_w < L$ , is expressed as:

$$f_2 \sim \frac{c}{4(L+H-R_w)} \quad 3.7$$

Including the relative permittivity of the substrate we can express  $f_2$  as:

$$f_2 \sim \frac{c}{4\sqrt{\varepsilon_{eff}}(L+H-R_w)} \quad 3.8$$

Where;

$f_2$  –The other resonant frequency with the case  $0 < R_w < L$

Effective Relative Permittivity,  $\varepsilon_{eff} = \frac{\varepsilon_r + 1}{2}$

$\varepsilon_r$  =Relative Permittivity of the substrate where the antenna is printed

The resonant frequency ( $f_r$ ) is a linear combination of resonant frequencies associated with the limiting case. For the simple antenna geometry above the resonant frequency can be written as:

$$f_r = r \cdot f_1 + (1 - r)f_2 \quad 3.9$$

Where;

$f_1$ - The resonant frequency related to  $R_w$

$f_2$  – The other resonant frequency with the case  $0 < R_w < L$

$f_r$  –Resonant frequency

$$r = \frac{R_w}{L}$$

Equation 3.1 also reflects the similarity that a PIFA has with a monopole antenna. Like a monopole, a PIFA forms a radiating structure through the interaction of the main radiating arm with its image on the ground plane (resembling a dipole) [33]. For this reason, the ground plane plays an important role in the radiation characteristics of a PIFA.

Empirical data from simulations carried out in research works such as [33, 34] suggests that the optimum performance can be achieved when the ground plane is at least  $\lambda/4$  in length in the direction of the dominant current distribution on the ground plane.

An attractive feature of a PIFA is the ability to control the imaginary component of its input impedance by changing its layout parameters. Specifically, the distance, D, between the

shorting arm and the vertical portion of the radiating arm (the feeder arm) can be used to control the reactive impedance of the antenna. The value of the reactive impedance is inversely proportional to the value of  $D$  [33]. By varying the distance  $D$ , the reactive impedance may be canceled, resulting in real input impedance.

$$X_A \propto \frac{1}{D} \quad 3.10$$

Where:

$X_A$ -Reactive impedance of the PIFA

$D$ - Distance between Feeder arm and Shorting arm

The width  $R_W$  of the main radiating arm of the PIFA is the second parameter that controls different characteristics of the antenna. The first characteristic is the reactive impedance. Increasing the width  $R_W$  of the antenna arm brings it closer to the ground plane (for fixed  $H$ ) thereby creating a higher capacitance. Another characteristic is the bandwidth, which is directly proportional to the value of  $R_W$ . Increasing the width of the radiating arm extends the operating bandwidth [33].

$$X_A \propto R_W \quad 3.11$$

$$BW \propto R_W \quad 3.12$$

Where:

$X_A$ -Antenna Reactive Impedance

$R_W$ -Width of the radiating arm of the PIFA

$BW$ -Operating Bandwidth

The final characteristic affected by the width is the resonance frequency. Alternatively, if the resonance frequency of the antenna must be kept constant, the width allows for the length,  $L$ , to be changed. This fact can be utilized to miniaturize the antenna length. For example, if the width is increased, the length of the antenna can be reduced.

### **GSM-900 PIFA antenna design**

To design a PIFA antenna for a given resonance frequency, the first step to consider is the constraints of the height or length of the structure. For example, the board investigated in this work cannot accommodate an antenna whose height is longer than 20mm and a length longer than 120mm since that could mean increasing the size of the board dimensions. But currently there is a demand for smaller mobile devices thus this increasing the board could mean failing to meet this demand.

Handset users generally receive more data than they transmit and thus the antenna designed for mobile devices need to provide a larger bandwidth for the downlink than that of the uplink to enable users utilize higher data-rate services such as video streaming.

As a starting point the dimensions for the GSM-900 PIFA antenna are determined as follows:

Setting the resonant frequency of the PIFA to be equal to the centre frequency of the GSM-900 band;

$$f_r = \left( \frac{890 + 960}{2} \right) \text{MHz} = 925 \text{MHz}$$

Using equation 3.1 the PIFA's effective length  $\lambda/4$ , in free space medium ( $\epsilon_r = 1$ ) can be approximated as follows:

$$f_r = \frac{C}{4(L + H)}$$

$$925 \text{MHz} = \frac{3.0 \times 10^8}{4(L + H)}$$

$$(L + H) = \frac{3.0 \times 10^8}{4 \times 925 \times 10^6}$$

$$(L + H) = 0.081 \text{M} = 81 \text{mm}$$

Thus the total effective PIFA length assuming free space medium,  $\lambda/4=81\text{mm}$ . This implies that the wavelength at 925MHz (centre frequency for GSM-900 band) is 324mm i.e.  $\lambda_{925\text{MHz}} = 324\text{mm}$ .

From [42];

$$H \sim \frac{\lambda_{925\text{MHz}}}{14} = 23\text{mm}$$

$$R_W \sim \frac{\lambda_{925\text{MHz}}}{40} = 8\text{mm}$$

And  $L = (81 - 23 - 8) = 50\text{mm}$  since  $R_W$  is part of  $L$ .

But constraints from the board ( $H < 20\text{mm}$  and  $L < 120\text{mm}$ ) force us to reduce H to 16mm and increase the length to 57mm since we still have room to increase .L

From literature too,  $D \ll \lambda$  and for this case it was chosen to be  $\sim \frac{\lambda}{45}$  (i.e. = 7.2mm) and  $S_W = F_W = 2\text{mm}$ .

And the ground plane from literature [44] was suggested to be approximately  $\lambda/4$ . Thus  $G_L \sim 0.25\lambda_{925\text{MHz}} = 81\text{mm}$  and  $G_W \sim 0.2\lambda_{925\text{MHz}} = 65\text{mm}$ .

Once the PIFA dimensions are determined mathematically and board constraints applied, an iterative process may be required to obtain the correct combination. Once the resonant frequency is obtained, the value of D can be varied in order to obtain the desired

input impedance. This generally causes a slight shift in resonance, requiring the length or height to be readjusted [33]. If the PIFA doesn't satisfy the bandwidth requirements, the parameter  $R_w$  can be increased. This once again causes the resonance frequency to shift but can be corrected by varying the length  $L$  of the antenna [33]. This iterative process may require several simulations before a final design provides acceptable results. However, the use of optimization procedures in AADS simulation tool simplifies this task greatly.

### Multi-branch PIFA antenna design for multiband operation

By combining a PIFA antenna with an inverted-L element, *a printed inverted-FL antenna* can be formed for dual band operation [48] as shown in the figure 3.4 below.

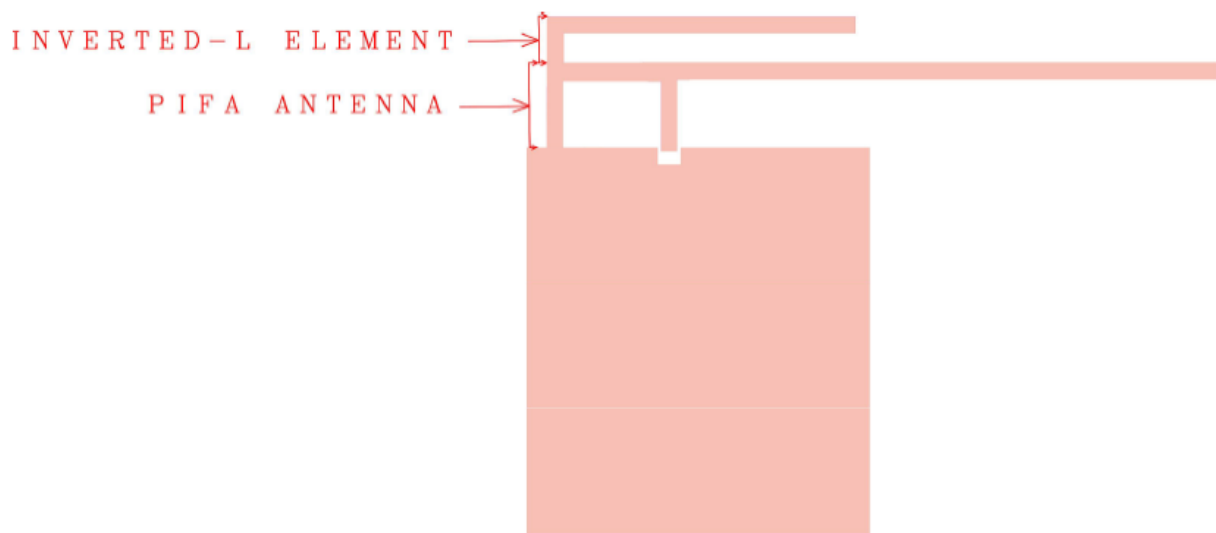


Figure 3.4: Printed Inverted-FL Antenna

The inverted-L element decides the resonance of the higher frequency band (i.e. 1975MHz) and whereas the PIFA controls the impedance matching at the lower frequency band (i.e. 925MHz). A well dimensioned printed inverted-FL antenna structure that could help us in understanding the design process of this type of antenna is shown in the figure 3.5 below.



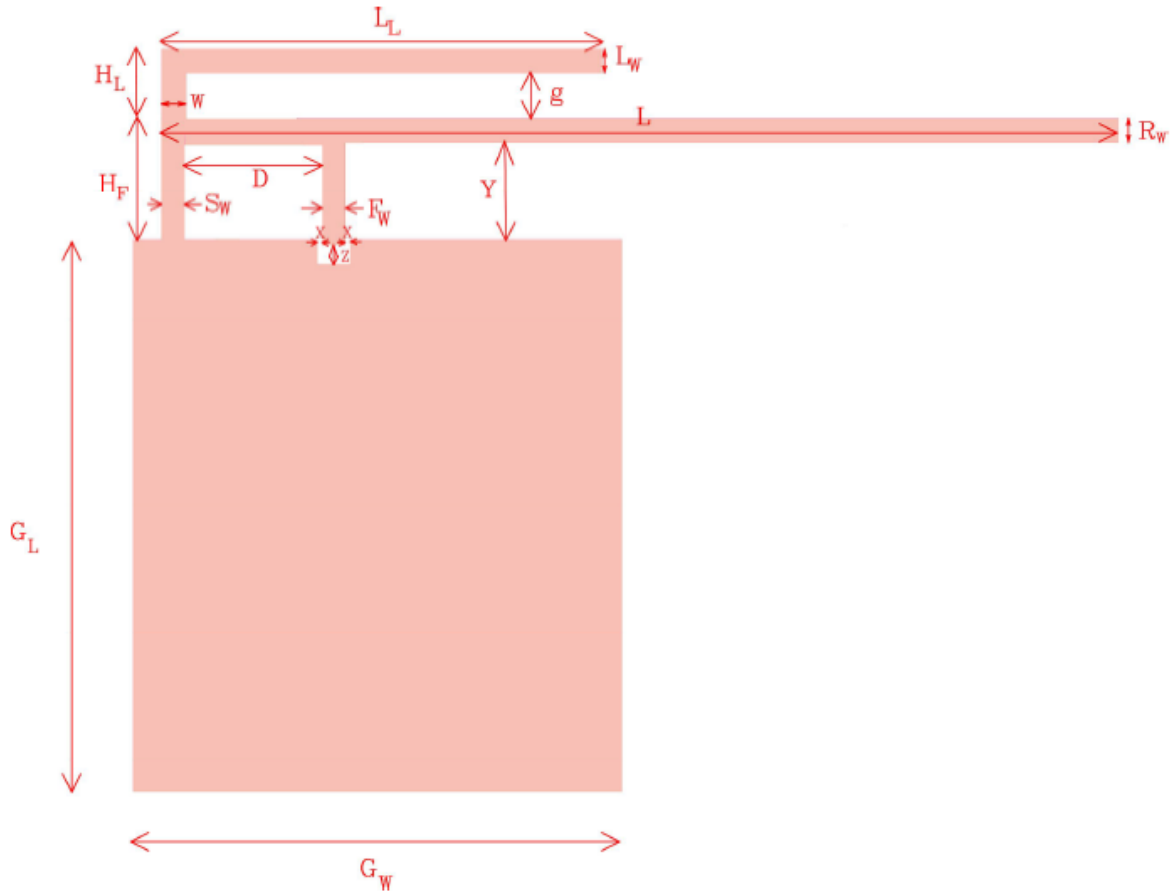


Figure 3.5: Printed Inverted-FL antenna with dimensions

Where:

- $L$ -Length of the radiating arm of the PIFA antenna
- $H_F$ -PIFA antenna height
- $R_W$ -Width of the PIFA antenna radiating arm
- $S_W$ -Shorting arm width of the PIFA antenna
- $F_W$ -The width of the Feed for the Printed Inverted-FL antenna
- $D$ -Distance between shorting arm and feed of the PIFA antenna
- $G_L$ -Length of the ground plane
- $G_W$ -width of the ground plane
- $X$ -The side gap between the PIFA feed and the notch on the ground plane
- $Z$ - Distance between the lower end of the feed and the notch on the ground plane
- $Y$ -Distance between the main radiating arm and the ground plane
- $G$ -Gap between the arm of the Inverted-L element and the arm of the PIFA antenna
- $L_W$ -The width of the horizontal arm of the inverted-L element
- $L_L$ -The length of the horizontal arm of the inverted-L element
- $H_L$ -Height of the inverted-L element
- $W$ -Width of the vertical arm of the inverted-L element

This Printed Inverted-FL antenna for dual band operation is made of a thin conducting film, having a flat structure as shown in figure 3.5 above, where both the radiating element (Inverted-F and inverted-L strip lines) and the ground plane lie in the same plane. In other

words, the Printed Inverted-FL antenna has a coplanar ground plate, forming a card-type structure.

The final structural parameters for the Printed Inverted-FL antenna are obtained through a step-by-step investigation of the following structures:

- i) The PIFA antenna element designed in the previous section
- ii) An Inverted-L element
- iii) A compound of the PIFA antenna and the Inverted-L element to form the radiating element for the dual-band Printed Inverted-FL antenna.
- iv) Modification of the dimensions for the radiating element (a compound of the PIFA antenna and the inverted-L element) and its coplanar ground plane to obtain the two resonant frequencies i.e. 925MHz (centre frequency for GSM-900) and 1795MHz (the centre frequency for GSM-1800).

Since the GSM-900 PIFA is designed in the previous section, then the design of the inverted-L element is as follows;

Setting the resonant frequency of the inverted-L to be equal to the centre frequency of the GSM-1800 band;

$$f_r = \left( \frac{1710+1880}{2} \right) MHz = 1795MHz$$

Using equation 3.1 the PIFA's effective length  $\lambda/4$ , in free space medium ( $\epsilon_r = 1$ ) can be approximated as follows:

$$f_r = \frac{C}{4(LL + HL + HF)}$$

$$1795MHz = \frac{3.0 \times 10^8}{4(LL + HL + HF)}$$

$$(LL + HL + HF) = \frac{3.0 \times 10^8}{4 \times 1795 \times 10^6}$$

$$(LL + HL + HF) = 0.042M = 42mm$$

Thus the total effective inverted-L length assuming free space medium,  $\lambda/4=42mm$ . This implies that the wavelength at 1795MHz (center frequency for GSM-1800 band) is 168mm i.e.  $\lambda_{1795MHz} = 168mm$ .

From [48];

$$HL + HF = 0.113\lambda_{1795MHz} = 19mm$$

$$LL = 42 - 19 = 23mm$$

$$Lw = W = g = 0.012\lambda_{1795MHz} = 2mm$$

Compounding this inverted-L element with the GSM-900 PIFA designed in the previous section while retaining the same ground plane for the GSM-900 PIFA antenna

( $G_L \sim 0.25\lambda_{925\text{MHz}} = 81\text{mm}$  and  $G_w \sim 0.2\lambda_{925\text{MHz}} = 65\text{mm}$ ) the dual band PIFA simulated and optimized using AADS software.

Thus, the length of the longer branch (see figure 3.5) is about 81mm (determined earlier in the design of the single band GSM-900 PIFA), which is one-quarter of the wavelength at 925MHz will act as the resonator for the lowest resonant mode i.e. GSM-900 (890-960 MHz) band. On the other hand, the shorter branch which has been determined above to around 42mm (which is about one-quarter wavelength at 1795MHz) will act as the resonator for the DCS (1710-1880 MHz) band.

An iterative process may be required to obtain the correct combination. Once the resonant frequency is obtained, the value of  $W$ ,  $w$ ,  $G_L$  and  $G_w$  can be varied in order to obtain the desired input impedances for the two resonances (i.e. 925MHz and 1795MHz). This generally causes a slight shift in the resonances, requiring the lengths  $L$ ,  $LL$  or the heights  $HL$  or  $HF$  to be readjusted [48]. If the Printed Inverted-FL antenna doesn't satisfy the bandwidth requirements for both bands, the parameters  $R_w$  and  $L_w$  can be increased while reducing  $g$  to attain the desired bandwidths. This once again cause the resonance frequency to shift but can be corrected by varying the lengths  $L$  and  $LL$  of the dual band antenna [48].

Although creating multiple resonant paths of the inverted-F antenna generates multiple resonances, the coupling between each resonant path makes it difficult to match the antenna at each resonant frequency [49]. However, modification of the size of the gap between the two arms i.e.  $g$ , the individual lengths and widths of the arms can help us match the antenna at each resonant frequency. This iterative process may require several simulations before a final design provides acceptable results.

## CHAPTER 4

### SIMULATION RESULTS FOR THE DESIGNED MULTIBAND PIFA ANTENNA

#### 4.1 Introduction

Having designed the single band and multiband PIFA antennas using the methods presented in Chapter Three, this chapter presents the simulation results and their interpretation. Results for the single band GSM-900 PIFA are presented and interpreted first followed by those for the dual band PIFA covering GSM-900 and GSM-1800 bands.

#### 4.2 Simulation results for the GSM-900 PIFA antenna

Using the method presented in Chapter Three for designing the single band GSM-900 PIFA antenna, the optimal dimensions for both the PIFA and its coplanar ground plane are tabulated in table 4.0 below.

PARAMETER	VALUE(mm)
$L$	$72.175$
$H$	$10.83$
$D$	$8.975$
$R_W$	$6.95$
$S_W$	$8.325$
$F_W$	$1.604$
$G_L$	$63.5$
$G_W$	$52.33$
X	$0.425$
Y	$3.85$
Z	$1$

Table 4.0 Dimensions for the optimized GSM-900 PIFA antenna

The far field antenna parameters for the optimized GSM-900 PIFA antenna resonant at 925MHz are tabulated in the table 4.1 below.

ANTENNA PARAMETER	MAGNITUDE	VALUE
Frequency(GHz)		0.925
Input Power(Watts)		0.00249953
Radiated Power(Watts)		0.00208675
Directivity(dBi)		2.36781
Gain(dBi)		1.58392
Radiation Efficiency (%)		83.4856
Maximum Intensity(watts/Steradian)		0.000286444
Effective Angle(Steradians)		7.285
Angle of U Max(mag, phase)	153	326
E( $\theta$ ) max(mag, phase)	0.0435527	100.098
E( $\phi$ ) max(mag, phase)	0.462523	96.3424
E(x) max(mag, phase)	0.226547	95.8094
E(y) max(mag, phase)	0.405105	96.5434
E(z) max(mag, phase)	0.0197725	-79.9015

Table 4.1 Parameters for the optimized GSM-900 PIFA antenna

Figure 4.0 below shows the surface current distribution for the optimized GSM-900 PIFA antenna resonant at 925MHz. It is important to note that at 925MHz, there is a stronger current distribution on the PIFA's radiating arm compared to other parts of the PIFA as well as on the ground plane.

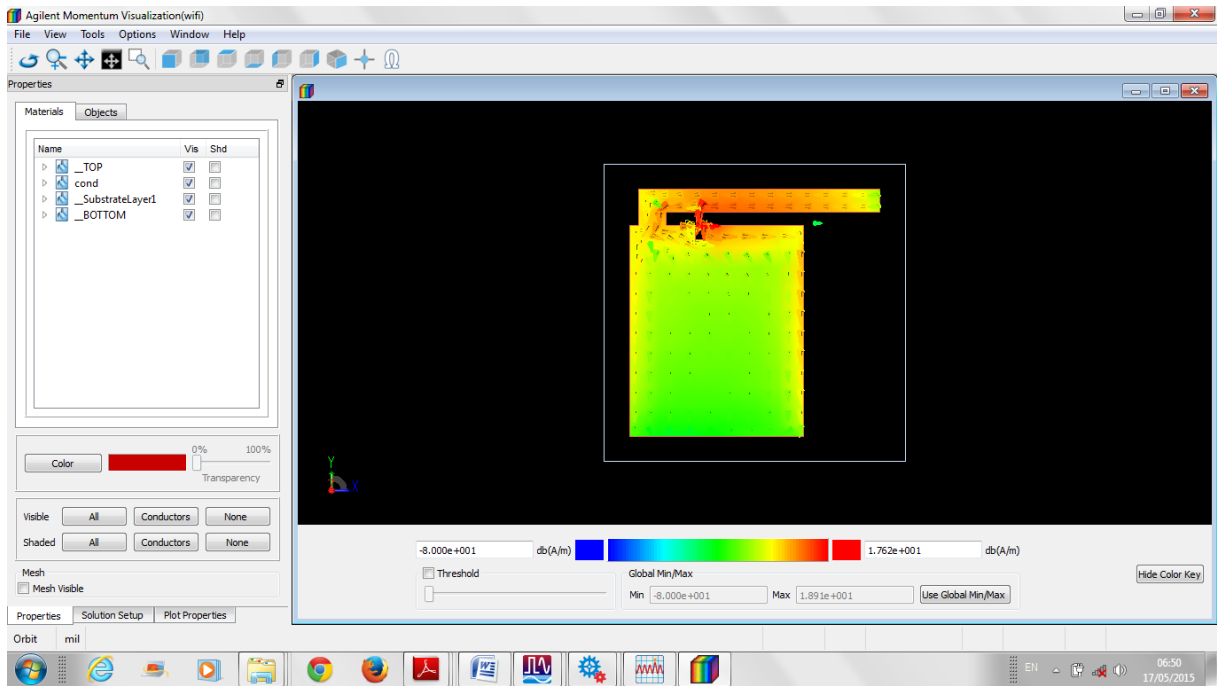


Figure 4.0: Steady state surface current magnitudes at 925MHz for the GSM-900 PIFA

Figure 4.1 shows the return loss for the single band PIFA. As depicted by marker m4, the antenna has the lowest return loss of -37.251dB at 925MHz. Using markers m2 and m1, the -10dB bandwidth for this PIFA antenna is 94.7MHz i.e. (978.2-883.5) MHz

m4  
freq=925.0MHz  
dB(S11\_fitted)=-37.251

m1  
freq=883.5MHz  
dB(S11\_fitted)=-10.319

m2  
freq=978.2MHz  
dB(S11\_fitted)=-10.397

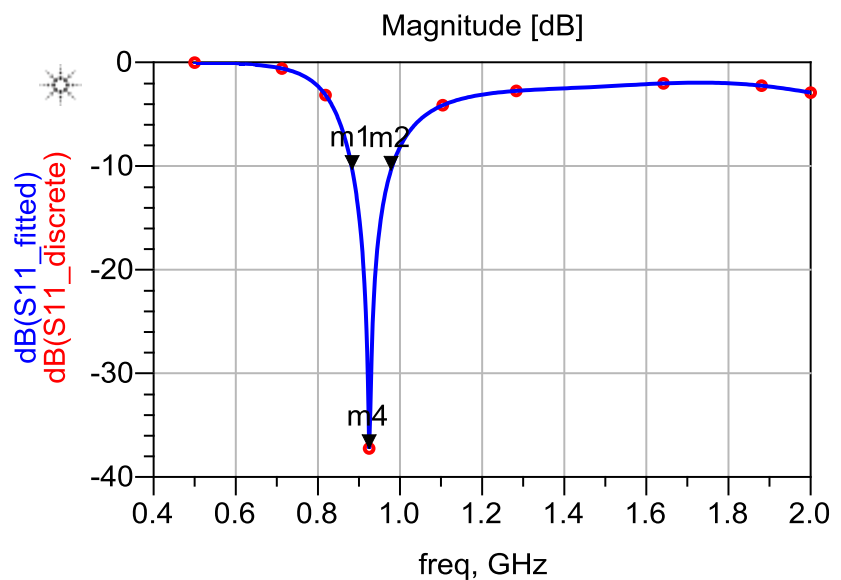


Figure 4.1: Return Loss for the designed GSM-900 PIFA antenna

The PIFA's impedance matching is illustrated in figure 4.2. Using marker m3, we can deduce that the antenna is almost perfectly matched to the transmission line impedance i.e.

$Z_A \sim Z_0$  ( $Z_A$  is the antenna's impedance and  $Z_0$  is the transmission line impedance)

since at 925MHz the antenna's impedance is close to the centre of the smith chart.

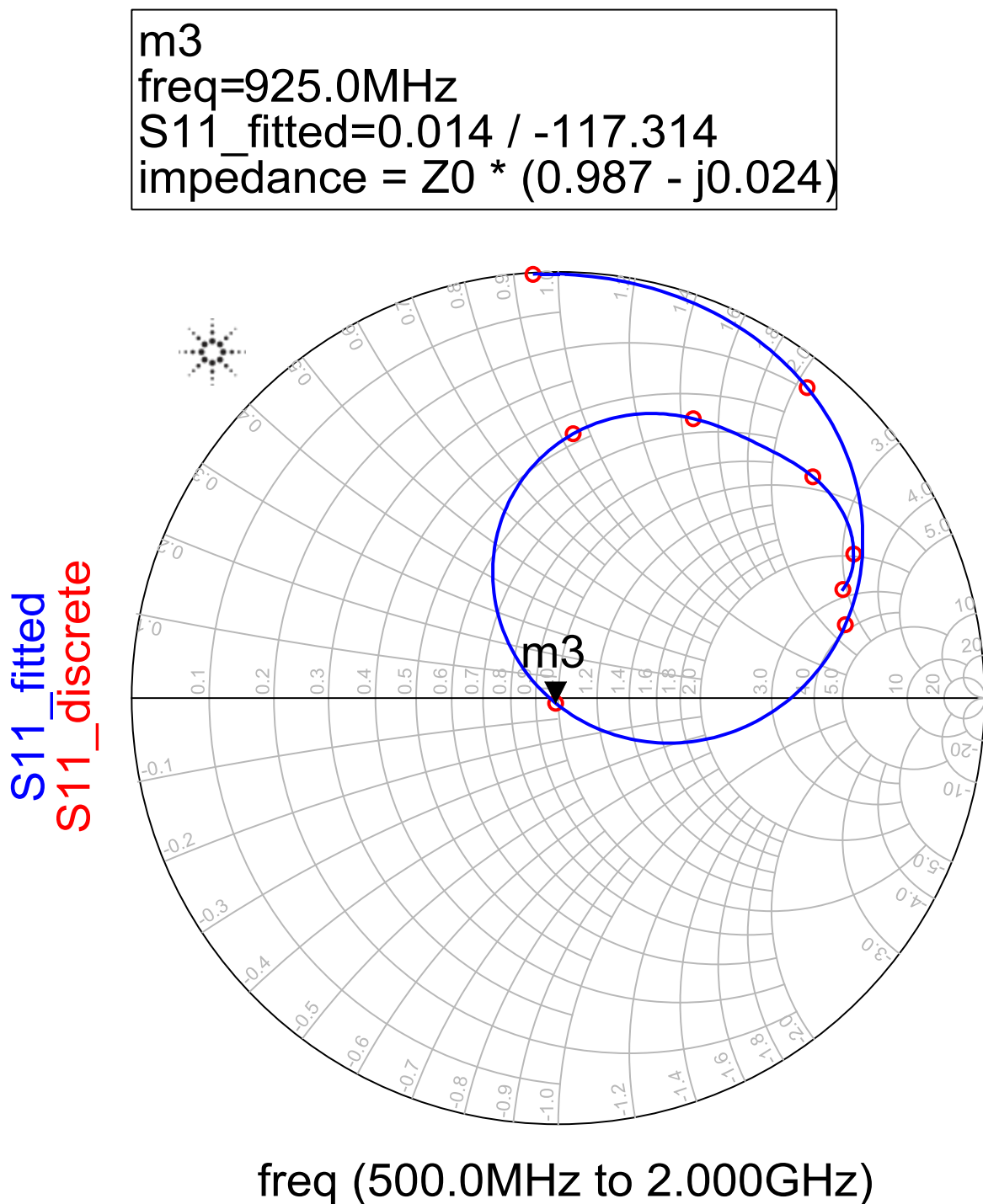


Figure 4.2: The simulated Input Impedance of the designed GSM-900 PIFA antenna

Figure 4.3 below illustrates the 3D radiation pattern for  $\phi=0$  for the optimized GSM-900 PIFA antenna. With ADS momentum, high level radiated power regions are indicated in red while low level radiated power regions are indicated in green. Thus it can be deduced

from the figure below that the designed PIFA antenna radiates power equally in all directions (i.e. Omni-directional radiation pattern).

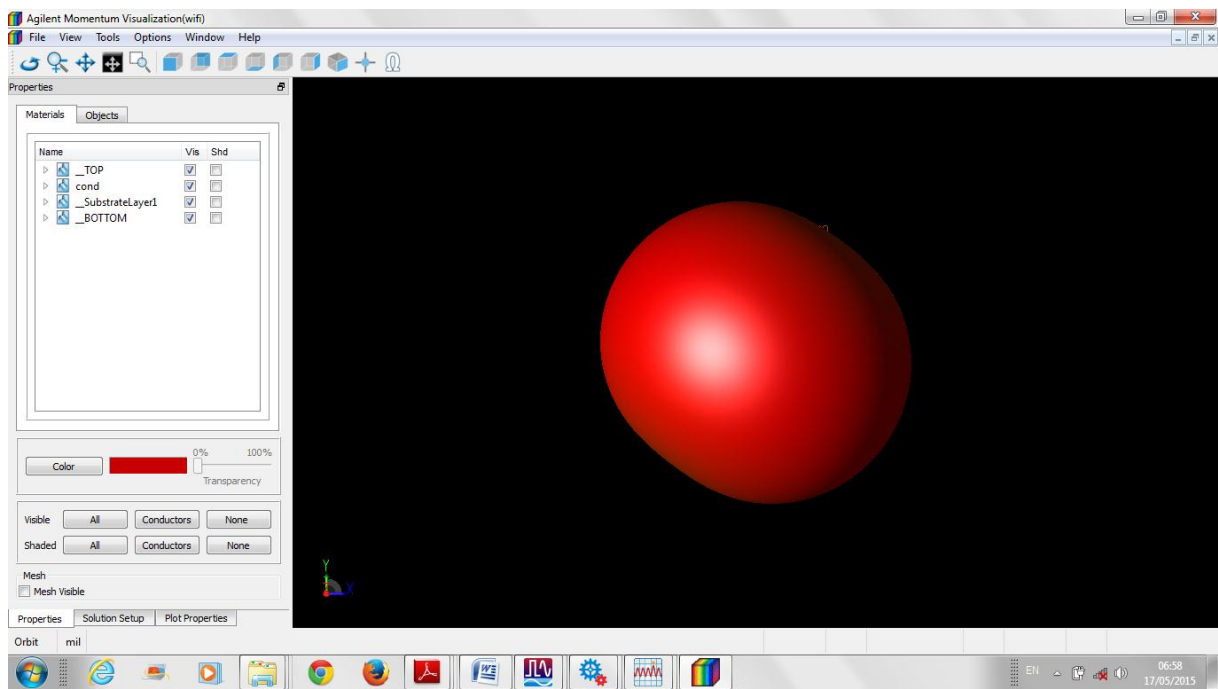


Figure 4.3: 3D radiation pattern for the designed GSM-900 PIFA antenna for  $\phi=0$



Frequency	E_max	Theta_max	Phi_max	Directivity_max	Gain_max	RadiatedPower	InputPower	Efficiency	CutType	CutAngle
9.250E8	0.465	153.000	326.000	2.368	1.584	0.002	0.002	0.835	Phi	0.000

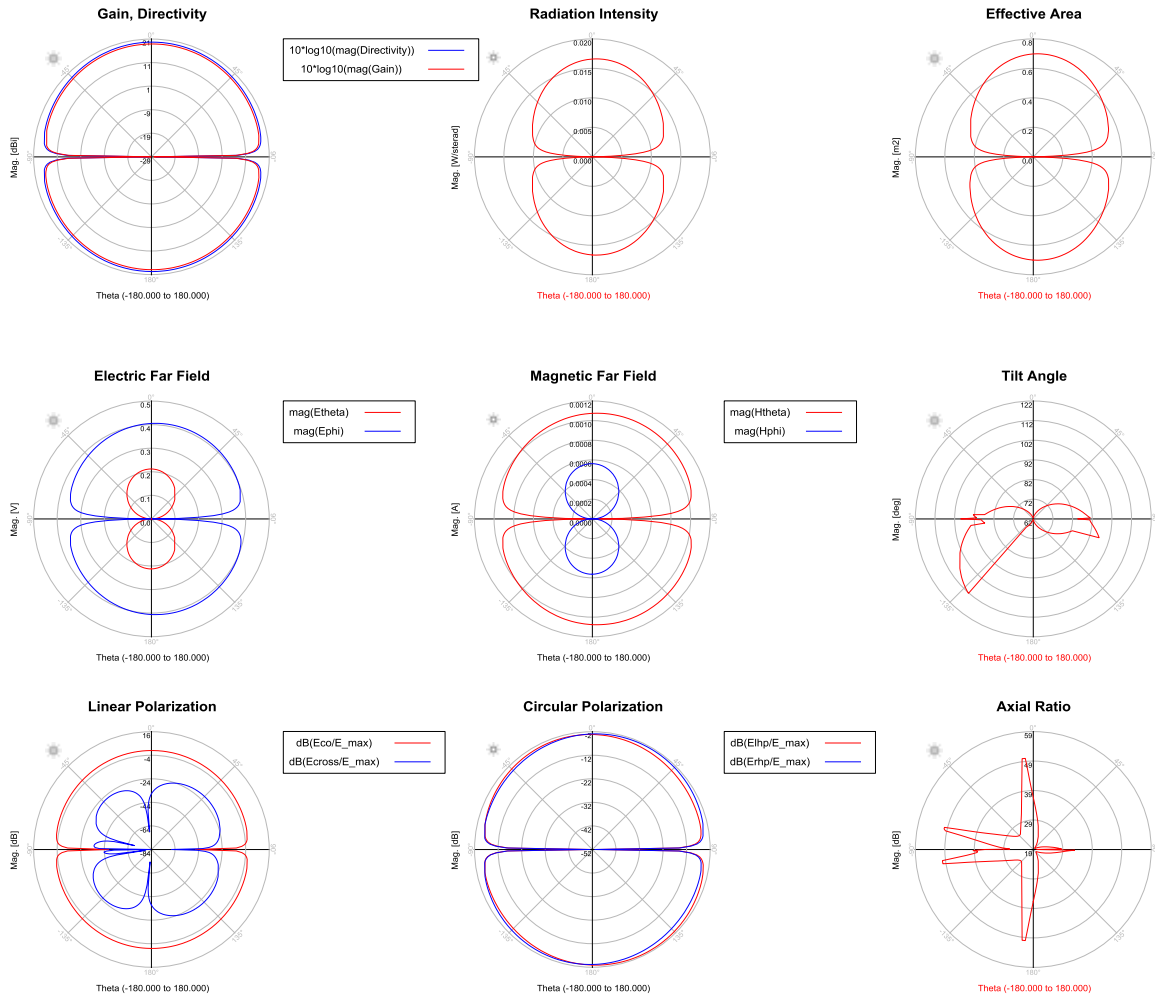


Figure 4.4: XY-plane radiation patterns for the designed GSM-900 PIFA antenna for  $\varphi=0$

#### 4.2.1 An interpretation of the simulation results for the designed GSM-900 PIFA Antenna

The simulation results show that the PIFA operate efficiently at the GSM-900 band. One reason for this is that at 925MHz (centre frequency for GSM-900), the ground plane is  $0.2\lambda_{925MHz} \times 0.16\lambda_{925MHz}$  which is therefore large enough to supply a full resonant current distribution. The gain/Directivity diagram in figure 4.4 above depict an almost Omni-directional radiation pattern since the PIFA antenna/ground plane combination behaves as an asymmetric dipole, the difference in current distribution on the two-dipole arms being responsible for some distortion of the radiation pattern. The optimal location of the PIFA in order to achieve this Omni-directional far field pattern and a  $50\Omega$  impedance matching was found close to the edge of the ground plane as shown in figure 4.0.

For maximum power to be transferred from the RF generator to the antenna, then the antenna impedance should be equal to the complex conjugate of the RF generator impedance. But since many RF generators (Radio chips) have a real impedance of  $50\Omega$  then the antenna has to be matched to  $50\Omega$ . At high frequency, transmission lines will transform the impedance of the antennas, making it very difficult to deliver power, unless these antennas are matched to the transmission lines as well. When an antenna is matched to the transmission line, the input impedance normally measured at the end of the transmission line doesn't depend on the length of the transmission line and thus a longer transmission line can be used to deliver an RF signal to the antenna. Thus if an antenna is not matched, the input impedance will vary widely with the length of the transmission line, and if the input impedance is not well matched to RF source impedance, not much power will be delivered to the antenna. This power ends up being reflected back to the generator which can be a problem in itself especially if high power is transmitted. Hence having tuned impedance as shown in figure 4.2 for the designed GSM-900 PIFA antenna is extremely important.

Electrically small antennas (i.e. antennas of size  $\lambda/4$  to  $\lambda/2$ ) normally achieve low directivity while electrically large antennas (i.e. antennas that are many wavelengths in size) have high directivity. This is due to the properties of the Fourier transform. Taking the Fourier transform of a short pulse, you get a broad frequency spectrum. This analogy too is present in determining the radiation of an antenna; the pattern can be thought of as the Fourier transform of the antenna's current or voltage distribution. As a result, small antennas have broad radiation patterns (i.e. low directivity) while antennas with large uniform voltage or current distributions have very directional patterns (and thus, a high directivity). This explains well why the designed PIFA antenna which is  $\lambda/4$  attained a directivity of 2.36781 (see table 4.1). However it was also found out that trying to make the antennas much smaller than  $\lambda/4$  degrades both the antenna's efficiency and bandwidth.

A high efficiency antenna has most of the power present at the antenna's input radiated away while a low efficiency antenna has most of the power absorbed as losses within the antenna, or reflected away due to *impedance mismatch*. The losses associated with an antenna are typically the *conduction losses* (due to finite conductivity of the antenna) and *dielectric losses* (due to conduction within a dielectric which may be present within the antenna). A good impedance matching for a given designed antenna can greatly improve the efficiency of the antenna. This is well explained by the antenna efficiency obtained

(83.4856%) for the designed antenna (see table 4.1) as a result of the antenna tuning close to  $50\Omega$ .

The designed PIFA antenna achieved a gain of 1.58392dBi, which imply that the power received far from the antenna will be 1.58392dB higher than what could be received from a lossless isotropic antenna (reference antenna) with the same input power. This is also due to the fact that electrically small antennas can be very inefficient with antenna gains lower than -10dB even without accounting for impedance mismatch.

The required GSM-900(890-960MHz) bandwidth is 70MHz with a reflection coefficient below -5dB as per the Research In Motion (RIM) recommendation. From figure 4.1, the designed antenna radiates best at 925MHz (the Centre frequency for GSM-900 band), where the reflection coefficient  $S_{11}=-37.251$ dB. Defining the bandwidth as the frequency range where  $S_{11}<-10$ dB the bandwidth would be roughly 95MHz, with 978.2MHz as the high end and 883.2MHz the low end of the frequency band. Though -10dB (a value still below the required reflection coefficient reference of -5dB from table 3.1) was used as the reference, still the antenna achieved sufficient bandwidth as per the RIM requirement. This bandwidth is wide enough to allow the antenna to cover both the uplink and downlink bands for the GSM-900 standard.

The Fractional Bandwidth (FBW) which is a measure of how wideband an antenna is was determined for the designed antenna as:

$$FBW = \frac{f_1 - f_2}{f_c} \tag{4.0}$$

$$FBW = \frac{978.2 - 883.2}{925}$$

= 0.1027(10.27%)

While the Q factor (a reciprocal of the Fractional Bandwidth) for this antenna was determined as follows;

$$Q = \frac{f_c}{f_2 - f_1} \tag{4.1}$$

$$= \frac{925}{978.2 - 883.2}$$

=9.7368

Although the designed PIFA antenna covers the whole GSM-900 band it is still narrow band since its Q factor as calculated above is relatively high. Antennas with a low Q factor are termed as wideband. The higher the value of Q a given type of antenna, the more

sensitive the antenna's input impedance is to small changes in frequency. This well explains why it is difficult to correctly match PIFA to 50Ω input impedance.

The PIFA's height is the antenna's dimension that is closely related to the impedance bandwidth where the Q factor can be reduced by increasing the antenna's height to broaden the bandwidth and vice versa. But since the antenna has attained sufficient bandwidth and we are further constrained by the space available on the board (i.e.  $H < 20\text{mm}$ ) where the antenna will be utilized, we live with this optimized PIFA.

A plane electromagnetic(EM) wave is characterized by travelling in a single direction(with no field variation in the two orthogonal directions) while the electric field and the magnetic field are perpendicular to each other and to the direction the plane wave is propagating. If the E-field of this plane wave stays along a single plane, this field would be termed as *linearly polarized*. An E-field of a given plane wave is termed as *circularly polarized* if the E-field has two orthogonal components which must have equal magnitude and 90° out of phase. If the E-field has two perpendicular components that are out of phase by 90° but are equal in magnitude, the field will end up being *elliptically polarized*.

From table 4.1, considering E(x), E(y) and E (z) components of the E-field of the designed PIFA antenna, it can be deduced that this antenna is elliptically polarized since these components have different magnitudes and are roughly 90° out of phase. Thus we can say that the radiation fields produced by this antenna evaluated in the far field are elliptically polarized.

Due to *reciprocity theorem*, antennas transmit and receive in exactly the same manner. This implies that a linearly polarized antenna transmits and receives linearly polarized fields. In general, for two linearly polarized antennas that are rotated from each other by an angle  $\varphi$ , the power loss due to this polarization mismatch will be described by the *polarization loss factor(PLF)* given by:

$$PLF = \text{Cos}^2 \varphi \quad 4.2$$

Hence, if antennas have the same polarization, the angle between their radiated E-fields is zero (i.e.  $\varphi = 0$ ) and there is no power loss due to polarization mismatch. If one antenna is vertically polarized and the other is horizontally polarized, the angle is 90° and no power will be transferred. This explains why moving the mobile phone on your head to a different angle can sometimes increase reception. Many cell phones antennas are often linearly polarized, so rotating the phone can often match the polarization of the phone and thus increase reception.

Circular polarization is a desirable characteristic for many mobile device antennas since two antennas that are both circularly polarized do not suffer signal loss due to polarization mismatch but practically this is not easily attainable a reason why many mobile devices end up either being linearly or elliptically polarized. An elliptically polarized antenna has a better reception compared to a linearly polarized one since it can receive both vertical and horizontally polarized electromagnetic waves, which can be proven beneficial in indoor environments where depolarization is a dominant phenomenon and the choice of the best polarization difficult.

From figure 4.0, the large resonant current distributions for the designed PIFA antenna resonating at 925MHz are indicated by the red colour. This reveals that the proposed antenna has much independency of the resonant current path on the PIFA's radiator thus we are able to design and tune the antenna to satisfy the bandwidth and resonant frequency required.

### 4.3 Simulation results for the dual band Printed Inverted-FL for GSM-900 and GSM-1800 bands

The dimensions for the optimized dual band inverted-FL antenna are tabulated in table 4.2 below.

PARAMETER	VALUE(mm)
$L$	74
$H_F$	5.36
$D$	11.87
$R_W$	5.33
$S_W$	7.143
$F_W$	1.604
$G_L$	61.22
$G_W$	45.87
$X$	0.5
$Y$	1.025
$Z$	3.55
$g$	1
$L_W$	5.35
$L_L$	37
$H_L$	4.34
$W$	29

Table 4.2 Dimensions for the optimized dual band PIFA antenna

The far field antenna parameters for the optimized dual band PIFA antenna resonant at both 925MHz and 1795MHz are tabulated in the table 4.3 below.

ANTENNA PARAMETER	ANTENNA PARAMETER VALUES FOR THE DUAL PIFA RESONANT AT 925MHz		ANTENNA PARAMETER VALUES FOR THE DUAL PIFA RESONANT AT 1795MHz	
	MAGNITUDE	VALUE	MAGNITUDE	VALUE
Frequency(GHz)		0.925		1.795
Input Power(Watts)		0.00249768		0.00249761
Radiated Power(Watts)		0.00208402		0.0017554
Directivity(dBi)		2.35781		4.73659
Gain(dBi)		1.57146		3.20512
Radiation Efficiency (%)		83.4382		70.2835
Maximum Intensity(watts/Steradian)		0.000285412		0.000415744
Effective Angle(Steradians)		7.30178		4.22234
Angle of U Max(mag, phase)	153	316	120	313
E( $\theta$ ) max(mag, phase)	0.0380787	109.063	0.121464	3.59377
E( $\phi$ ) max(mag, phase)	0.462165	102.639	0.546345	-32.5239
E(x) max(mag, phase)	0.296807	102.113	0.366926	-36.339
E(y) max(mag, phase)	0.355884	103.064	0.409325	-28.8567
E(z) max(mag, phase)	0.0172874	-70.937	0.105191	-176.406

Table 4.3 Parameters for the optimized dual band PIFA antenna resonant at 925MHz and 1795MHz

Figure 4.5 below shows the surface current distribution for the optimized dual band PIFA antenna resonant at 925MHz. It is important to note that at 925MHz, there is a stronger

current distribution on the PIFA's longer arm compared to other parts of the PIFA as well as on the ground plane.

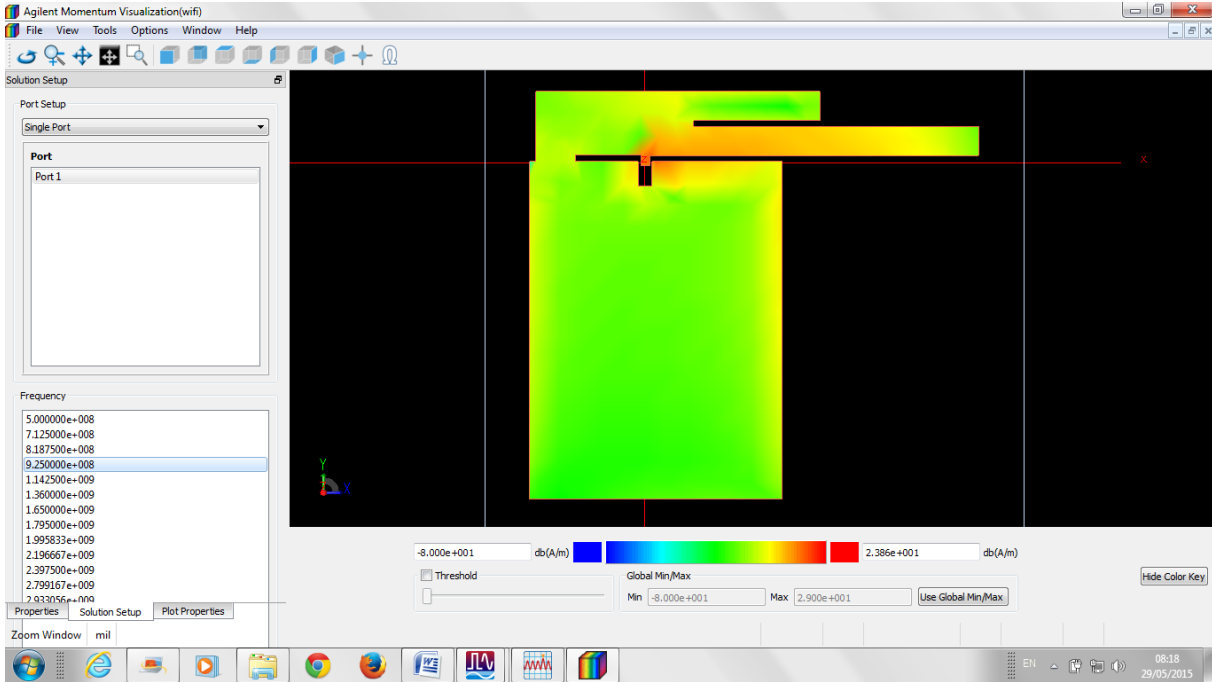


Figure 4.5: Steady state surface current magnitudes at 925MHz for the dual band PIFA

Figure 4.6 below shows the surface current distribution for the optimized dual band PIFA antenna resonant at 1795MHz. It is important to note that at 1795MHz, there is a stronger current distribution on the PIFA's shorter arm compared to other parts of the PIFA as well as on the ground plane.

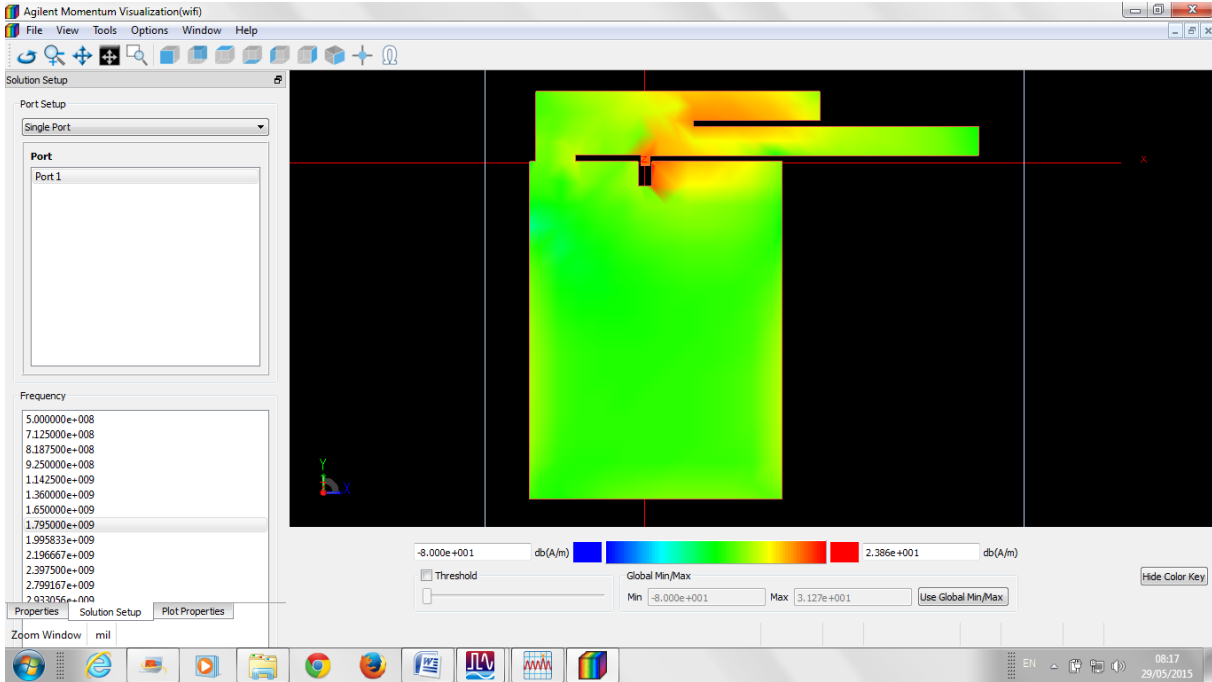


Figure 4.6: Steady state surface current magnitudes at 1795MHz for the dual band PIFA

Figure 4.7 shows the return loss for the dual band PIFA. The antenna has the lowest return loss of -30.319dB at 925MHz the centre frequency for GSM-900 band and -30.187dB at 1795MHz the centre frequency for the GSM-1800 band as depicted by markers m1 and m2 respectively.

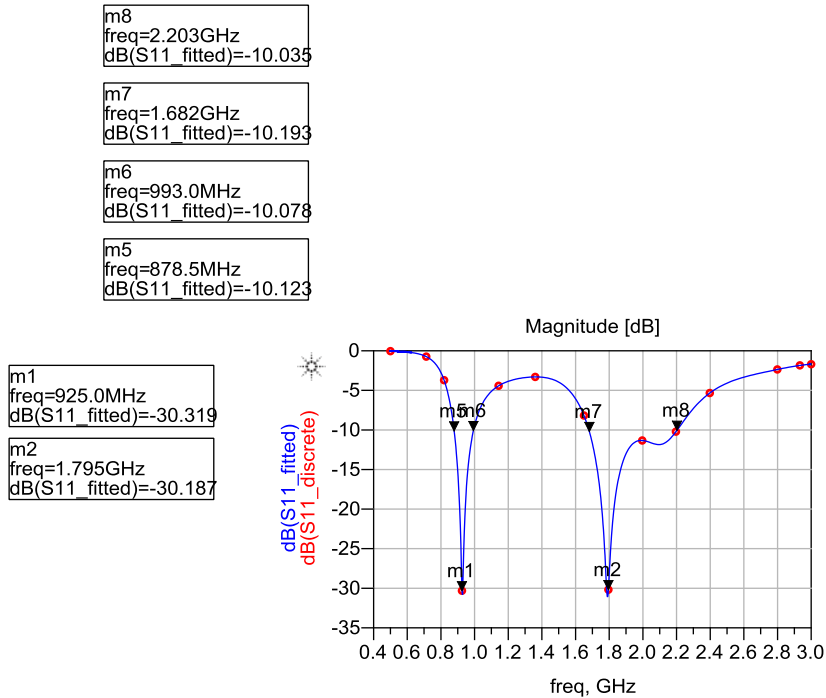


Figure 4.7: Return Loss for the designed dual band PIFA antenna

The dual band PIFA’s impedance matching is illustrated in figure 4.8. Using markers m3 and m4, we can deduce that the antenna is almost perfectly matched to the transmission line impedance i.e.  $Z_A \sim Z_O$  ( $Z_A$  is the antenna’s impedance and  $Z_O$  is the transmission line impedance) since at both 925MHz and 1795MHz the antenna’s impedance is close to the centre of the smith chart.



```

m4
freq=925.0MHz
S11_fitted=0.030 / -95.565
impedance = Z0 * (0.992 - j0.060)

```

```

m3
freq=1.795GHz
S11_fitted=0.031 / -177.785
impedance = Z0 * (0.940 - j0.002)

```

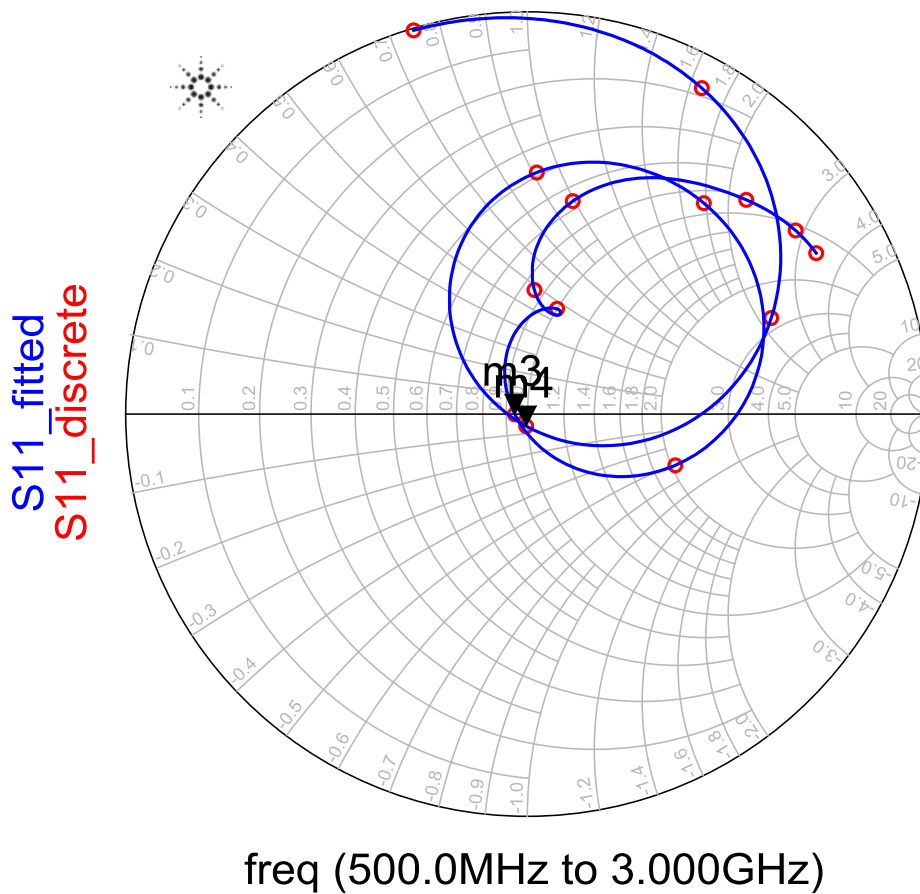


Figure 4.8: The simulated Input Impedance of the designed dual band PIFA antenna

Figures 4.9 and 4.10 below illustrates the 3D radiation pattern for  $\phi=0$  for the optimized dual band PIFA antenna. With ADS momentum, high level radiated power regions are indicated in red while low level radiated power regions are indicated in green. Thus it can be deduced that the antenna seems directional when resonant at 1795MHz compared to 925MHz resonant frequency.

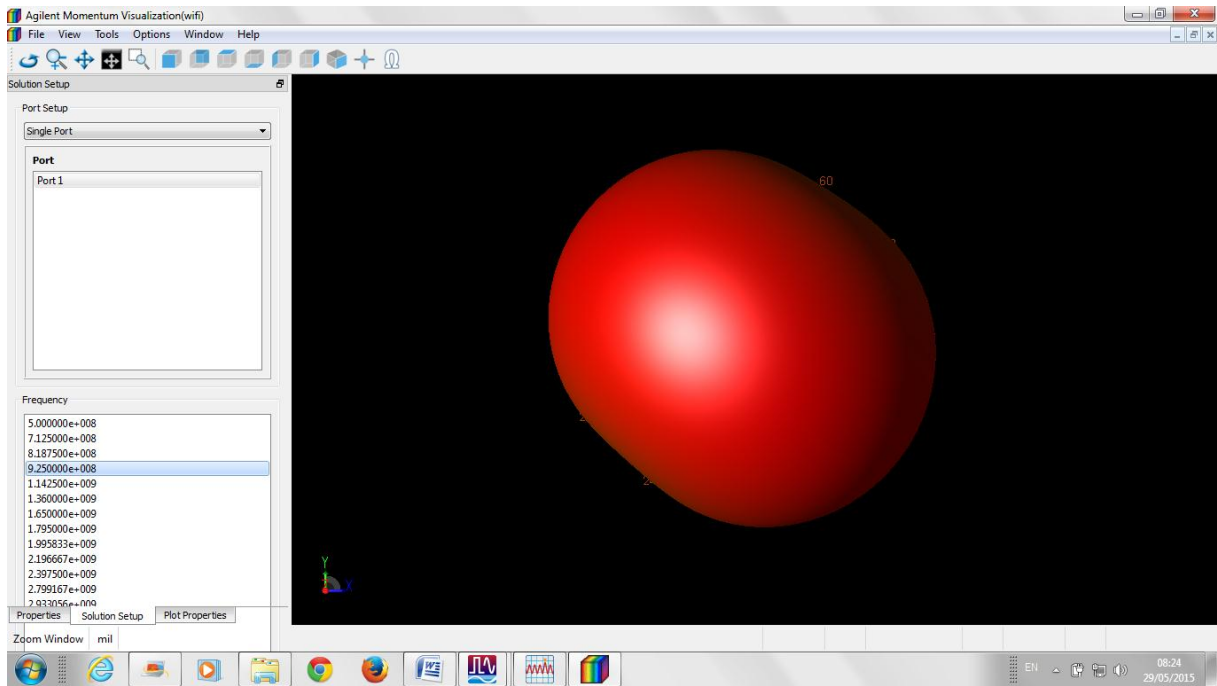


Figure 4.9: 3D radiation pattern for the designed dual band PIFA antenna resonant at 925MHz for  $\varphi=0$

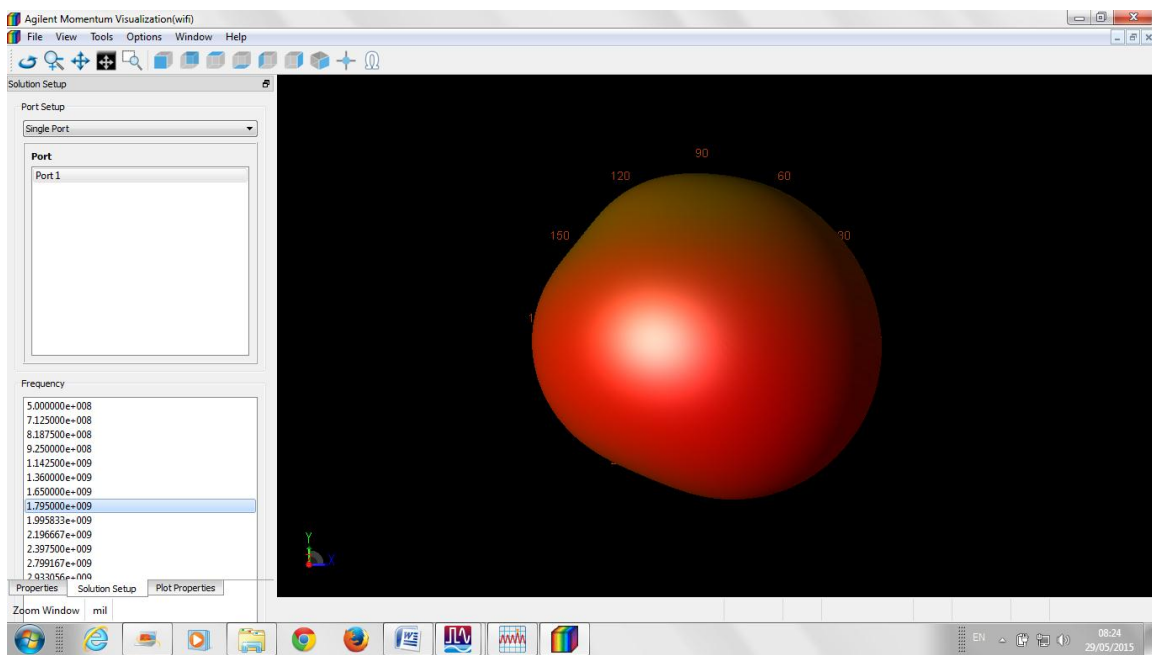


Figure 4.10: 3D radiation pattern for the designed dual band PIFA antenna resonant at 1795MHz for  $\varphi=0$

Dataset: emFar - May 29, 2015

Frequency	E_max	Theta_max	Phi_max	Directivity_max	Gain_max	RadiatedPower	InputPower	Efficiency	CutType	CutAngle
9.250E8	0.464	153.000	316.000	2.358	1.571	0.002	0.002	0.834	Phi	0.000

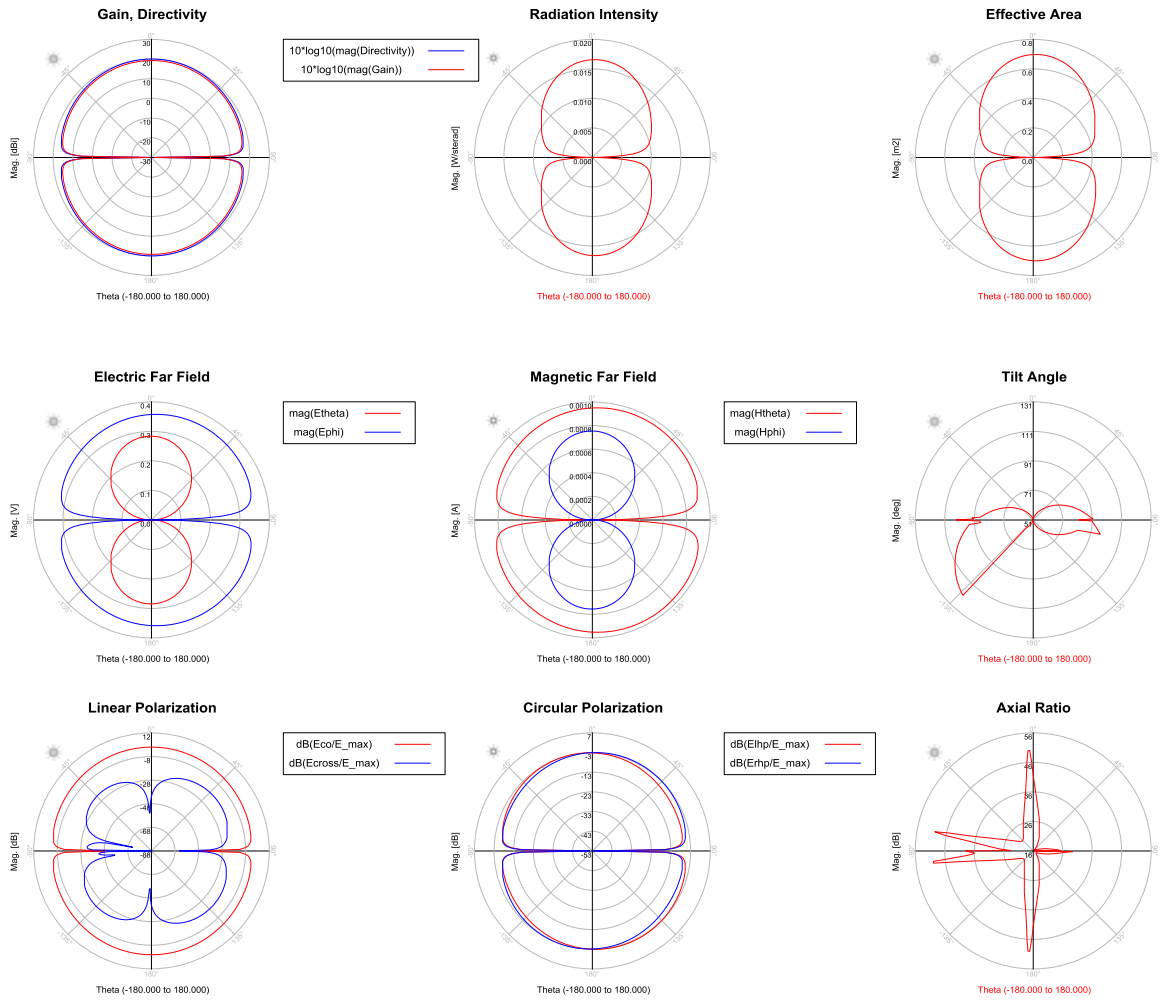


Figure 4.11: XY- plane radiation patterns for the designed dual band PIFA antenna resonant at 925MHz for  $\phi=0$

Dataset: emFar - May 29, 2015

Frequency	E_max	Theta_max	Phi_max	Directivity_max	Gain_max	RadiatedPower	InputPower	Efficiency	CutType	CutAngle
1.795E9	0.560	120.000	313.000	4.737	3.205	0.002	0.002	0.703	Phi	0.000

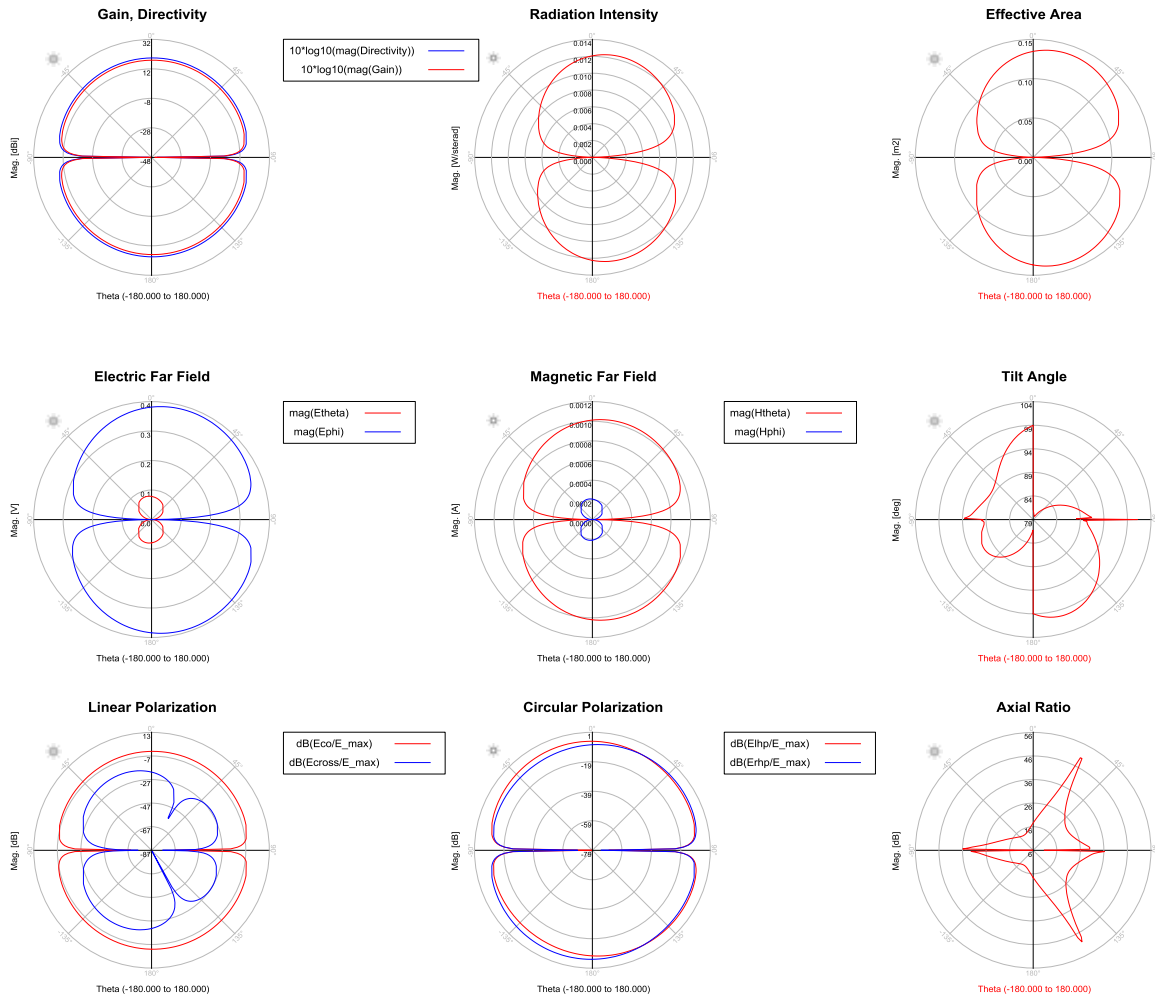


Figure 4.12: XY-plane radiation patterns for the designed dual band PIFA antenna resonant at 1795MHz for  $\phi=0$

### 4.3.1 An interpretation of the simulation results for the designed Dual Band PIFA Antenna for GSM-900 and GSM-1800 Bands

From the simulation results above, a compound of the inverted L and F elements to form a dual band PIFA operates efficiently at both GSM-900 and GSM-1800 bands. This is primarily because at both 925MHz (i.e. the centre frequency for the GSM-900) and 1795MHz (i.e. centre frequency for GSM-1800), its coplanar ground plane is  $0.19\lambda_{925MHz} \times 0.15\lambda_{925MHz}$  and  $0.36\lambda_{1795MHz} \times 0.27\lambda_{925MHz}$  respectively which is therefore large enough to supply a full resonant current distribution at both bands.

From figures 4.5 and 4.6, it is clear that the dual band PIFA has two arms. The longer arm which is 74mm from table 4.3 covers the GSM-900 band while the shorter arm which is 37mm covers the GSM-1800 band. Both arms are slightly less than one-quarter wavelength at

the operating frequencies (i.e. 925MHz and 1795MHz). This is largely due to the effect of the supporting FR4 substrate which tends to reduce the resonant length of the radiating elements. Figure 4.7 shows the return loss of the dual band PIFA antenna. It is seen that the two operating bandwidths are obtained. The lower bandwidth determined at -10dB reaches 114.5MHz and covers the GSM-900 band (890-960 MHz). The upper band has a bandwidth as large as 521MHz and covers the DCS (1710-1880 MHz), PCS (1850-1990 MHz) and UMTS (1920-2170 MHz) bands. These sufficient bandwidths were attainable majorly due to the PIFA's widths (i.e.  $R_W = 5.33mm$  and  $L_W = 5.35mm$ ) that was finally settled at.

The excited surface current distributions obtained from the ADS momentum simulation at 925MHz and 1795MHz are presented in figures 4.5 and 4.6 respectively. For the 925-MHz excitation, a stronger surface current distribution is observed along the longer arm element of the dual band PIFA antenna. This suggests that this arm is the major radiating element at the GSM-900 band. At 1795MHz, the surface current distribution on the shorter arm of the PIFA becomes stronger. This indicates that the shorter inverted-L element is the major radiating element for the higher operating frequency.

Considering the dual band PIFA's geometry, the inverted-L element acts as a capacitive load to the inverted-F element [50]. However from the figure 4.8, it is evident that the input impedance for the dual band PIFA is closer to the centre of the smith chart (i.e. it is matched). This is because the capacitive loading introduced by the inverted-L element was compensated by widening W (i.e.  $W=29mm$ ) which introduced an equivalent inductance to neutralize it. Thus we were able to introduce a new resonant mode at 1795MHz which didn't change the initial resonant mode at 925MHz.

From figures 4.11 and 4.12, it is evident that the designed dual band PIFA antenna has dual-polarization radiation patterns that have suitable characteristics for mobile devices. From table 4.3, more energy for E ( $\varphi$ ) is radiated in both lower and higher bands compared to E ( $\theta$ ) in the XY-plane (a plane being considered). This is probably due to the current cancellation on the strips and the co-planar ground plane. Both figures too show dipole-like radiation patterns at both resonant frequencies. This is mainly because the PIFA/ground plane combination behaves as an asymmetric dipole, the differences in current distribution on the two-dipole arms being responsible for some distortion of the radiation pattern.

The **Friis Transmission Formula**[23], a fundamental equation in antenna theory, is used to calculate the power received by one antenna (with gain  $G_R$ ), when transmitted from another antenna (with gain  $G_T$ ), separated by a distance R, and operating at a frequency

$f$ . This formula relates the free-space path loss, antenna gains and wavelengths to the received and transmit power. One useful form of the Friis Transmission Formula is expressed below:

$$P_R = \frac{P_T G_T G_R C^2}{(4\pi R f^2)} \quad 4.3$$

Where;

$P_R$ -power received by the receiving antenna

$P_T$ -power delivered to the transmitting antenna

$G_T$ -antenna gain of the transmitting antenna in the direction of the receiving antenna

$G_R$ -antenna gain of the receiving antenna in the direction of the transmitting antenna

$C$ -speed of light

$f$ -operating frequency

$R$ -distance between the transmitting and receiving antenna.

Equation 4.3 shows that more power is lost at higher frequencies. This is the fundamental result of the Friis Transmission Equation. This means that for antennas with specified gains, the energy will be highest at lower frequencies. The difference between the power received and the power transmitted is known as **Path Loss**. Friis Transmission equation show that the Path Loss is higher for higher frequencies. That is why mobile phones generally operate at less than 2GHz. There may be more frequency spectrum available at higher frequencies, but the associated Path Loss will not enable quality reception. This is one of the major reasons too as to why GSM-900 band is superior to the GSM-1800 band. This too explains why at very high frequencies (i.e. 60GHz), only point-to-point communication is possible since the Path Loss is very high.

Although equation 4.3 suggests that low Path Losses are incurred at low frequency transmissions, another challenge crops up at low frequencies. For example at the new LTE(4G) band, that operates at 700MHz, the mobile device designers will have to fit an antenna with a larger wavelength in a compact device and so the antenna designer's job gets more complicated.

Circularly polarized antennas are preferred though they are not practically realizable. This is because; they can receive both horizontally and vertically polarized electromagnetic waves. This is also important because if the transmitting and receiving antennas are not polarization matched, the power received by the receiving antenna will be reduced by the Polarization Loss Factor (PLF) to properly account for the mismatch as shown below:

$$P_R = (PLF) \frac{P_T G_T G_R C^2}{(4\pi R f^2)} \quad 4.4$$

#### **4.4 Summary of the simulated results**

This chapter has reported the simulation results that were obtained in the process of developing a multi-band PIFA antenna. The dual band PIFA antenna comprises of a single PIFA antenna that was capacitively loaded with an inverted-L element to cover the GSM-900 band (890-960 MHz), the DCS (1710-1880 MHz), PCS (1850-1990 MHz) and UMTS (1920-2170 MHz) bands. Since the antenna can be printed directly on a single PCB, it is both low cost and easy to fabricate, making it suitable for any palm-sized mobile device applications.

In the next chapter, this dual band antenna is integrated into a populated multilayer PCB, tuned and its performance evaluated. The results obtained are also presented and discussed.

## **CHAPTER 5**

### **PERFORMANCE OF THE DESIGNED DUAL BAND PIFA ANTENNA ON A POPULATED MULTI-LAYER BOARD**

#### **5.1 Introduction**

Desirable electrical characteristics of a circuit and its PCB layout include low noise, low distortion, low crosstalk and low radiated emissions [49, 51, 52, 53, 55, 56, 59, 61]. The three goals in designing PCBs for electrical performance and signal integrity are:

- i) The PCB should be immune to interference from other systems.
- ii) It should not produce emissions that cause problems for other systems.
- iii) It should demonstrate the desired signal quality.

When electromagnetic waves get into a given PCB system, it is referred to as electromagnetic interference (EMI). On the flip side, this PCB system can also be a source of EMI and cause problems for other systems. The ability for systems to work together effectively is termed as electromagnetic compatibility (EMC). Proper layout of a PCB can greatly reduce EMI and improve EMC [54].

The method by which systems and circuits interfere with each other is inductive and capacitive coupling of their related electromagnetic fields. In the 1820s Faraday and Henry showed that an electric current could be produced in a conductor by changing the current in another nearby conductor. And years later Maxwell showed that changing electric fields also produce magnetic fields. These fields are a source of many problems in PCB designs [54].

This chapter outlines basic concepts for RF PCB design while providing recommended RF design guidelines which allows the designers to have designs with optimum performance on their first board fabrications reducing design time and the costs involved. Secondly, following these guidelines, the dual band PIFA antenna is integrated into multi-layer PCB and its performance evaluated.

#### **5.2 Basic concepts of RF PCB Design**

There are four areas for electrical considerations when designing and routing RF PCBs namely [54]:

- i) Component placement
- ii) PCB layout stack-up
- iii) Bypass capacitors
- iv) Trace width
- v) Spacing width between traces
- vi) Trace corners



vii) Continuity of the return path that is tightly coupled to the RF traces (Ground plane)

viii) Embedded antenna placement considerations

### **5.2.1 Proper component placement for electrical considerations**

It is important for one to consider component placement with electrical performance and PCB manufacturability in mind. Usually these two goals complement each other but occasionally they conflict. When conflicts do occur an attempt should be made to resolve the conflict in a way that is mutually beneficial. If that is not possible, electrical considerations usually have priority over mechanical considerations unless doing so will result in mechanical failure of the PCB board.

PCBs can be designed for analog circuits, digital circuits or mixed signals. Since analog circuits are susceptible to noise, the goal is usually to place the parts to minimize the possibility of degrading the signals. This usually means keeping the components as close as possible so that the traces can be as short as possible and keeping the signal path as straight as possible.

With digital circuits it is also desirable to keep related parts close together and lines short, but because digital circuits often contain many parallel paths and branches and may contain wide data buses it may be impossible to do so. Sometimes the best that can be accomplished is to keep the parts that are functionally related closer together or place parts together that have the highest speed clocks and rising edges in order to minimize the length of related signal lines.

Mixed signal boards are even more challenging in that analog, digital and high power circuits (such as switching regulators) exist on the same board. In this case the board should be segregated into different areas. The topology may vary but the idea is to keep the high power and noisy circuitry closer to the edge of the board if possible. This limits the amount of the return plane utilized by these circuits and therefore minimizes the amount of return plane that is common between them and the rest of the circuitry. Digital and analog circuits should also be kept apart from each other to minimize the effects of switching noise on analog circuitry. When dividing the circuit this way it is also necessary (and beneficial) to utilize split and isolated power and ground planes [51, 54].

Figure 5.1 is an example of a mixed signal board illustrating proper component placement.

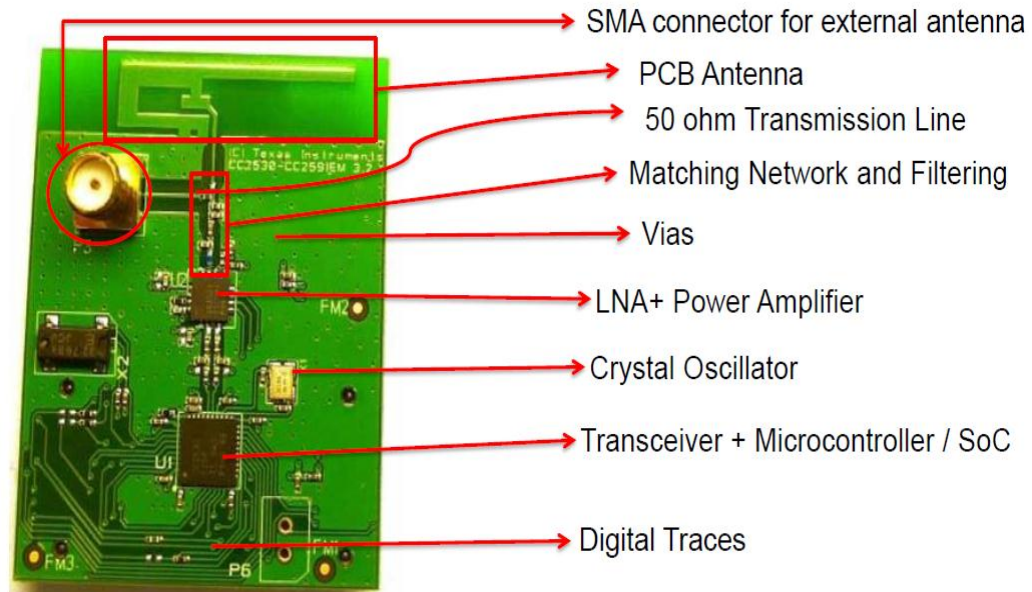


Figure 5.1: Proper component layout for an optimised RF PCB design [49]

### 5.2.2 Multi-layer PCB stack-up planning

For EMC performance consideration, once the working frequency in mobile device product is over 5MHz, or the rise-up/fall-down time of digital signals is less than 5ns, then multi-layer PCB should be considered. The more common multi-layer PCB structure are 4-layers,6-layers and 8-layersPCB.Thus, if a product is designed using multi-layer PCB technology, then the stack-up design of these multi-layer PCBs will become very important(61).

Planning the multi-layer PCB stack-up configuration is one of the most important aspects in achieving the best possible performance of a product. A poorly designed substrate, with inappropriately selected materials, can degrade the electrical performance of signal transmission increasing emissions and crosstalk and can also make the product more susceptible to external noise. These issues can cause intermittent operation due to time glitches and interference dramatically reducing the products performance and long term reliability [54, 55].

In contrast, a properly built PCB substrate can effectively reduce electromagnetic emissions, crosstalk and improve the signal integrity providing a low inductance power distribution network. And, looking from a fabrication point of view, can also improve manufacturability of the product. Suppressing the noise at the source rather than trying to elevate the problems one the product has been built makes sense.

The PCB layer stack-up and thickness are assigned to the manufacturer when the board is ordered and not during the PCB routing process. However, the PCB layers, stack-up

and thickness need to be defined early in the design stage before working on the PCB layout since the stack-up determines how many layers to enable efficient routing and how many power and ground planes to establish [54].

The strategy for stacking up a PCB depends on a number of things such as:

- i) The capability of the board manufacturer
- ii) The circuit density(both routing and components)
- iii) The frequency(analog) and rise/fall times(digital) of the signals
- iv) The acceptable cost of the board

As circuits become denser, additional routing and plane layers are required. Digital circuits commonly require more layers than analog circuits since digital circuits are typically consist of parts with greater pin count per chip and because they have a higher number of parallel connections.

High speed circuits (whether analog or digital) may require a greater number of layers even if they are not very dense. This is because multilayer boards can provide better impedance control and shielding since they can have additional ground planes.

The more layers a board has the more it costs, but once a PCB stack-up exceeds four layers the cost increase per layer usually become less for additional layers. Additionally the benefits of shielding and impedance control can considerably outweigh the increased cost of extra layers.

Boards containing copper planes allow signals to be routed in either microstrip or stripline controlled impedance transmission line configurations creating much less radiation than the indiscriminate traces on a two layer PCB. The signals are tightly coupled to the planes (either ground or power planes) reducing crosstalk and improving signal integrity. Planes, in multi-layer PCBs, provide significant reduction in radiated emission over two layer PCBs. As a rule of thumb, a four layer board will provide 15dB less radiation than a two layer PCB board.

In designing a layer stack-up there are a few important guidelines to follow [55]:

- i) Since PCBs are constructed of double-sided cores bonded together with prepreg, multilayer PCBs usually contain even number of layers. Odd-layered boards can be made, but in most cases there is no cost benefit to adding only one layer instead of a layer pair. For example if one needs five layers it is wise to consider six layers since the extra layer can be an extra return/ground plane and the symmetry of an even number of layers help minimize board warpage (twisting). This is because as the board

cools after multilayer lamination, it can twist to relieve the different lamination stresses on the foil side and the core side. Boards constructed with one core on one side and foil on the other side has a very high risk of twisting, especially as the board thickness increases. The key to eliminating a warp is to create a balanced/even stack-up.

- ii) A signal layer should always be adjacent (and close) to a plane layer (preferably a return/ground plane) to minimize loop inductance, which minimizes electromagnetic radiation and crosstalk. Power planes should also be adjacent (and close) to a return plane as this adds interplane capacitance, which helps minimize power supply noise and radiation. If one has to choose between a signal layer being adjacent to the return plane and a power plane being adjacent to the same return plane, a signal layer should be given priority, since one can add more bypass and bulk capacitors between the power planes to make up for the loss in interplane capacitance.
- iii) A signal's return current will be on the ground or power plane that is closest to the signal line (if possible) and the relative dimensions determine the trace/plane routing pairs. Ideally all return currents will need to end up at the ground/return pin of the PCB's power connector. It may be beneficial to stack-up and route a PCB to try and make it easier for the return currents of critical high-speed traces to be paired up with certain ground planes (so that they are not forced to go through capacitor leads or vias to get back to the ultimate return point), but there is no guarantee they will follow it.
- iv) For an AC signal, there is really a difference between the power plane and the ground plane because they are all shorted together with bulk and bypass capacitors. So when the signal traces transit from one layer to another the return currents may not have an easy path from one ground plane to another and may choose to return to the source on a power plane until they find a convenient path back to the preferred ground through a bypass capacitor. While the return current is not flowing on the preferred plane the impedance of the transmission line can be significantly different from what is expected. To assist the return current in staying with the signal line when it changes layers, return current bridges can be installed by using free vias connected to the ground planes or capacitor fan-out vias near vias used to transmit signals from one layer to another.

### **Effects of the Soldermask on the Board Impedance**

Since PCBs are normally covered by a soldermask, then the effects of the conformal coating should be considered when calculating impedance. Generally, the soldermask will

reduce the impedance by 2 to 3Ω on thin traces. As the trace thickness increases the soldermask has less effect [55].

ICD STACKUP PLANNER – www.icd.com.au 4/28/2011												Total Board Thickness: 88.6
Layer		Material	Dielectric		Copper	Trace		Current	Impedance	Edge Coupled	Broadside Coupled	Description
Number	Name	Type	Constant	Thickness	Thickness	Clearance	Width	(Amps)	Characteristic(Zo)	Differential(Zdiff)	Differential(Zdbs)	
1	Top	Conductive			1.4	4	4	0.31	55.64	93.54		Signal
		Dielectric	4.3	3								Prepreg
2	GND	Conductive			1.4							Plane
		Dielectric	4.3	6								Core

ICD STACKUP PLANNER – www.icd.com.au 4/28/2011												Total Board Thickness: 88.6
Layer		Material	Dielectric		Copper	Trace		Current	Impedance	Edge Coupled	Broadside Coupled	Description
Number	Name	Type	Constant	Thickness	Thickness	Clearance	Width	(Amps)	Characteristic(Zo)	Differential(Zdiff)	Differential(Zdbs)	
		Dielectric	3.3	0.5								Soldermask
1	Top	Conductive			1.4	4	4	0.31	53.53	89.98		Signal
		Dielectric	4.3	3								Prepreg
2	GND	Conductive			1.4							Plane
		Dielectric	4.3	6								Core

Figure 5.2: Effects of the soldermask coating on the PCB impedance [55]

Figure 5.2 above illustrates the effect of the soldermask coating on microstrip impedance. The example is of commonly used liquid photoimageable having a thickness of 0.5MIL and a dielectric constant of 3.3. The soldermask drops the microstrip characteristic impedance by two Ω and the differential impedance by 3.5Ω. So if one doesn't consider the soldermask then the calculation could be out by as much as 3 to 4%.

**Dielectric Materials**

The most popular dielectric material is FR4 and may be in the form core or Prepreg (Pre-impregnated) material. The core material is thin dielectric (core fibreglass epoxy resin) with copper foil bonded to both sides. For instance ISOLA's FR406 materials include 5,8,9.5,14,18,21,28,35,39,47,59 and 93 MIL cores. The copper thickness is typically 1/2 to 2oz (17 to 70µM).

The prepreg material is thin sheets of fibreglass impregnated with uncured epoxy resin which hardens when heated and pressed the PCB fabrication process. ISOLA's FR406 material include 1.7, 2.3, 3.9 and 7.1 MIL prepreg that may be combined to achieve the desired prepreg thickness.

The most common stack-up called the '*Foil Method*' is to have prepreg with copper foils bonded to the outside of the outermost layers (top and bottom) then are alternating with prepreg throughout the substrate. An alternative stackup is called the '*Caped Method*' which is the opposite of the Foil Method. The most common multilayer configurations include 4, 6, 8,10,12,14 and 16 layers, but in this research considering the number of signal nets that must break out from a BGA, the number of power supplies required by the BGAs, the component density and package types an 8-layer PCB will be considered [55].

In this guideline, a classical PCB stack-up of 8-layers is described. An effective layer function assignment attains best RF performance and significantly reduces electromagnetic interface (EMI) problems. In the table below, S1 indicates the first signal layer; S2 indicates the second signal layer and so on.

**Stack-up for 8-layers PCB**

The stackup shown in table 5.1 below demonstrates an example of an 8-layer stackup. This stackup has two plane layers at the centre of the substrate which allows tight coupling between the centre planes and isolates each signal plane (i.e. top, bottom, inner 3 and inner 6) reducing coupling and hence crosstalk dramatically. It is the commonly used stack-up for high speed signals of Double Data rate two and three (DDR2 and DDR3) designs where the crosstalk due to tight routing has to be considered [55].

ICD STACKUP PLANNER – www.icd.com.au 4/28/2011												
Layer		Material	Dielectric		Copper	Trace		Current	Impedance	Edge Coupled	Broadside Coupled	Description
Number	Name	Type	Constant	Thickness	Thickness	Clearance	Width	(Amps)	Characteristic(Zo)	Differential(Zdiff)	Differential(Zdbs)	
		Dielectric	3.3	0.5								Soldermask
1	Top	Conductive			0.7	5	5	0.22	50.05	87.69		Signal
		Dielectric	4.3	3								Prepreg
2	GND	Conductive			1.4							Plane
		Dielectric	4.3	8								Core
3	Inner 3	Conductive			1.4	12	5	0.37	51.96	90.66		Signal
		Dielectric	4.3	8								Prepreg
4	VDD	Conductive			0.7							Plane
		Dielectric	4.3	14								Core
5	GND	Conductive			0.7							Plane
		Dielectric	4.3	8								Prepreg
6	Inner 6	Conductive			1.4	12	5	0.37	51.96	90.66		Signal
		Dielectric	4.3	8								Core
7	VCC	Conductive			1.4							Plane
		Dielectric	4.3	3								Prepreg
8	Bottom	Conductive			0.7	5	5	0.22	50.05	87.69		Signal
		Dielectric	3.3	0.5								Soldermask

Table 5.1: Stack-up for 8-layer PCB [55]

**5.2.3 Bypass capacitors and fan-out**

Bypass capacitors serve two main functions:

- i) To short high frequency noise to ground
- ii) To act as current reservoirs.

Consequently, there are two basic methods to fanning out power pins. First, one can route the power pin to the bypass capacitor before the fan-out via and to the power plane as shown in figure 5.3. Alternatively one can route the power pin to the power plane first by placing the fan-out via between the power pin and the bypass capacitor as shown in figure 5.4. Figure 5.3 is recommended for analog circuits while figure 5.4 for digital circuits [54].

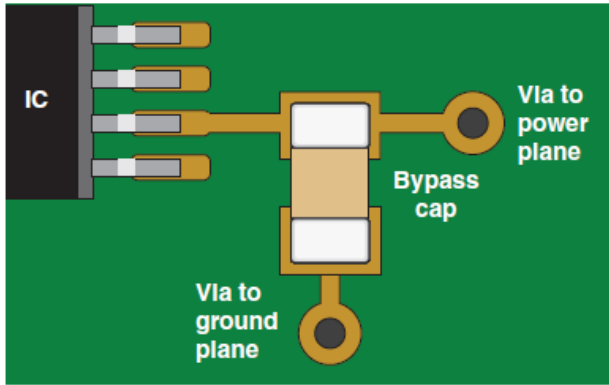


Figure 5.3: Power pin to bypass capacitor

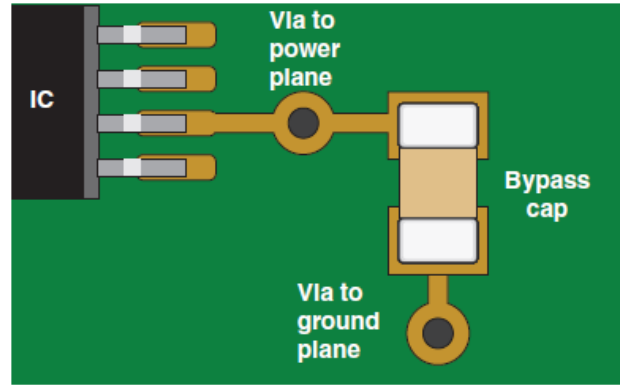


Figure 5.4: Power pin to via to bypass Capacitor

### 5.2.4 Trace width for current carrying capability

When current flows through a conductor it will heat up due to  $I^2R$  losses. Wider traces exhibit less resistance and therefore less heating. To determine the minimum trace width required to minimize heating, determine the maximum current a trace will carry and the thickness of the copper one will use on the board equation 5.1 below can be used to calculate the minimum trace width.

$$w = \left( \frac{1}{1.4xh} \right) \left( \frac{I}{kx\Delta T^{0.421}} \right)^{1.379} \quad 5.1$$

Where;

$w$ -the minimum trace width (in mils)

$h$ -the thickness of the copper cladding (in  $oz/ft^2$ )

$I$ -current load of the trace (in Amps)

$k=0.024$  is used for inner layers and  $0.048$  for outer (top and bottom) layers

$\Delta T$ -the maximum permissible rise in temperature ( $O_C$ ) of the conductor above ambient temperature.

Instead of calculating manually the trace width using equation 5.1, the graphs shown in figure 5.5 can be used to determine minimum trace widths for 1oz inner and outer layer copper with  $\Delta T = 10 O_C$ .

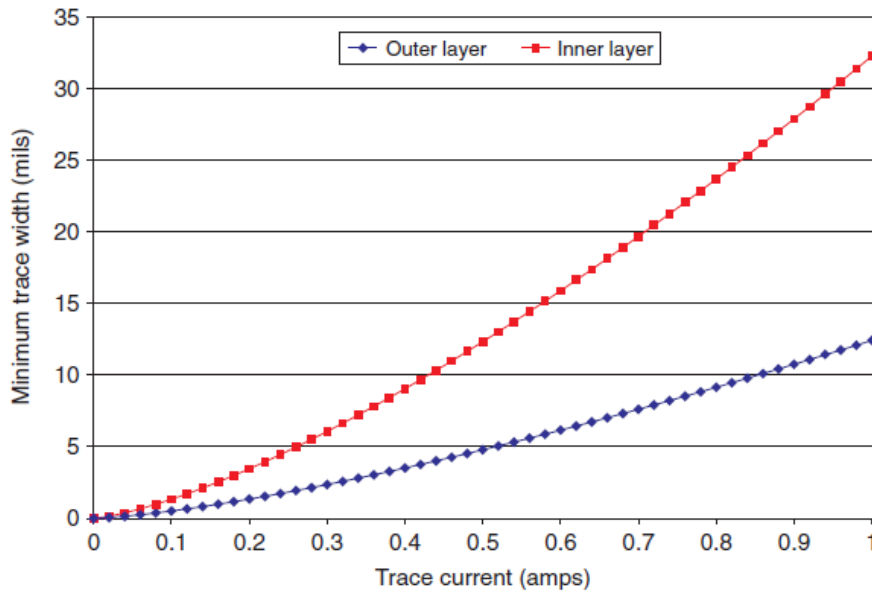


Figure 5.5: Minimum trace widths for 1oz copper for  $\Delta T = 10 \text{ }^\circ\text{C}$  [54]

From figure 5.5, with 6-mil traces you can run up to about 300mA on inner traces and about 600mA on outer traces. Usually of concern are power supply lines for large circuits and power supply boards in general [54].

### 5.2.5 Trace width for controlled impedance

Figure 5.15 below is a representation of signal propagation on a PCB trace.

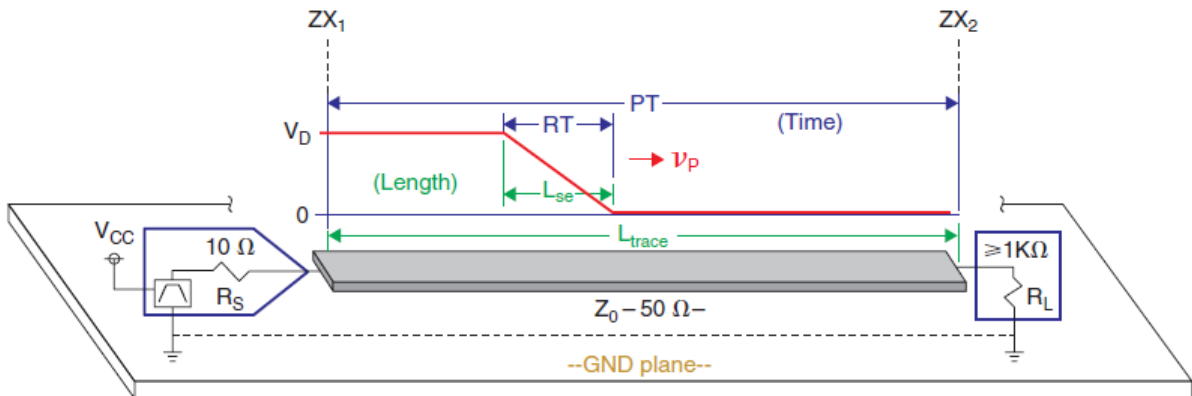


Figure 5.6: Representation of a signal propagation on a PCB trace [54]

The circuit in figure 5.6 above consists of a driver that is powered by VCC and has a low output impedance,  $R_s$  ( $10\Omega$ ), a transmission line with a characteristic impedance,  $Z_o$  ( $50\Omega$ ) and a receiver with a high output impedance,  $R_L$  (usually  $1K\Omega$  or higher). The dashed lines indicate the interfaces of the mismatched impedances and are labelled  $ZX_1$  and  $ZX_2$ . The dimensions in green represent length and the dimensions in blue represent time. This circuit can be used to represent either an analog or digital circuit.

Consider the following from figure 5.6;



*RT*-the rise time; the time it takes for an output of a driver to transit from a minimum value to a maximum value.

$L_{trace}$ -is the length of a trace (transmission line) on the PCB

$V_P$ -the propagation velocity of a wave. It is determined by  $Z_o$  which in turn is determined by  $\epsilon_r$  and the transmission line dimensions (trace width and the distance to the ground plane).

*PT*-the propagation time; the time it takes for the wave to propagate from one end of the transmission line to the other.

$L_{SE}$ -the effective length of the rising edge (also called transition distance or the spatial extent of the transition or edge length).

Length and time are related by the propagation velocity of the wave,  $V_P$  (M/s), where

$$PT = \frac{L_{trace}}{V_P} \text{ (S)} \text{ and } L_{SE} = V_P \times RT \text{ (M)}$$

If the length of the trace,  $L_{trace}$ , is longer than the spatial extent of the rising edge,  $L_{SE}$  (i.e.  $L_{trace} > L_{SE}$ ) then the rising edge of the signal will fit entirely within the length of the trace and the reflection voltage will be an amplitude-scaled copy of the entire rising edge, for which the scaling is determined by the reflection coefficient,  $\rho$ . Another way to look at it is that if *RT*(rise time) is faster than the *PT*(propagation time), then the rising edge will have time to be fully reflected.

The goal is to design a PCB trace such that propagation time (*PT*) is less compared to signal rise time (*RT*) i.e.  $PT < RT$  or a trace's length ( $L_{trace}$ ) is shorter compared to a signal's spatial extents ( $L_{SE}$ ) i.e.  $L_{trace} < L_{SE}$ . If a PCB trace doesn't meet these conditions, then it is termed as "**Electrically long**" and must be treated as a transmission line. Proper treatment of a transmission line means controlling its impedance over the entire length of the trace and matching of the impedance of the line with the source and load impedances so that reflections do not occur.

Much of the literature states that the propagation time should be less than one-half of the rise time (i.e.  $PT < \frac{1}{2}RT$ ) or the length of the trace should be less than one-half of the spatial extent of the signal's rising edge (i.e.  $L_{trace} < \frac{1}{2}L_{SE}$ ). When these two conditions are met, the trace is termed as "**Electrically short**". The length of a trace or a transmission line for which these conditions are just barely met is called **the critical length**. These relationships define the limits and not the goals. *The shorter trace lengths are, or slower the rise times the better will it for the PCB designer [54].*

For digital systems, the critical length (i.e. the maximum allowable trace length) of a PCB trace is determined by the following equation;

$$L_{trace} = \frac{RT}{2 t_{PD}} \tag{5.2}$$

Where;

*RT*- (or Fall time- *FT*) can be obtained from the datasheet of the driver IC driving the trace and will have units of time (e.g. nS). Since both the rise time and the fall time must fall within limits the smaller value should be used in the calculations.

$t_{PD}$ -the intrinsic propagation delay whose formula is dependent on the transmission line types

For analog systems the critical length is determined with respect to the wavelength rather than the rising edge.

The wavelength  $\lambda$  is determined using equation 5.3 below;

$$\lambda = \frac{v_p}{f} \quad 5.3$$

Where;

$v_p$ -is the intrinsic propagation velocity given by ( $v_p = \frac{1}{t_{PD}}$ ) thus  $\lambda$  becomes,

$$\lambda = \frac{1}{fxt_{PD}} \quad 5.4$$

$f$ -is the frequency of the signal on the trace

Various critical length limits are stated in literature: anywhere from  $L_{trace} < \frac{1}{6} \lambda$  to  $L_{trace} < \frac{1}{20} \lambda$ . IPC-2251 standard recommends  $L_{trace} < \frac{1}{15} \lambda$ , whereby  $L_{trace}$  is the length of the trace as measured on the PCB and  $\lambda$  is determined using the equations 5.3 and 5.4 above but using the highest frequency component of the signal (i.e it is the shortest wavelength).

Tables 6-6 and 6-7 [54] can be used to determine  $t_{PD}$  (ps/in) for critical length calculations for both analog and digital circuits. If it is determined using equation 5.2 or 5.4 that a trace is electrically long, then source, load resistance and the transmission line (PCB trace) need to be impedance controlled.

### 5.2.6 Trace spacing for voltage withstanding

There are two reasons for controlling the spacing between traces namely;

- i) To ensure adequate voltage-withstanding capability(insulation resistance) between high voltage lines
- ii) To minimize crosstalk between signal lines

Table 5.2 below, which is a bridged version of a similar table given in IPC-2221A (the Association connecting Electronics Industries whose aim is to standardize PCB assembling) shows the required trace spacing in mils for various voltage ranges on internal and external

layers. The spacing in external traces depends on both the voltage and the external coating of the PCB board.

Voltage between conductors ( $V_{DC}$ or $V_{P.P}$ )	Internal traces	External traces		
		Bare	Soldermask only	Conformal coating
0–15	2	4	2	5
16–30	2	4	2	5
31–50	4	24	5	5
51–100	4	24	5	5

After IPC-2221A.

Table 5.2: Minimum conductor spacing in mils for both internal and external traces of a multilayer PCB [54]

### 5.2.7 Trace spacing to minimize crosstalk

The typical trace spacing used in PCB layouts is shown in figure 5.7 below, in which the edge-to-edge spacing between traces is typically one conductor width.

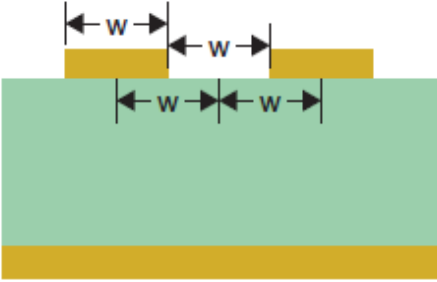


Figure 5.7: Typical trace spacing

If a trace is susceptible to crosstalk from adjacent traces then it should be kept a minimum of two trace widths apart (edge-to-edge) from other traces as shown in figure 5.8.

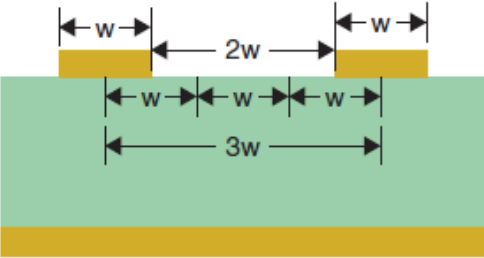


Figure 5.8: 3W spacing to minimize crosstalk

The trace spacing method illustrated in figure 5.8 above is referred to as *the 3W rule* since the centre-to-centre spacing is 3W. At 3W, the traces are out of reach of about 70% of each other’s magnetic field if the traces are controlled impedance transmission lines. Keeping

the traces 10W apart at the centres will keep the traces out of about 98% of each other's if the traces are controlled impedance transmission lines.

**5.2.8 Trace with acute and 90° angles**

Routing high-frequency analog or high-speed digital traces with acute or 90° angles has been long discouraged, but not everyone agrees anymore as to how much of a problem really is [54]. The argument is that the trace width increases by a factor of 1.414 at the corner of the trace as shown in figure 5.9 below and causes a change in the characteristic impedance due to an increase in the capacitance of the trace.

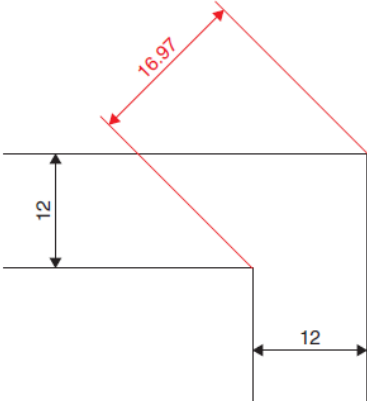


Figure 5.9: Trace geometry of a sharp 90° corner [54]

The resultant impedance mismatches will cause reflections and which in turn will cause ringing in digital circuits with fast rise times and standing or travelling waves in high-frequency analog circuits. In theory then, 90° corners should be avoided at least when routing controlled impedance transmission lines. Figure 5.10 below is an illustration of good and bad trace geometries.

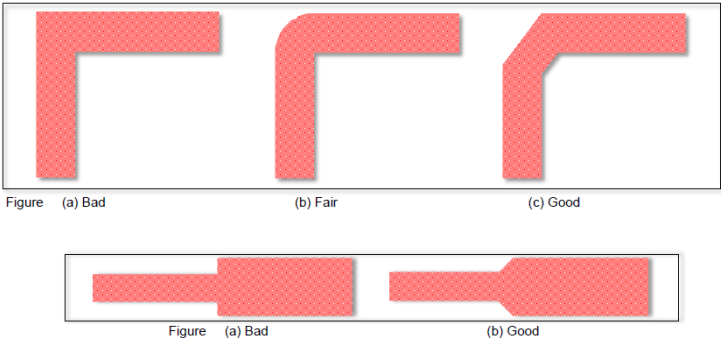


Figure 5.10: An illustration of good and bad trace geometries

**5.2.9 Ground Plane requirement for RF PCB design**

Return currents on RF PCB designs follow the path of least impedance. If the ground plane, which is normally the return path, is divided under the RF section as shown in figure

5.11, the return current paths may become larger leading to higher spurious emission .In addition, divided ground planes add undesirable inductance leading to poor RF performance [49].

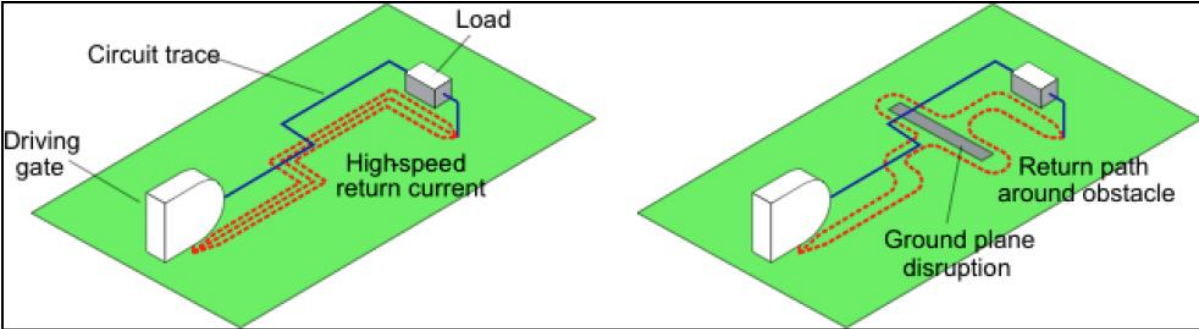


Figure 5.11: Effect of a slotted ground plane on RF return current path [49]

A continuous ground plane also provides for easy connection to the ground by allowing one to drop vias from the RF module pads and antenna to be grounded and thus no additional traces are required to connect the RF circuitry to ground which eliminates unwanted inductance [49].The following two techniques can be employed in the design of RF PCB boards to minimize board radiations and coupling:

- i) In the case where RF routing is done on the top layer, and there happens to be unused areas on this plane. It is recommended to fill these unused areas with ground planes, which are then connected with the reference ground plane which is normally in the second layer with several vias spaced about  $\frac{1}{10} \lambda_{operating\ wavelegth}$  apart.
- ii) **Via Fencing:** Having a grounded via shield around the RF section to protect the RF section from coupling to other sections on a larger board or from nearby interfering sources. This technique also helps to reduce unwanted board edge radiations. Figure 5.12 illustrates an example showing RF design with grounded via shield.

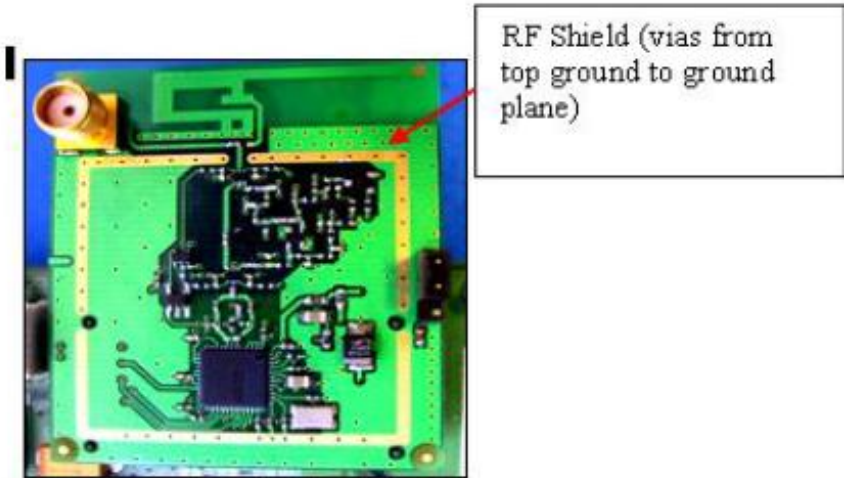


Figure 5.12: RF PCB design with grounded via shield [49].

Embedded antennas (PCB antennas) are generally quarter wave monopole antennas. They are only half of the antenna structure with the other half being a ground plane on PCB designed for RF operation. This antenna/ ground plane combination will behave as an asymmetric dipole. The required PCB ground plane length is roughly  $\frac{1}{4} \lambda_{operating\ wavelength}$ . If the ground plane is not sufficient, the antenna's resonant frequency will be shifted higher and even pushed out of the band if it is too small. While a large ground plane will shift the antenna's resonant frequency lower, but the amount of shift will not be as much as the shift caused by a smaller ground plane.

#### **5.2.10 RF PCB design considerations for embedded PCB antennas**

- i) If the design uses a battery, the battery will act as a ground plane and therefore should not be placed under the antenna.
- ii) Changes to the feed line length will change input impedance matching
- iii) PCB and chip antennas should not have any ground plane under them.
- iv) Any metal in close proximity, plastic enclosure, and human body will change the antenna's input impedance and resonance frequency, which must be considered in the design.
- v) For chip antennas verify that the spacing from and orientation with respect to the ground plane is correct as specified in the datasheet.

### **5.3 Integrating the dual band PIFA antenna into a multilayer board**

#### **5.3.1 Defining the layer stack-up for designed multilayer PCB board**

Since the multilayer PCB is a mixed analog and digital design, the problem of digital noise being injected into analog circuitry is experienced. The solution to this problem is segregating the analog circuitry from the digital circuitry and eliminating common return paths. Segregating the components is easy and straight forward since the components are physically placed in different places on the board. Eliminating common return paths can be accomplished by splitting ground and the power planes into separate areas or utilizing separate continuous planes without separating them. This concept with the guidelines for multilayer PCB stacking outlined in section 5.2.2 above led us to structure the PCB stacking as shown in figure 5.13 below.

	Subclass Name	Type	Material	Thickness (MIL)	Conductivity (rho/cm)	Dielectric Constant	Loss Tangent	Negative Artwork	Shield	Width (MIL)	Impedance (ohm)
1		SURFACE	AIR			1	0				
2		DIELECTRIC	SOLDERMASK	0.5	0	3.3	0				
3	TOP	CONDUCTOR	COPPER	0.411	595900	1.001	0	<input type="checkbox"/>		4.76	51.975
4		DIELECTRIC	FR-4	2.756	0	4.2	0.035				
5	L2_GND_1	PLANE	COPPER	0.69	595900	1.001	0	<input type="checkbox"/>	<input checked="" type="checkbox"/>		
6		DIELECTRIC	FR-4	3.937	0	4.2	0.035				
7	L3_INT_1	CONDUCTOR	COPPER	0.69	595900	1.001	0	<input type="checkbox"/>		3.70	49.991
8		DIELECTRIC	FR-4	7.0866	0	4.2	0.035				
9	L4_Pwr_1	PLANE	COPPER	0.69	595900	1.001	0	<input type="checkbox"/>	<input checked="" type="checkbox"/>		
10		DIELECTRIC	FR-4	27.559	0	4.2	0.035				
11	L5_POWER_GND	PLANE	COPPER	0.69	595900	1.001	0	<input type="checkbox"/>	<input checked="" type="checkbox"/>		
12		DIELECTRIC	FR-4	7.0866	0	4.2	0.035				
13	L6_INT_2	CONDUCTOR	COPPER	0.69	595900	1.001	0	<input type="checkbox"/>		5.50	41.514
14		DIELECTRIC	FR-4	3.937	0	4.2	0.035				
15	L7_GND_2	PLANE	COPPER	0.69	595900	1.001	0	<input type="checkbox"/>	<input checked="" type="checkbox"/>		
16		DIELECTRIC	FR-4	2.756	0	4.2	0.035				
17	BOTTOM	CONDUCTOR	COPPER	0.411	595900	1.001	0	<input type="checkbox"/>		4.76	51.975
18		DIELECTRIC	SOLDERMASK	0.5	0	3.3	0				
19		SURFACE	AIR			1	0				

Figure 5.13: Multilayer PCB stack-up

Since the circuit density of (both routing and components) is dense, the board utilizes 8 layers; four routing layers (TOP, L3\_INT\_1, L6\_INT\_2 and the BOTTOM), two continuous ground planes (L2\_GND\_1 and L7\_GND\_2) and two split power planes (L4\_PWR\_1 and L5\_POWER\_GND—a mixture of power and ground split planes). The goal of such a stacking is to provide a multitude of routing capabilities and better coupling of signal traces to return planes to minimize crosstalk and loop inductances.

The RF components and the dual band PIFA antenna placement and their routing was done on the top layer while utilizing the continuous ground plane on layer two. The top and this ground layer (L2\_GND\_1) are tightly coupled (<10 mils) to reduce the crosstalk and minimize loop inductance for the RF signals being transmitted on the microstrip transmission lines done on top layer. The top layer of the PCB stack-up above showing the dual band PIFA antenna and its adjacent RF circuitry is as shown in figure 5.14 below and the continuous GND plane on layer 2 is shown in figure 5.15.

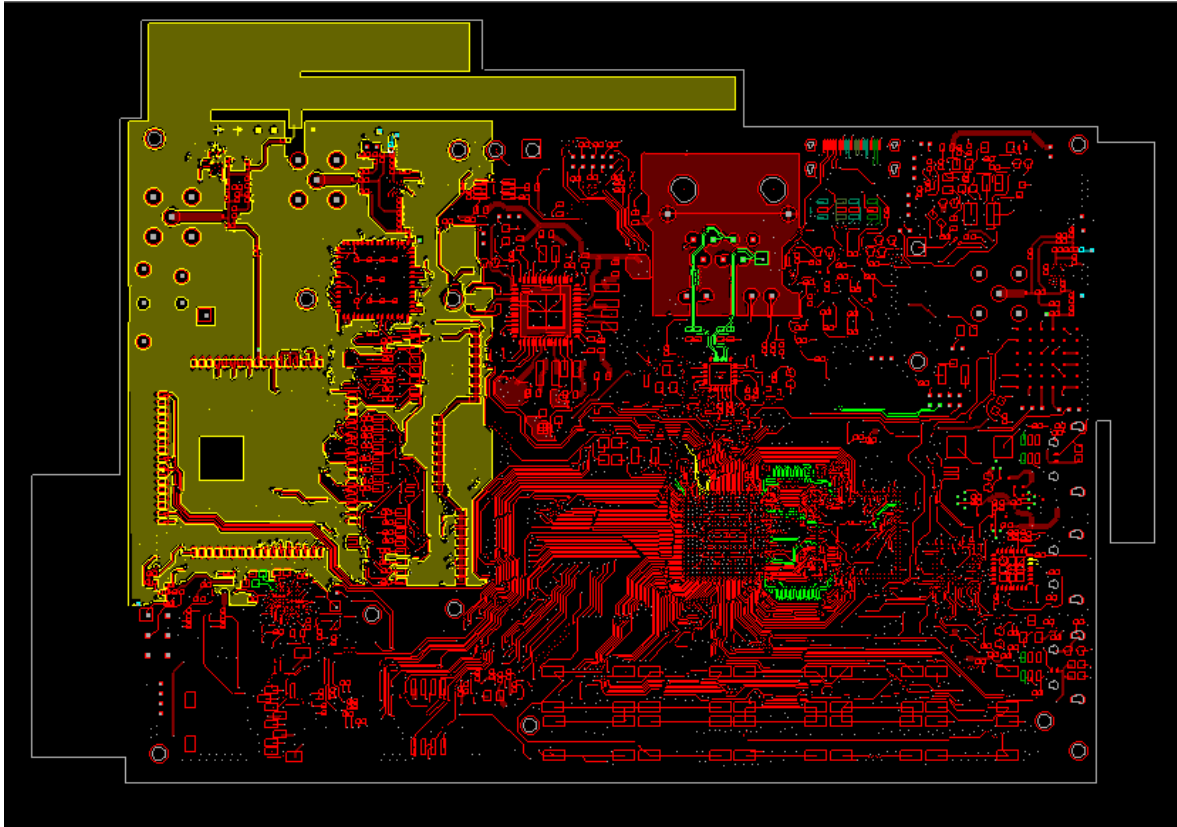


Figure 5.14: Top layer of the designed multilayer stacking

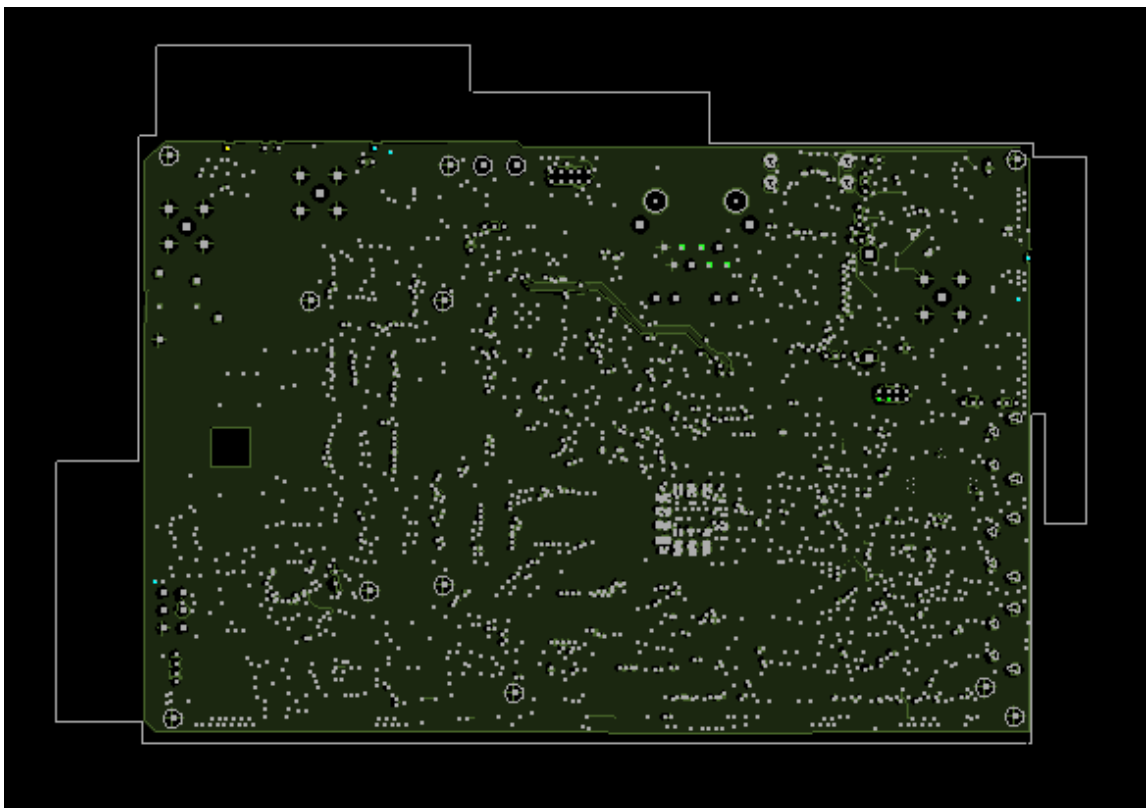


Figure 5.15: Layer 2(L2\_GND\_1) of the designed multilayer stacking



### 5.3.2 Suitable location and placement of the dual PIFA on the designed PCB board

Close proximity to components or housing affects the electrical performance of all antennas. When placed on a non-conductive area of the board, there should be a clearance of at least 5mm in all directions from metal components for maximum efficiency. A reduction in the efficiency of the antenna and a shift in tuned frequencies will be observed if these clearances are not followed. Proximity effects will also have an adverse effect on the radiation pattern of the antenna. Device housings should never be metal, polycarbonate and/or coated with EMI absorption material. Below 1mm clearance around the antenna, major issues do arise, such as antenna detuning and low radiation efficiency.

Conductive blocking structures and other components adjoining an antenna significantly degrade radiation performance because such components serve as EM field scatterers and create unwanted parasitic inductance and capacitance. Thus under no circumstance should they be placed in close proximity to the antenna[36].Figure 5.14 above shows the suitable location of the dual band PIFA antenna in the presence of components.

### 5.3.3 Designing a 50Ω controlled impedance surface microstrip transmission line for connecting the antenna to the GSM module

The transmission line from the RF module to the antenna is a surface microstrip whose width and critical length were determined as follows using the equations shown in figure 5.16 below.

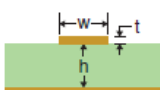
Microstrip transmission lines		Characteristics	Intrinsic propagation delay
Surface	<p>Topology</p> 	<p>Characteristic impedance</p> $Z_0 = \frac{k}{\sqrt{\epsilon_r + 1.41}} \ln \left( \frac{5.98h}{0.8w + t} \right) \text{ ohms}$ <p> <math>k = 87</math> for <math>15 &lt; w &lt; 25</math> mils [1, 2, 3, 4]  <math>k = 79</math> for <math>5 &lt; w &lt; 15</math> mils [3, 4] </p> <p><b>Restrictions</b></p> <p> <math>0.1 &lt; \frac{w}{h} &lt; 3.0</math> [1]  <math>1 &lt; \epsilon_r &lt; 15</math> [1] </p> <p><b>Design equations</b></p> <p>Trace routing width to use in Layout</p> $w = 7.475h \cdot e^{\frac{-Z_0 \sqrt{\epsilon_r + 1.41}}{k}} - 1.25t$ <p>(use <math>k = 87</math>, then check against width rules, use <math>k = 79</math> if necessary)</p>	$t_{PD} = 84.75 \sqrt{0.475\epsilon_r + 0.67}$ (ps/in.)

Figure 5.16: surface microstrip design equations [54]

First the intrinsic propagation delay ( $t_{PD}$ ) of the intended surface microstrip for GSM application is determined as follows:

From figure 5.16 above,

$$t_{PD} = 84.75\sqrt{0.475\epsilon_r + 0.67} \text{ (ps/in)} \quad 5.5$$

From figure 5.13, FR4 is the material used as the substrate between the TOP and L2\_GND\_1 whose relative permittivity is 4.2, thus;

$$t_{PD} = 84.75\sqrt{0.475 \times 4.2 + 0.67} \text{ (ps/in)}$$

$$t_{PD} = 138.35 \text{ (ps/in)}$$

Since RF circuits, like the one being considered here, are analog systems, the critical length of the trace is determined with respect to the wavelength using equation 5.4 above and since the highest frequency component for GSM applications is 1900MHz the wavelength is calculated as follows;

$$\lambda = \frac{1}{f \times t_{PD}}$$

$$\lambda = \frac{1}{1900 \times 10^6 \times 138.35}$$

$$\lambda = 3.8 \text{ inches (96.63mm)}$$

Utilizing the IPC-2251 standard recommendations ( $L_{trace} < \frac{1}{15} \lambda$ ), the critical length of the trace is determined as follows;

$$L_{trace} = \frac{1}{15} \times 96.63$$

$$L_{trace} = 6.44 \text{ mm}$$

Due to the board spacing constraints the antenna and the GSM module were placed some distance apart. Therefore the connection of RF pin of the RF chip to the feed of the antenna uses a trace longer than the critical length determined above ( $PCB \text{ trace} > L_{trace}$ ) i.e. **the PCB trace is electrically long**. Since the GSM module RF pin and the PIFA antenna characteristic impedances are at 50Ω, the PCB trace need to impedance controlled.

From figure 5.16, the width of the 50Ω controlled impedance trace can be determined using the following equation;

$$w = 7.475 \times h \times e^{\left(\frac{-Z_0 \sqrt{\epsilon_r + 1.41}}{87}\right)} - 1.25t \quad 5.7$$

From figure 5.13, the dielectric material utilized is FR4 whose dielectric constant is 4.2 and thickness (h) is 2.756mils. The copper thickness (t) of traces on the top is set to 0.411mils (equivalent to 0.3oz) and since the target impedance is 50Ω, the trace width was determined as follows;

$$w = 7.475 \times 2.756 \times e^{\left(\frac{-50\sqrt{4.2+1.41}}{87}\right)} - 1.25 \times 0.411$$

$$w = 4.76 \text{mils}$$

Thus the desired RF trace width for the intended 50Ω controlled surface microstrip transmission line is 4.76mils. Then the minimum trace width of the GSM traces is set to 4.75mils and the maximum trace width is set to 25mils on the networks spreadsheet as shown in figure 5.17 below.

Type	Objects	Referenced Physical C Set	Line Width	
			Min	Max
			mil	mil
*	*	*	*	*
Net	GPS_RF_OUT	DEFAULT	4.75:5.50:5.50:5.50:5.50:5.50:4.75	0.00
Net	GPS_SDA	DEFAULT	4.75:5.50:5.50:5.50:5.50:5.50:4.75	0.00
Net	GPS_SMA_A	DEFAULT	4.75:5.50:5.50:5.50:5.50:5.50:4.75	0.00
Net	GPS_SMA_B	DEFAULT	4.75:5.50:5.50:5.50:5.50:5.50:4.75	0.00
Net	GSM_ALT_A	DEFAULT	4.75:5.50:5.50:5.50:5.50:5.50:4.75	25.00
Net	GSM_ALT_B	DEFAULT	4.75:5.50:5.50:5.50:5.50:5.50:4.75	25.00
Net	GSM_ANTENNA	DEFAULT	4.75:5.50:5.50:5.50:5.50:5.50:4.75	25.00
Net	GSM_RF_IN	DEFAULT	4.75:5.50:5.50:5.50:5.50:5.50:4.75	25.00
Net	GSM_RF_OUT	DEFAULT	4.75:5.50:5.50:5.50:5.50:5.50:4.75	25.00

Figure 5.17: Maximum and minimum trace width setting from the nets spreadsheet

Once the extents of the transmission widths are set, the trace is routed manually, disabled and locked to avoid being shifted or altered while routing other traces.

**5.3.4 Simulation results of the multiband PIFA antenna in the presence of components**

The DXF import feature in Agilent ADS momentum allows the original PCB and the dual band PIFA model file to be imported, along with all networks, power and ground planes and all various components on the PCB board ready for electromagnetic simulation. This feature allows engineers to investigate the performance of embedded antennas in realistic environments. Figure 5.18 below is the complete PCB with dual band PIFA antenna model ready for electromagnetic simulation.

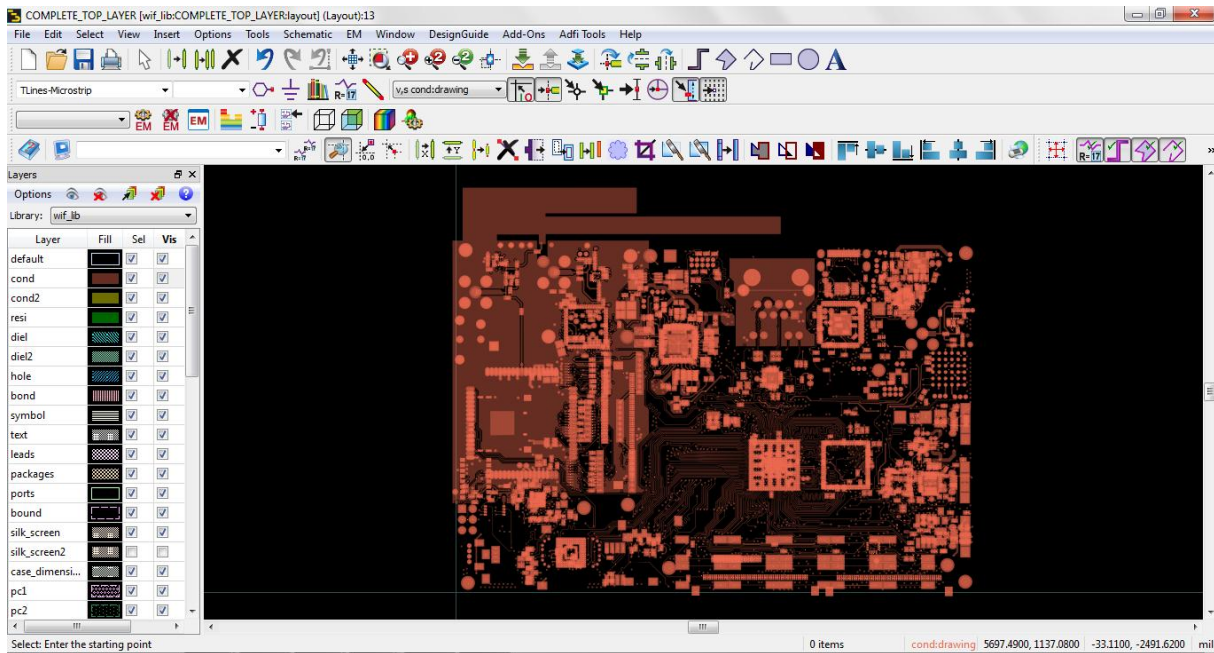


Figure 5.18: Complete PCB with the dual band PIFA antenna model ready for simulation

#### 5.4 Simulated results of the antenna on a populated PCB board

An antenna is a function of its environment. Whether it is sitting on a PCB prototype or a final product, all these two scenarios result in different performance. Unlike most components that can be used in a design with an expected effect on the circuit, an antenna is affected by everything around it.

The radiated electromagnetic fields from an antenna interact with nearby materials, and can shift its intended frequencies of operation. This is evident by comparing the simulated return loss obtained when the antenna was alone (see figure 4.7) and when it was incorporated into a populated PCB board (see figure 5.19 below). The centre frequency of the lower band was shifted downwards from 925MHz to 916MHz, while the centre frequency of the upper band was shifted upwards from 1.795GHz to 1.931GHz. Thus it is always a good idea to place a designed antenna in its final environment and match its impedance so that it operates in the desired frequency bands. A poorly matched antenna can degrade one's link budget by 10-30dB and severely reduce range. All antennas, whether they are off-the-shelf or designed in the laboratory require matching.

From figure 5.20, the antenna is not impedance matched as the markers m7 and m8 are not coinciding at the centre of the smith chart. When the antenna is placed on a populated board, its electromagnetic fields develop differently than they would have developed on a non-populated PCB board. Its coplanar ground is etched out by through holes, vias, tracks etc. of other circuitry routed on the PCB. This is evident from figure 5.18 above. An etched

antenna's coplanar ground plane ultimately changes the antenna's surface current distribution and consequently its impedance. In addition, new parasitic resonant frequencies emerge as well as shown in figure 5.19 due to this etching .The number of these parasitic resonant frequencies depend on how much the coplanar ground plane is etched out and the clearance of the any material and other components around the antenna area.

m6  
freq=1.931GHz  
dB(S11\_fitted)=-13.962

m5  
freq=1.978GHz  
dB(S11\_fitted)=-8.956

m4  
freq=1.848GHz  
dB(S11\_fitted)=-9.122

m3  
freq=916.7MHz  
dB(S11\_fitted)=-30.805

m2  
freq=948.5MHz  
dB(S11\_fitted)=-10.156

m1  
freq=884.1MHz  
dB(S11\_fitted)=-9.398

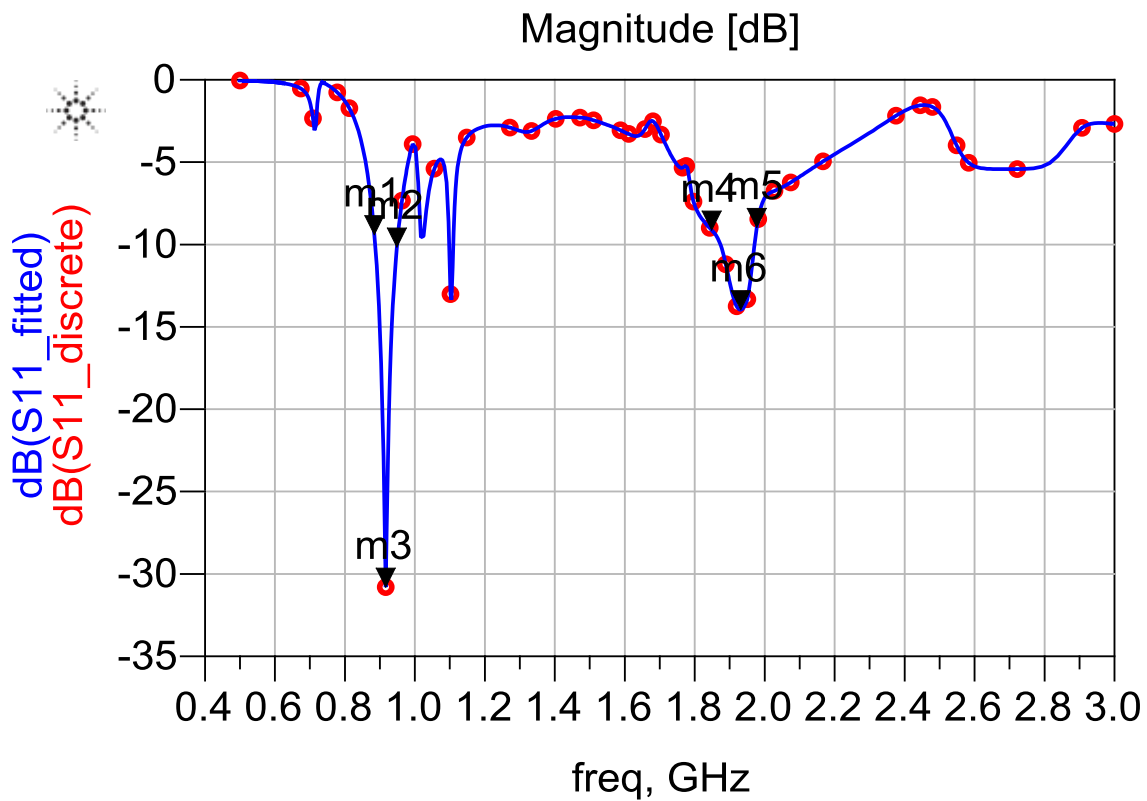


Figure 5.19: Return Loss for the designed dual band PIFA antenna on a populated PCB board

m8  
 freq=1.931GHz  
 S11\_fitted=0.200 / -136.110  
 impedance =  $Z_0 * (0.722 - j0.209)$

m7  
 freq=916.7MHz  
 S11\_fitted=0.029 / -121.155  
 impedance =  $Z_0 * (0.969 - j0.048)$

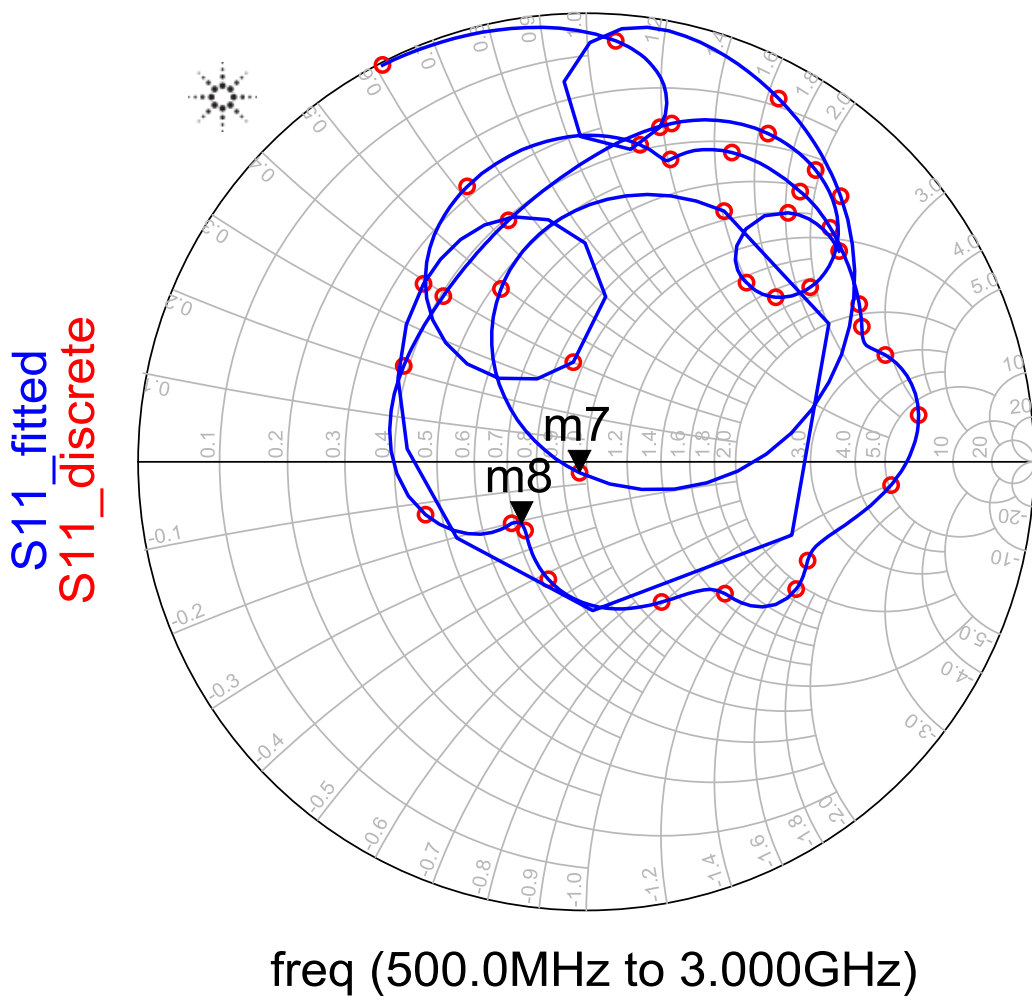


Figure 5.20: simulated Input Impedance of the designed dual band PIFA antenna on a populated PCB board

The antenna's impedance will shift depending on the proximity, electrical properties, and the size of the surrounding materials. Thus it is paramount to keep off large and metallic

components around the antenna area as the antenna’s electromagnetic fields will induce current on them, which will in turn become small radiators. This will not only interfere with the antenna’s impedance matching, but it will also significantly reduce the gain pattern of the antenna. Therefore the antenna needs matching to the correct resonant frequencies which can be achieved by means of three element PI network, placed at the input of the antenna. Usually a capacitor pair and an inductor, or an inductor pair and a capacitor, will give sufficient tuning ability. In addition, to facilitate the antenna debugging and certification testing of RF performance, an RF test connector is added in series between the GSM module’s RF port and the antenna matching circuit. The recommended antenna matching circuit by the sim900 module vendors that was employed in our design is shown in figure 5.21 below.

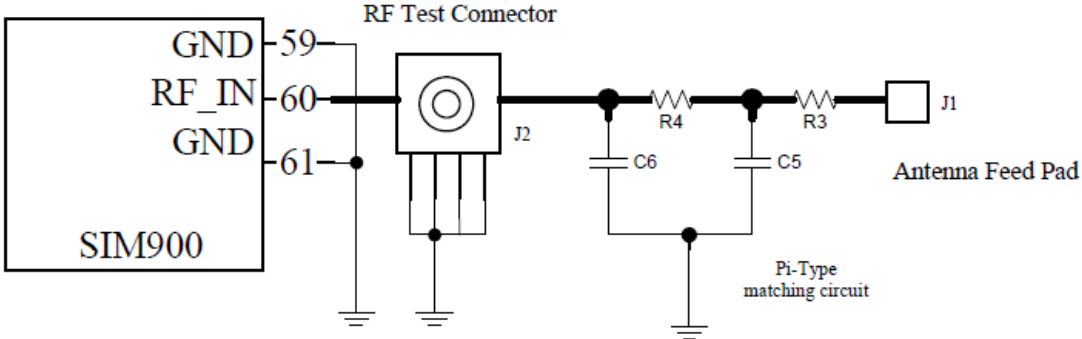


Figure 5.21: Antenna matching circuit [61]

The components R4, C5 and C6 in figure 5.20 above make up a PI-type circuit structure. The component J2 is the RF test connector, which is used to conduct the RF test. The trace in bold type should be 50Ω impedance controlled and was designed and routed as it was explained in section 5.3.3 above. It is important that the components selected be of smaller footprints since small footprints will introduce less parasitic effects. The component values are not given since tuning the matching PI-network will be done by changing the component values, and since the final tuning will be done in a device with a plastic enclosure, the values are yet to be determined.

Thus a good practice is to review all components in the RF section of the layout and remove all excess metal. In addition, it is an important to avoid routing of traces near or parallel to RF transmission lines or RF bias lines. RF signals will couple to these pieces of metal, which are usually connected to ground and can distort the signal. Maintaining a continuous ground plane under an RF trace is critical to maintaining the characteristic impedance of the trace. In addition, it is also important to avoid any form of routing on the



ground plane layer that will result in disruption of the continuity of this ground layer under the RF traces.

## CHAPTER 6

### CONCLUSION AND RECOMMENDATIONS

#### 6.1 Conclusion

The aim of this research work was to design, optimize and tune a dual band PIFA antenna for mobile devices in the presence of active components on a typical mobile device measuring 120mm by 80mm while the designed antenna occupies an area of 72mm by 10mm. Thus the designed antenna can fit within these devices if it is positioned at the edge of the longer side mobile device PCB, enabling mobile device designers to utilize the space within the handset for other on board circuitry more effectively. The minimum size of the antenna's co-planar ground plane was determined to be 63mm by 52mm which can easily be obtained from one of the ground layers used on the multilayer PCB stacking of these devices. To make this research a success, below is a summary of the steps that were taken.

First, the design and optimization of a printed inverted-FL antenna, where the radiating element is a compound of a PIFA antenna and inverted-L elements, adjacent to a coplanar ground plane is presented. The design procedure for dual-band operation at frequencies 900MHz and 1800MHz is described in four steps. In the first step, a PIFA antenna is designed to operate at 900MHz. In the second step, an inverted-L element operating at 1800MHz is designed. Thirdly, the PIFA antenna element is capacitively loaded with the inverted-L element for dual band operation. And lastly, structural adjustments are carried out on the compounded inverted-FL antenna and its co-planar ground to obtain optimal dual frequency operation at the desired frequencies. It is found out that the antenna's lower and upper bandwidths determined at -10dB reach 114.5MHz and 512MHz respectively which covers the above mentioned bands very well with very low return losses of -30.319dB and -30.189dB at resonant frequencies 925MHz and 1.795GHz respectively.

Secondly, the designed GSM dual band inverted-FL is integrated into a populated multilayer mixed-signal PCB board and its performance evaluated through electromagnetic simulation. Good PCB stacking, effective PCB partitioning, proper component orientation and placement, routing discipline combined with right selection of antenna location are the keys to successful integration of the dual band PIFA into a mixed signal multilayer PCB, improved continuity and uniformity of the dual band PIFA antenna's co-planar ground plane and an improved overall integrated antenna performance. Good multilayer PCB stacking, is an important factor in determining the Electromagnetic Compatibility (EMC) of a product, it is effective in reducing radiation from the loops of the PCB (differential-mode emission), as

well as the cables attached to the board (common-mode-emission). Proper component orientation and placement ease component identification, inspection and testing. Effective PCB partitioning and discipline in routing minimizes track lengths. Moreover, a properly done layout ensures that digital currents remain in the digital section of the board and will not interfere with analogue signals. Finally, a good antenna location selection facilitates easier antenna tuning and minimizes interference. Though a slight antenna detuning is evident, the results obtained show that the lower and upper bandwidths determined at -10dB is over 60MHz and 130MHz with return losses -30dB and -14dB at resonant frequencies 915MHz and 1931MHz.

## **6.2 Recommendations for future work**

The results obtained so far are simulation based due to the time constraints. Since the multilayer PCB board has been designed and manufactured, it will serve as a workbench for practical RF measurements.

In this research work only the GSM PIFA antenna has been tuned and its performance evaluated in the presence of components. However, the designed PCB board has both WIFI and GPS antennas as well. It will be important to study and evaluate how these antennas couple while other practical RF measurements will also be carried out.

## REFERENCES

- [1] D. O. Kim, C. Y. Kim and D. G. Yang, "Design of Internal Multi-band Mobile Antenna for LTE700/WCDMA/UMTS/WiMAX/WLAN Operation," *PIERS Proceedings*, pp. 1490-1493, March 2012.
- [2] M. Karkkainen, "Meandered multiband PIFA with coplanar parasitic patches," *IEEE Microwave and Wireless Components Letters*, vol. 15, pp. 630-632, 2005.
- [3] D. K. Karmokar, A. R. Himel and A. N. Rakib , "Broadband Tiny Triple Inverted-F Antenna for 5 GHz WLAN and Bluetooth Applications," *ACEEE International Journal on Communications*, vol. 3, pp. 25-29, March 2012.
- [4] S. O. Park, Y. S. Yoon, J. K. Oh, K. J. Lee, and G. Koo , "Hexaband Planar Inverted-F Antenna With Novel Feed Structure for Wireless Terminals," *IEEE Antennas and Wireless Propagation Letters*, vol. 6, pp. 66-69, February 2007.
- [5] M. K. Kumar<sup>2</sup> and R. Shantha, "A Modern Approach for Planar Inverted F Antenna Miniaturization," *International Journal of Emerging Technology and Advanced Engineering*, vol. 2, no. 3, pp. 343-351, March 2012.
- [6] Zhijun Zhang, ANTENNA DESIGN FOR MOBILE DEVICES, 1st ed. Asia: John Wiley & Sons Pte Ltd, 2011.
- [7] Motorola Incorporation, Financial Highlights 1983.
- [8] M. Hirose and M. Miyake, "Pattern Control of a  $1/4\lambda$  Monopole Antenna on a Handset by Passive Loading," *International Conference on Universal Personal Communications*, vol. 1, pp. 44-48, October 1993.
- [9] S. Sekine and T. Maeda, "The radiation characteristic of a  $\lambda/4$ -monopole antenna mounted on a conducting body with a notch [portable telephone model]," *Antennas and Propagation Society International Symposium*, vol. 1, pp. 65-68, June 1992.
- [10] S. N. Hornsleth and J. B. Toftgard, "Effects on Portable Antennas of the Presence of a Person," *IEEE Transactions on Antennas and Propagation*, vol. 41, no. 6, pp. 739-746, August 2002.
- [11] P. Haapala and P. Vainkainen, "Helical antennas for multi-mode mobile phones," *European Microwave Conference*, vol.1, pp. 327 - 331, September 1996.
- [12] I. Egorov and Z. Ying, "A non-uniform helical antenna for dual band cellular phones," *IEEE Antennas and Propagation Society International Symposium*, vol. 2, pp. 652 - 655, July 2000.
- [13] G. F. Pedersen and J. B. Andersen, "Integrated Antennas for Hand-held Telephones with Low Absorption," *Proceedings of Vehicular Technology Conference*, vol. 3, pp. 1537-1541, June 1994.
- [14] P. Nowak and E. Bonek Fuhl, "Improved internal antenna for hand-held terminals," *Electronics Letters*, vol. 30, no. 22, pp. 1816-1818, October 1994.
- [15] R. Staraj, G. Kossiavas and C. Luxey P. Ciaisi, "Design of an Internal Quad-Band Antenna for Mobile Phones," *IEEE Microwave and Wireless Components Letters*, vol. 14, no. 4, pp. 148-150, 2004.

- [16] A. A. H. Azremi, R. B. Ahmad, P. J. Soh and F. Malek N. A. Saidatul, "Multiband Fractal Planar Inverted F Antenna (F-PIFA) for Mobile Phone Application," *Wireless Communication Systems*, vol. 14, pp. 671 - 675, September 2010.
- [17] K. Wong and W. Chen, "Compact Microstrip Antenna with dual-band frequency operation," *Electronics Letters*, vol. 33, no. 8, pp. 646-647, 1997.
- [18] P. S. Hall and D. Wake Z. D. Liu, "Dual-Frequency Planar Inverted-F Antenna," *IEEE Transactions on Antennas and Propagation*, vol. 45, no. 10, pp. 1451-1458, October 1997.
- [19] J. F. Zurcher, O. Staub and J. R. Mosig A. K. Shrivervik, "PCS Antenna Design: The Challenge of Miniaturization," *IEEE Antennas and Propagation Magazine*, vol. 43, no. 4, pp. 12- 27, August 2002.
- [20] S. D. Targonski and D. M. Kokotoff R. B. Waterhouse, "Design and Performance of Small Printed Antennas," *IEEE Transactions on Antennas and Propagation*, vol. 46, no. 11, pp. 1629-1633, November 1998.
- [21] John Huang, "A Review of Antenna Miniaturization Techniques for Wireless Applications," *California Institute of Technology: Jet Propulsion Laboratory*, 2001.
- [22] C. A. Balanis, *Antenna theory : analysis and design*, 2nd ed.: Wiley, 1997.
- [23] J. D. Kraus, *Basic Antenna Concepts*, 2nd ed. New York: McGraw-Hill, 1988.
- [24] J. D. Kraus and R. J. Marhefka, *Antenna Basics*, 3rd ed. New York: McGraw-Hill, 2002.
- [25] (2014,October) Electromagnetic Spectrum. [Online].  
<http://www.vlf.it/frequency/bands.html>
- [26] (2014, October) Definition of frequency bands. [Online].  
<http://www.vlf.it/frequency/bands.html>
- [27] (2014, October) Spherical coordinate system. [Online].  
<http://019ed12.netsolhost.com/photometry.htm>
- [28] (2014, October) Radar Terms and Definitions. [Online].  
[http://www.interfacebus.com/Electronic Dictionaty Radar Terms Lo.html](http://www.interfacebus.com/Electronic_Dictionaty_Radar_Terms_Lo.html)
- [29] K.-L. Wong, "Modified Planar Inverted-F Antenna," *Electronics Letters*, vol. 30, no. 1, pp. 7-8, 1998.
- [30] Freescale Semiconductor, "Compact Integrated Antennas," *Application note,AN2731*, December 2012.
- [31] W. L. Stutzman and G. A. Thiele, *Antenna Theory and Design.*: Wiley, 1997.
- [32] Q. Rao, S. Ali and D. Wang W. Geyi, "Handset Antenna Design: Practice and Theory," *Progress in Electromagnetics Research*, pp. 123-160, 2008.
- [33] Amin M Abbosh and Marco A Antoniadis Ahmad Rashidy Razali,.., ch. 4.
- [34] Agilent, Advanced Design System inbuilt manual.
- [35] Nariman, and Mahmoud Shirazi Firoozy, "Planar Inverted-F Antenna (PIFA) Design Dissection for Cellular Communication Application," *Journal of Electromagnetic Analysis and Applications*, vol. 3, no. 10, 2011.
- [36] Richard Wallace, Antenna Selection Guide, Application Note AN058,2012.

- [37] A. Hollister, *Scattering Parameters & Smith Charts*, 2007.
- [38] M. Karaboikis, G. Tsachtsiris and V. Makios C. Soras, "Analysis and Design of an Inverted-F Antenna Printed on a PCMCIA Card for the 2.4 GHz ISM Band," *IEEE Antenna and Propagation Magazine*, vol. 44, no. 1, pp. 37-44, February 2002.
- [39] Y.W. Chi and K. L. Wong, "Very-small-size printed loop antenna for GSM/DCS/PCS/UMTS operation in the mobile phone," *Microwave and Optical Technology Letters*, vol. 51, no. 1, pp. 184-192, January 2009.
- [40] H. Kim<sup>2</sup>, M. Ali<sup>1</sup>, S. K. Park<sup>1</sup> and S. Eom<sup>1</sup>, "Embedded Antenna for Metallic Handheld Communication Devices," *Progress In Electromagnetics Research B*, vol. 57, pp. 127-138, 2014.
- [41] E. ÖJEFORS, "*Integrated Antennas*", *ACEEE International Journal on Communications*, vol. 03, no. 01, March 2006.
- [42] Iulian Rosu, "Small Antennas for High Frequencies", *Microwave and Optical Technology Letters*, vol. 51, no. 1, pp. 200-207, January 2009.
- [43] M. Karaboikis, G. Tsachtsiris and V. Makios C. Soras, "Analysis and Design of an Inverted F Antenna Printed on a PCMCIA Card for the 2.4 GHz ISM band", *IEEE Antenna and Propagation Magazine*, vol. 44, no. 1, pp. 37-44, February 2002.
- [44] "Broadband Tiny Triple Inverted-F Antenna for 5 GHz WLAN and Bluetooth Applications," *ACEEE Int. J. on Communications*, vol. 03, no. 01, March 2012.
- [45] A. M. Abbosh, M. A. Antoniadou and A. R. Razali, *Compact Planar Multiband Antennas for Mobile Applications*, Intech Open Science, 2013.
- [46] X. Zhung and Z. Zhang, "Bandwidth enhancement of multiband handset antennas by opening a slot on mobile chassis," *Microwave and Optical Technology Letters*, vol. 51, no. 7, pp. 1702-1706, 2009.
- [47] A. Hossa, R. Bialkowski and K. Byndas, "Investigations into operation of single- and multi-layer configurations of planar inverted-F antenna," *IEEE Antennas and Propagation Magazine*, vol. 49, no. 4, pp. 22-33, 2007.
- [48] Y. Sato, H. Mimaki, J. Yamauchi and H. Nakano, "An Inverted-F Antenna for Dual-frequency Operation," *IEEE Transactions on Antenna and Propagation*, vol. 53, no. 8, pp. 2417-2421, August 2005.
- [49] Suyash Jain, "Low Power RF Designs Layout Review Techniques", January 2011.
- [50] John Lienau, "Antenna Matching within an Enclosure: techniques and guidelines," *LS Research Wireless Product Development*.
- [51] Rick Hartley. *RF/Microwave PC Board Design and Layout*.
- [52] Freescale Semiconductor, "High Speed layout Design Guidelines", April 2006.
- [53] Lattice Semiconductor Corporation, "High Speed PCB Design Considerations", April 2011.
- [54] Kraig Mitzner, : Elsevier Inc., 2007, ch. 6, pp. 109-164.
- [55] Barry Olney, "Multilayer PCB Stackup Planning", February 2011.
- [56] Semtech, "RF design guidelines: PCB Layout and Circuit Optimization", 2006

- [57] LearnEMC:Introduction to EMC. [Online]. <http://learnemc.com/introduction-to-emc,2015>
- [58] LearnEMC: PCB Layout. [Online]. <http://learnemc.com/pcb-layout,2015>
- [59] Dave Neperud,LS Research. [Online]. <http://www.lsr.com/white-papers/7-antenna-design-considerations,2015>.
- [60] Peter Joseph Bevelacqua: Antenna-Theory.com. [Online]. <http://www.antenna-theory.com/2014>
- [61] Simcom,"SMT Module RF Reference Design Guide",2010.